CREATION RESEARCH SOCIETY

QUARTERLY

Volume 61 Fall 2024 Number 2

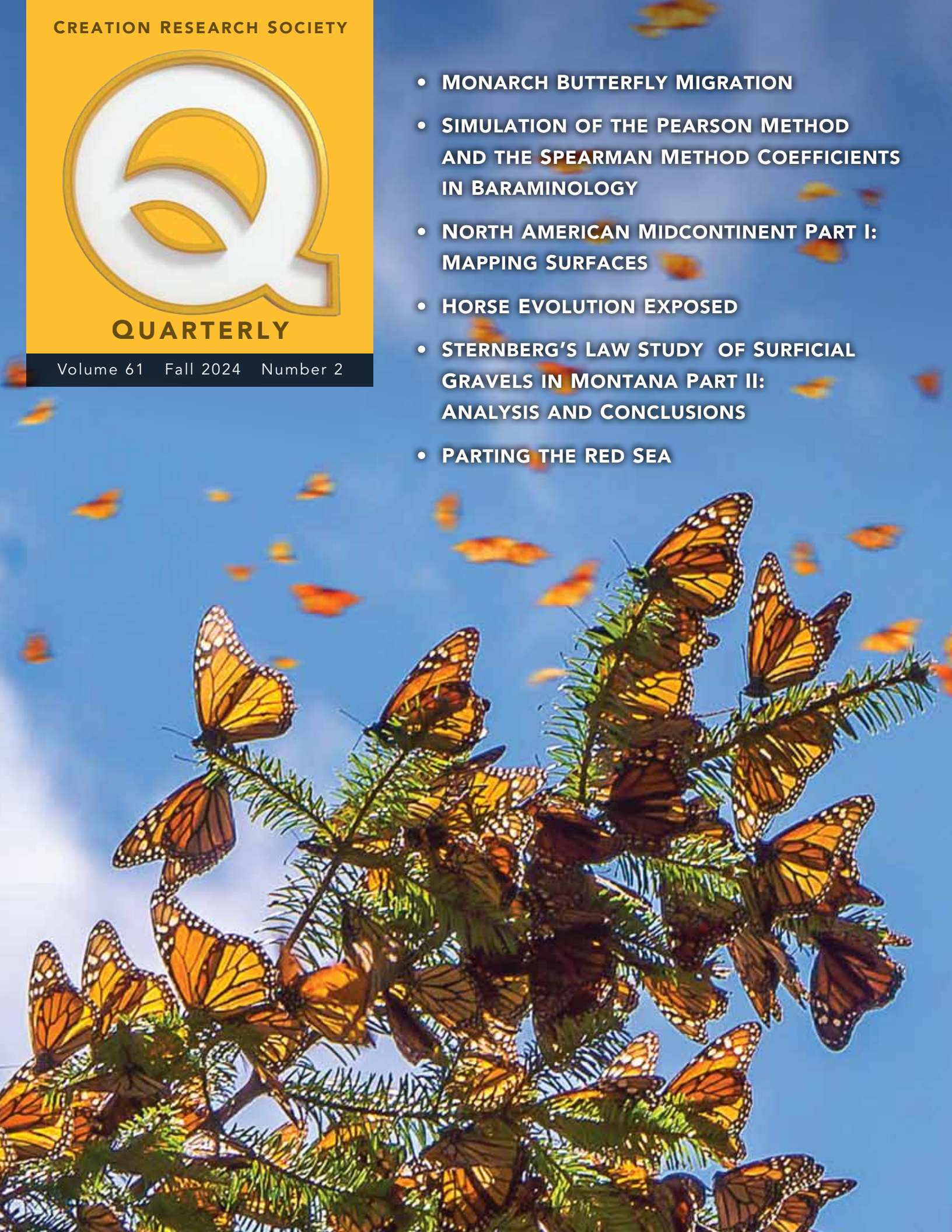

- MONARCH BUTTERFLY MIGRATION
- SIMULATION OF THE PEARSON METHOD AND THE SPEARMAN METHOD COEFFICIENTS IN BARAMINOLOGY
- NORTH AMERICAN MIDCONTINENT PART I: MAPPING SURFACES
- HORSE EVOLUTION EXPOSED
- STERNBERG'S LAW STUDY OF SURFICIAL GRAVELS IN MONTANA PART II: ANALYSIS AND CONCLUSIONS
- PARTING THE RED SEA

CREATION RESEARCH SOCIETY

QUARTERLY

Volume 61

Number 2 | Fall 2024

Articles

Departments

CREATION RESEARCH SOCIETY

QUARTERLY

Volume 61

Number 2 | Fall 2024

Haec Credimus

For in six days the Lord made heaven and earth, the sea, and all that in them is, and rested on the seventh. —Exodus 20:11

Cover by Michael E. Erkel, Afton, Virginia

Design services by Cindy Blandon, cblandon@aol.com

The *Creation Research Society Quarterly* is published by the Creation Research Society, 1 W. Firestorm Way #145, Glendale, AZ 85306, and it is indexed in the *Christian Periodical Index* and the *Zoological Record.*

Send papers on all subjects to the Editor: CRSQeditor@creationresearch.org or to Tim Clarey, 1806 Royal Lane, Dallas, TX 75229.

Send book reviews to the Book Review Editor: Mary Beth De Repentigny, Book Review Editor, marybethd4@gmail.com.

ISSN 0092-9166

Printed in the United States of America

A Study of Monarch Butterfly (*Danaus plexippus* L.) Migration and Its Establishment

Eugene F. Chaffin*

Abstract

The fact that the monarch butterfly (*Danaus plexippus* L.) migrates from Canada to central Mexico is a well-known fact. Here, the migration of the Eastern and Western populations of monarchs is described. This article will not be a field study but an attempt to synthesize a theory of how this migration could originate in a young-Earth context, given that butterflies were created essentially as seen today or will be assumed to have originated this way. The Uvarov Phase Theory is discussed as it applies to desert locusts and its possible relation to the unique migratory generation of monarchs, that is, the larger size of the Fall migratory individuals, and the importance of diapause. The establishment of this interesting migratory pattern is discussed in terms of geography and topography and related to the unique flight abilities of these butterflies.

Key Words: design in nature, insect host plants, insect migration, instinctual reactions, monarch migration

Introduction

Monarch butterflies (*Danaus plexippus* L.) have an interesting life cycle in which the larvae feed upon several species of toxic milkweed. The plants are toxic due to high concentrations of cardenolides in their latex (Agrawal et al., 2015), but monarch larvae are able to tolerate and gain protection from predators by ingesting the milkweed contents (Figure 1). Milkweeds cannot grow in the cold winter, and the monarch itself has a frail constitution which needs warmer climates to survive (Dingle, 1996, p. 247). The eastern population of monarch butterflies follows various paths south in the Fall. Butterflies originating in Indiana or other Midwestern states follow a roughly-defined route south towards Oklahoma and then Texas. Butterflies from Eastern Canada or the eastern United States generally may follow the Appalachian Mountains, but others follow the shores of the Atlantic Ocean. Western monarchs find winter sanctuaries in coastal California.

The eastern population of monarch butterfly spends the winter in the mountains of central Mexico, seeming to prefer to flock together on fir trees on the sides of these mountains (Urquhart, 1976; Brower et al., 2009). Considering that these mountains may be the result of tectonic forces, possibly colliding plates or other Genesis Flood events,

* Eugene F. Chaffin, Ph.D., Simpsonville, SC, ChaffinEF@aol.com
Accepted for publication February 29, 2024

Figure 1. A monarch butterfly flying above a patch of common milkweed (*Asclepias syriaca*), a common happening during late Spring, Summer, and early Fall. Photo by Gene Chaffin.

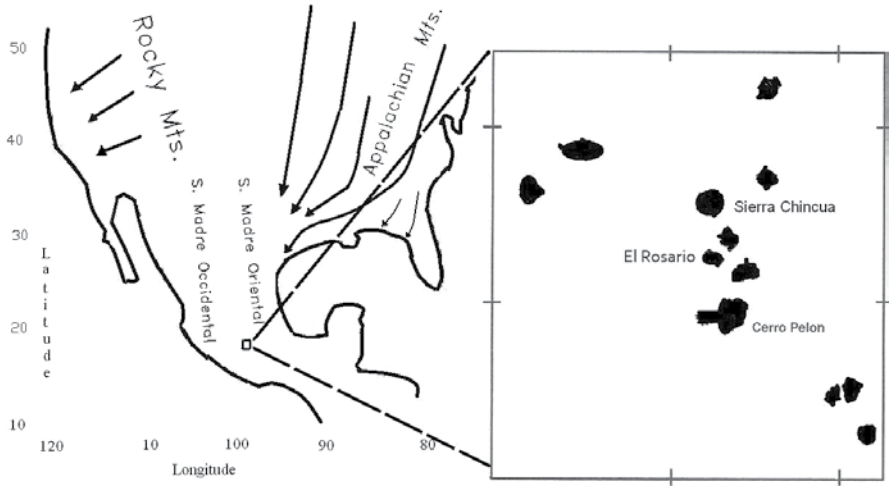

Figure 2. This map shows how the paths flown in Fall by the eastern population of monarchs are funneled towards the Transvolcanic Mountains of central Mexico by the Sierra Madre Oriental Mountains on the West and the shores of the Gulf of Mexico on the East. The black areas of the inset represent the sites in the Transvolcanic Mountains where the monarchs overwinter, although the exact shapes, monarch population densities, and locations vary from year to year. Drawn by Gene Chaffin.

we consider the monarch migration and how the monarch routes could become established on the post-Flood Earth. The Sierra Madre Oriental Mountains in Mexico, together with the Gulf Coast shores sort of form a "funnel" for directing the butterflies (Figure 2). Like sand falling through an hourglass, the monarchs are directed towards their winter home. However, when one considers the path that some of the monarchs must follow along the Gulf Coast starting from the southeastern United States, one is left wondering what directs them? Other species of butterflies besides monarchs migrate, including the cloudless sulphur (*Phoebis sennae*) (Walker, 1985), the painted lady (*Vanessa cardui*) (Abbot, 1951; Nesbit et al., 2009; Stefanescu et al., 2012), and red admiral (Brattström, et al., 2018). Gulf fritillaries (*Agraulis vanillae*) migrate, although over much shorter distances (Arbogast, 1966). However, monarchs are the marathon champions prominent in the minds of anyone who has ever paid any attention to butterflies. In recent years, biophysicists have been studying mathematical models to try to explain migratory movements. Vilk et al. (2022) tried to formulate a non-Markovian model to explain animal movement. "Markovian" in this context means that the behavior at each time interval is independent of the behavior at preceding intervals. But when an animal moves, its decisions are non-Markovian—its choice of direction and speed is balanced against its desire to seek a new foraging spot. Vilk et al. tried to insert input called "preferential returns" to take this into account.

Nearly a couple of decades ago, Dingle (1996, p. 391) wrote:

> In addition to conceptual models, there have also been attempts to generate some formal mathematical statements regarding insect movements. One approach is to assume a set of "rules" for movement and see if insect examples actually conform to those rules. Diffusion, random walk, and Markov chain models are of this sort and have been used effectively to describe within-patch foraging movements of insects, most notably by Peter Kareiva (1982, 1983a,b; Kareiva and Shigesada, 1983).

Kareiva and Shigesada (1983) considered a random walk process, a series of straight-line movements in which the future pattern of movement is not influenced by the pattern of movement that previously transpired. Although this process can result in dispersal away from a starting point, as when insects are seeking nectar from flowers, it does not move the majority of individuals toward a goal (Mexico).

The way monarchs or other butterflies fly is different from that of birds, bats, pterodactyls, locusts, dragonflies, mayflies, etc. Monarch wings are covered with tiny scales, about 100 micrometers in length. Experiments

Figure 3. Monarch butterflies roosting in an oak tree at Port Louisa National Wildlife Refuge in Iowa.

by Slegers et al., (2017) showed that butterflies' ability for climbing flight was decreased after scales were removed. Also, according to Lang (2023), the scales are of just the correct size to aid flight efficiency. Lang did not elaborate, but it appears that God has given a perfect design that enables butterflies to fly. It is difficult to imagine how slow changes in the genetics of scale size could lead to butterflies as observed, since decreased flight efficiency would not lead to viable individuals. The individual needs the perfect scale size.

For an insect to steadily move in a given direction, as for a monarch moving from Canada to central Mexico, it must be directed or attracted, perhaps by a God-given instinct. It also must be able to orient itself, perhaps using the polarization of sunlight (Chaffin, 2021) while soaring near the optimum height. But is there any way to explain how the route to Mexico was established? After all, the post-Flood butterflies had not been to Mexico before, and even today the individuals that return to Mexico are not the same individuals from the previous Spring.

Vilk et al. (2022) wrote:

> Notably, memory patterns must be properly balanced by the organisms with some level of behavioral plasticity to enhance flexibility and exploration (see, e.g., Ref. [14]). For all these reasons, correctly incorporating memory within stochastic models is an important research line for improving both predictive and descriptive tools of movement [6, 15–17].

Vilk et al.'s reference 14 was Krochmal et al. (2021), in which eastern painted turtles, *Chrysemys picta*, migrated the same routes based on memories of previous years, but juvenile individuals followed more varied routes. It would seem that perhaps the post-Flood monarchs were similar to the juvenile turtles in that the species had to learn the route.

In chaos theory one encounters an entity known as an "attractor state." One considers how a small change in an input parameter can cause a strategic change in a system's environment resulting in a branching from a critical point to a significantly different future trajectory. We could find that a new "attractor state" emerges, since from this critical point the trajectory can go in two different ways where each branch represents a trajectory into a new basin of attraction with a new regime and equilibrium.

Vilk et al. (2022) studied a "phase transition," occurring when their "preferential returns" got strong. In this case, a *phase transition* is defined as occurring when some smooth small change in a quantitative input variable that results in a qualitative change in the system's state. In the monarch, such a transition must occur when it is time for migration to begin.

Dingle (1996, p. 145) wrote:

> In many insects migration seems to involve a trade-off with reproduction. The frequently observed ontogenetic separation of migratory behavior from reproduction has been called an oogenesis-flight syndrome (above and Johnson 1969), and the assumption underlying the concept is that migration and reproduction are alternate physiological states.

Leong et al. (1991) studied the conditions, humidity, prevalent winds, temperatures, etc. at a site (San Luis Obispo County, California) where some monarchs of the western population overwinter. These conditions are attractive to monarchs. One might say that an "attractor state" exists at this site.

When an army gets ready to move, each soldier finds his place and each piece of equipment is moved as ordered. One might think of an attractor

state being chosen as a stable configuration into which the army settles. As long as a soldier knows his orders and is close enough when the order comes, he finds this place (Figure 3).

In the central Mexico sites, the monarchs spend the winter gathering over and over either on the branches or the trunks of fir trees on the sides of mountains. The altitude is right for what the monarchs need. There are about a dozen known sites that the monarchs use, called El Rosario, Cerro Pelon, Sierra Chincua, etc., spread over two states (Figure 2). The trees, by holding heat, provide something to cling to and help control moisture conditions, and otherwise shelter the monarchs (Brower et al., 2009). The monarchs are normally not too hot or too cold. One might say that the sites would be "attractor states" due to these optimal conditions. Monarchs which reach these sites have a better chance of survival until Spring.

This does not explain every question about establishing migration, but perhaps it is a step in that direction. Another factor for the eastern population is the funneling, mentioned before, caused by the path of the butterflies as it leads between the Sierra Madre Oriental Mountains on the west and the Gulf of Mexico on the east (Figure 2). The monarchs avoid the great mountain heights to the west and the unforgiving gulf waters to the east, and flying in the generally southern direction end up in the Transvolcanic Mountains of central Mexico. At this new latitude, the mountains have an acceptable climate, at least most of the time. Occasional winter storms unfortunately kill off many monarchs. Also, recent reports reveal that small numbers of monarchs survive in coastal areas of northern Florida, Georgia, and South Carolina (Journey North, 2024), although not inland. Southern Florida, of course has a year-around population (Brower et al., 2009).

Phase Theory and Migration

The Russian/English entomologist, Uvarov (1889–1970), proposed the phase theory of desert locusts (Uvarov, 1921). It stated that the locusts could change physiologically and morphologically, between two extreme types or phases: *solitaria* which led a solitary, settled life and was produced when the individuals were more separated from others, and *gregaria* which was highly gregarious and active and was produced when the population was dense.

Uvarov had observed two phases of the Old World desert locust, now called *Schistocera gregaria.* The two phases differ in coloration, size, as well as relative proportions. Environmentally-induced changes seem to be due to humidity, temperature, and crowding of individuals. The word *polyphenism* is used for differences in physiological or behavioral differences within an insect species (Dingle, 1996, pp. 273–274; Pener and Simpson, 2009, p. 5). It has been noticed in social insects as well as in several species of grasshoppers and locusts. The modern day desert locust is associated with crop decimation in East Africa and the Middle East, similar to the episode in the Book of Exodus, Chapter 10. In 1938 to 1940, an episode of crop decimation occurred in the Dakotas, Wyoming, Montana, North-Central Colorado, and parts of southern Canada, due to the migratory grasshopper *Melanoplus sanguinipes*, then known as *Melanoplus mexicana* (Parker et al., 1955). It was thought to be due to an extremely gregarious phase of this species. Drought caused the decline of native grasses, the emergence of weeds, and soon swarms of this gregarious, migratory phase of insect were causing serious crop damage.

If our concern is the monarch butterfly, one soon wonders whether the migratory "super generation" (aka the "Methuselah generation") qualifies as a "phase." The wing size of the migratory Eastern population of monarch was reported by Altizer and Davis (2010, Table III) to be 51.44±0.19 mm for males and 51.18±0.19 mm for females, whereas South Florida, Puerto Rican, and Costa Rican individuals, not thought to be migratory, averaged a few millimeters less. Li et al. (2016) did not find a difference in wing shape (aspect ratio) between migratory and nonmigratory populations, but agreed with the conclusion that the migratory monarchs had larger wings: "Our study indicates that size may play a larger role than shape in long-distance migratory capability."

Davis et al. (2023) reported larger white spots on migratory monarchs, and speculated that this change in reflectance may aid aerodynamic efficiency.

The so-called "juvenile hormone" is connected with the induction of reproductive organ growth in both male and female monarchs. The migratory generation is in a state called diapause from August or early September to November for males while for females, diapause typically does not end until December (Herman, 1981, p. 89). In the diapause condition reproductive activity ceases, reserving energy for migratory flight.

Conclusion

Thus, the unique migratory generation of monarchs seems to be indicative of a phase designed by the Creator to enable these insects to survive the winter. Physiological and size factors have been discussed which play important roles. While other species of butterflies may survive by other means, monarchs are an example of a long-distance migratory solution.

References

Abbot, C.H. 1951. A quantitative study of the migrations of the painted lady

butterfly *Vanessa cardui* L.—*Ecology* 32:155–171.

Agrawal, A.A., J.G. Ali, S. Rasmann, and M. Fishbein. 2015. "Macroevolutionary Trends in the Defense of Milkweeds Against Monarchs" (Chapter 4, pp. 47–54) in *Monarchs in a Changing World: Biology and Conservation of an Iconic Butterfly*. K.S. Oberhauser, K.R. Nail, and S. Altizer (editors). Cornell University Press (and Comstock Publishing Associates), Ithaca, NY.

Altizer, S., and A.K. Davis. 2010. Populations of monarch butterflies with different migratory behaviors show divergence in wing morphology. *Evolution* 64(4):1018–1028.

Arbogast, R.T. 1966. Migration of *Agraulis vanillae* (Lepidoptera, Nymphalidae) in Florida. *The Florida Entomologist* 49(3):141–145.

Brattström, O., A. Shapova, L.I. Wassenaar, K.A. Hobson, and S. Åkesson. 2018. Geographic origin and migration phenology of European red admirals (*Vanessa atalanta*) as revealed by stable isotopes. *Movement Ecology* 6(25), DOI: 10.1186/s40462–018–0143–3.

Brower, L.P., E.H. Williams, D.A. Slayback, L.S. Fink, M.I. Ramirez, R.R. Zubieta, M.I.L. Garcia, P. Gier, J.A. Lear, and T.V. Hook. 2009. Oyamel fir forest trunks provide thermal advantages for overwintering monarch butterflies in Mexico. *Insect Conservation and Diversity* 2(3):163–175.

Chaffin, E. 2021. Monarch migration. *Creation Matters* 26(1):1, 3.

Davis, A.K., B. Herkenhoff, C. Vu, P.A. Barriga, and M. Hassanalian. 2023. How the monarch got its spots: Long-distance migration selects for larger white spots on monarch butterfly wings. *PLos One* 18(6):e0286921.

Dingle, H. 1996. *Migration: The Biology of Life on the Move*. Oxford University Press. New York, NY.

Herman, W.S. 1981. Studies on the adult reproductive diapause of the monarch butterfly, *Danaus plexippus*. *Biological Bulletin* (Woods Hole) 160(1):89–106.

Johnson, C.G. 1969. *Migration and Dispersal of Insects by Flight.* Metheun, London, UK. Cited in Dingle (1996).

Journey North website. 2024. https://journeynorth.org/monarchs; accessed February 2024.

Kareiva, P.M., and N. Shigesada. 1983. Analyzing insect movement as a correlated random-walk. *Oecologia* (Berlin) 56:234–238.

Krochmal, A.R., T.C. Roth, and N.T. Simmons. 2021. My way is the highway: The role of plasticity in learning complex migration routes. *Animal Behavior* 174:161–167.

Lang, A.W. 2023. Microscopic scales enhance a butterfly's flying efficiency. *Physics Today* 76(9):54–55.

Leong, K.L.H., D. Frey, G. Brenner, S. Baker, and D. Fox. 1991. Use of multivariate analyses to characterize the monarch butterfly (Lepidoptera: Danaidae) winter habitat. *Annals of the Entomological Society of America* 84(3):263–267.

Li, Y., A.A. Pierce, and J.C. de Roode. 2016. Variation in forewing size linked to migratory status in monarch butterflies. *Animal Migration* 3(1):27–34.

Nesbit, R. L., J.K. Hill, I.P. Woiwod, D. Sivell, K.J. Bensusan, and J.W. Chapman. 2009. Seasonally-adaptive migratory headings mediated by a sun compass in the painted lady butterfly (*Vanessa cardui*). *Animal Behaviour* 78(5):1119–1125.

Parker, J.R., R.C. Newton, and R.L. Shotwell. 1955 Observations on mass flights and other activities of the migratory grasshopper. *U.S. Department of Agriculture Technical Bulletin 1109*. 46 pages.

Pener, M.P., and S.J. Simpson. 2009. Locust phase polyphenism. *Advances in Insect Physiology* 36:1–272.

Slegers, N., M. Heilman, J. Cranford, A. Lang, J. Yoder, and M.L. Habegger. 2017. Beneficial aerodynamic effect of wing scales on the climbing flight of butterflies. *Bioinspiration & Biomimetics* 12(1):016013. 14 pages.

Stefanescu, C., F. Páramo, S. Åkesson, M. Alarcón, A. Ávila, T. Brereton, J. Carnicer, L.F. Cassar, R. Fox, J. Heliölä, J.K. Hill, N. Hirneisen, N. Kjellén, E. Kühn, M. Kuussaari, M. Leskinen, F. Liechti, M. Musche, E.C. Regan, D.R. Reynolds, D.B. Roy, N. Ryrholm, H. Schmaljohann, J. Settele, C.D. Thomas, C.V. Swaay, J.W. Chapman. 2012. Multigenerational long-distance migration of insects: Studying the painted lady butterfly in the Western Palaearctic, *Ecography* 51(2). DOI:10.1111/j.1600–0587.2012.07738.x.

Urquhart, F.A. 1976. Found at last—The monarch's winter home. *National Geographic* 150(2): 161–173.

Uvarov, B.P. 1921. A revision of the genus *Locusta* L. (=*Pachytylus,* Fieb.), with a new theory as to the periodicity and migrations of locusts. *Bulletin of Entomological Research* 12(2):135–163. DOI: https://doi.org/10.1017/S0007485300044989.

Vilk, O., D. Campos, V. Méndez, E. Lourie, R. Nathan, and M. Assaf. 2022. Phase transition in a non-Markovian animal exploration model with preferential returns. *Physical Review Letters* 128:148301. 7 pages.

Walker, T.J. 1985. "Butterfly migration in the boundary layer" (pp. 704–723) in *Migration: Mechanisms and Adaptive Significance, Contributions to Marine Science*, Volume 27 supplement. M.A. Rankin (editor). Port Aransas Marine Laboratory, University of Texas Marine Science Institute, Port Aransas, TX.

Simulation of the Pearson Method and the Spearman Method Coefficients in Morphology-Based Baraminological Research

Harry F. Sanders, III

Abstract

Statistical baraminology has been a common research topic in creation biology for the last several decades. Several statistical methods have been employed but none have been tested against simulated data where the result is known. Therefore, both the original Pearson method and newly deployed Spearman method are tested in this paper against simulated data where the existing patterns were known. Multiple patterns of varying strengths were tested. In every case, the Pearson method outperformed the Spearman method. Based on these preliminary results, the Pearson method (aka the Pearson correlation coefficient) should be the preferred method of statistical baraminology. However, much more research is needed to ensure that baraminology is placed on a strong empirical foundation.

Introduction

Statistical baraminology is the methodology of choice for determining baramins for many in the creation science community. Statistical baraminology uses a distance correlation equation drawn from cladistics (Sokal and Sneath, 1963) to measure the distance between taxa, assuming the more closely related taxa have a lower distance (Robinson and Cavanaugh, 1998). These measurements are done using statistical algorithms, and the data is drawn from the secular phylogenetic literature. Such data is assumed to be completely free of bias (Wood, 2011), despite the evolutionary literature being open about possible biases (Winsor, 1994). The data is analyzed in the web applications BDISTMDS and/or BARCLAY and visualized in graphs and multidimensional scaling plots. For an extensive review of how statistical baraminology works, see Sanders and Cserhati, 2022.

The web applications BDISTMDS and BARCLAY are the primary tools used by baraminologists. The original

* Accepted for publication February 9, 2024

method, BDISTMDS (Wood, 2001), has recently been superseded by BARCLAY (Wood, 2021), though the original method's results have been deemed close enough to be accurate (Wood, 2021). BDISTMDS used the Pearson coefficient as its statistical base, while BARCLAY originally defaulted to the Spearman coefficient (Wood, 2020). BARCLAY now defaults to Pearson despite the original paper claiming Pearson did not meet the required assumptions for use (Wood, 2020). The current recommendation is to use multiple clustering techniques in baraminological analysis (Wood, 2021). However, no simulation studies testing either coefficient have ever been published. While the desire to apply statistical baraminological methods to real-life data is understandable, knowing whether the methods work as intended requires careful testing and simulations where the outcome is known. Therefore, this paper will perform simulation studies on both the Pearson method and the Spearman method to determine if they work as intended and what situations, if any, each one excels at.

Importantly, this is not intended to be the final word on simulation studies in baraminology. This study does not simulate MDS plots, nor does it deal with either PAM or FANNY clustering. Instead, it is intended to provide a foundation for future testing and provide a test for the statistical methods which has, as yet, not been done. Follow-up testing should be done to further tune and test statistical baraminology.

Methods

To perform these experiments, a dataset was generated in Microsoft Excel using the "RANDBETWEEN" function. The dataset was created using 100 simulated taxa and 1,000 simulated characters and randomized before each trial. Character states were permitted to be integers in a range from 0–4. This range of five numbers was selected to allow a wide range of possible characters that would match a wild-type dataset as well as make pattern detection easier. No question marks (representing unknown character states) were introduced into the data, as the desire was to give both methods a best-case scenario. Groups of ten, twenty, fifty, and one hundred taxa were compared using 50, 100, 200, 500, and 1,000 characters. These numbers were chosen as rough approximates of what is available in the mainstream scientific literature. It is rare that a dataset will have more than 100 taxa or 1,000 characters, therefore these were selected as the upper boundaries. It is also uncommon but not unheard of for a dataset to have less than ten taxa or 50 characters, therefore these served as the lower bounds.

The dataset was used in seven separate experiments. First, both Pearson and Spearman were exposed to purely random data. In the succeeding experiments, patterns were introduced to the data. For the second experiment, two taxa were given identical characters for X number of traits. For the third, a second pattern of equal strength but completely different from the first, was given to two different taxa. Effectively, this should have created two clusters. For the fourth experiment, a single pattern with three taxa was used. For the fifth experiment, two patterns with three taxa each were created. In the sixth experiment, there were three patterns given to three taxa each, which should create three clusters. In the final test, both methods were presented with patterns that were identical for all characters in the dataset at varying numbers of patterns and taxa.

For the purposes of this experiment, a pattern is a preset sequence of characters shared across multiple taxa. The pattern represents similarity due to potential ancestry. Taxa where a pattern was introduced might also share random characters generated due to the dataset, but these characters do not represent ancestry. As an example, two species might share number of vertebrae, dentition, eye structure, and specialized structures because of ancestry, but share similar diets, gut length, and size with a third species based purely on chance. The pattern based on ancestry is the pattern baraminologists want to find in the data.

Patterns varied from 0.5% to 50%. In practice, this means that if the experiment used 50 characters, no more than 25 were deliberately made similar between two or more simulated taxa. If an experiment used 1,000 characters, no less than five were deliberately made similar between two or more simulated taxa. When a pattern was introduced, it was given to a select number of taxa, varying from two to three. In some tests several different patterns were introduced to create multiple clusters. To introduce a pattern, the randomized character data was altered so that the states of anywhere from 5–500 characters were identical for the selected taxa. Each dataset was tested at the aforementioned number of characters and taxa. As an example, if 10 taxa were selected for analysis, along with 100 characters, a 10% strength of pattern would be 10 characters being placed in states that were identical. Character 1 for taxa A and B might be simulated as having a value of "1" while Character 3 for the same taxa might have a value of "0." No matter how many patterns were introduced, the same strengths of patterns were used for each number of characters. The tests were identical for each method, and each pair of tests was run using identical datasets. Each unique combination of number of taxa, number of characters, strength of pattern, and number of pattern was run once for the Pearson method and once

for the Spearman method. In total, 520 unique combinations were submitted to both algorithms. In total, 1040 tests were performed.

Note that for the purposes of this study, multidimensional scaling, a visualization tool used to represent calculated distances, was not performed. The goal here was not to interpret the results of the baraminic distance calculation, merely to determine how well the algorithms performed at detecting patterns and rejecting noise. Further, given the subjectivity of the MDS plots, they would not have been helpful in this scenario. FUZZY and PAM plots were also not performed as the point was to determine how well the Pearson method and the Spearman method coefficients performed compared to one another when the correct result was known. The Spearman method tests were performed using the BARCLAY algorithm, while the Pearson method tests were performed with the BDISTMDS algorithm. It is possible not using BARCLAY for both may have impacted the results slightly as the two algorithms are not identical. BARCLAY no longer provides the bootstrapping results (Wood, 2020), that BDISTMDS did (Wood, 2008) as an example. However, given that Wood has deemed the results of the two methods comparable (Wood, 2021) this seems unlikely.

Before going any further, it is important to define some terms. The first is the strength of pattern. When used, it refers to how strong of a pattern was introduced into the dataset. A higher strength of pattern means that more matching characters were placed in the data. The introduction of a pattern requires predefining a certain number of characters so that a given percentage of characters in taxa A and taxa B are identical. Thus, if taxa A and B have a 50% strength of pattern, they are predefined to be identical in 50% of the characters used for analysis. The remaining characters are allowed to vary randomly. If it is assumed that taxa with similar characters are likely related, then changing the strength of pattern reveals which of the current statistical programs is better at detecting those relationships.

The second important term is noise. For this study, noise was defined as any positive or negative correlation appearing on the graph that should not have been there based on the pattern placed in the data. No noise was deliberately introduced into the data. Instead, any character states not predefined in the experiment varied randomly. Effectively noise was the presence of a false positive or negative correlation between two taxa. The more false positives or negatives that are present, the larger the amount of noise. A false negative was marked as a failed test because it indicated that two taxa that should be seen as similar were being read as dissimilar. A false positive was marked as a failed test because it indicated that two taxa that should not be similar were found to be similar. Just one of these errors in a given test resulted in a failed test. The goal is to determine what was required to produce 100% accuracy in the results. If a negative correlation (discontinuity) was not present, but the positive correlation (continuity) was all correct, the test was marked as passed. Missing discontinuity was ignored because only continuity was built into the data and the presence of continuity does not necessarily imply discontinuity (Wood et al., 2003). In other words, just because two organisms are similar to each other, it is not necessarily implied that they are dissimilar to a third organism. However, if continuity was absent from where it should have been present, this was marked as a failed test, because continuity was built into the data. If discontinuity was present when continuity should have been present, this was also marked as a failed test. The goal was to determine how well each method detected continuity patterns in the data.

Results and Discussion

Random Data Experiment

When presented with purely random data, no matter how what combination of characters and taxa numbers were used, the Spearman method always found patterns of continuity. The more characters and taxa were added, the worse at filtering out noise the Spearman method became. As shown in Figure 1a and b, the Spearman method had some noise when combining ten taxa with fifty characters, but a much larger amount when comparing 100 taxa with 1,000 characters. The Pearson method showed no noise at the ten and twenty taxa levels. However, when the character to taxa ratio met or dropped below the 2:1 threshold, the Pearson method began to present noise as well.

The fact that the Spearman method always finds patterns in purely randomized data is disconcerting. That patterns potentially exist in randomized data is possible, given each cell in the dataset is filled randomly. If this were the case, however, it is concerning that the Pearson method does not also find these patterns. Further, given the data is created randomly for each test, if the problem were patterns within a given dataset, the Spearman method would not be expected to find patterns on every occasion. Given that only the Spearman method finds these patterns, it raises the possibility that the switch from the Pearson method to the Spearman method coefficients made when Wood (2020) introduced the BARCLAY algorithm has created a tendency to find much weaker patterns than had been done previously.

Single Pattern

For this test, a single pattern was introduced into the dataset. Taxa A

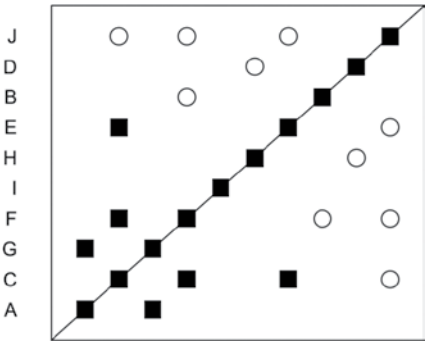

Figure 1A. Spearman coefficient result when presented with randomly generated data. Ten taxa and fifty characters were used for analysis.

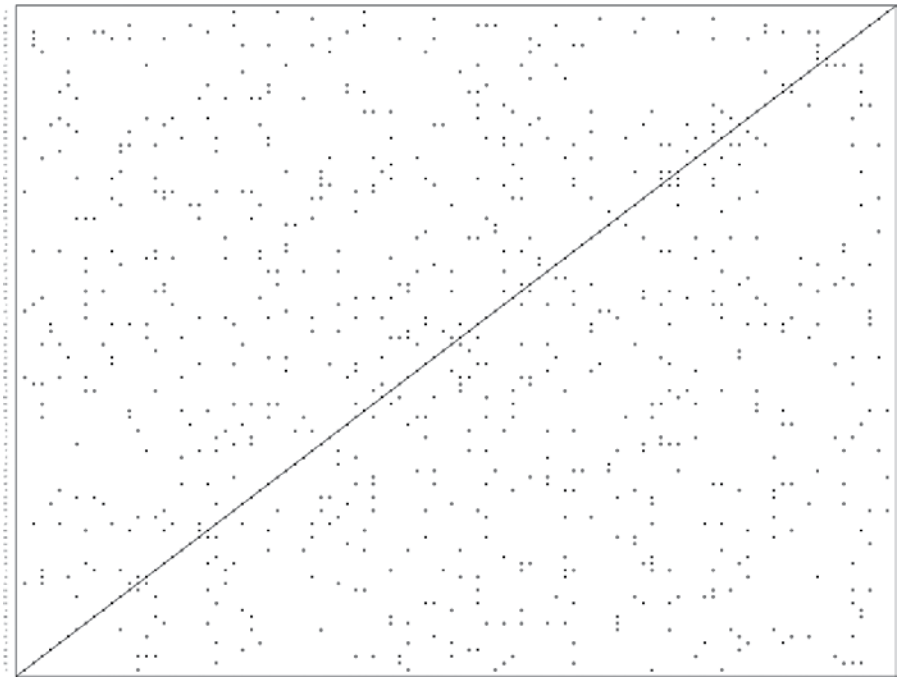

Figure 1B. Spearman coefficient result when presented with randomly generated data. 100 taxa and 1000 characters were used in this analysis.

and B were given a pattern that varied in strength as described above. Both methods performed poorly, when the number of taxa was equal to or greater than the number of characters, which is unsurprising. However, the Spearman method always produced much more noise than the Pearson method in this scenario (See Figure 2a and 2b for an example)[1].

When 50 characters were used, the Pearson method detected the pattern when it was fifty percent of the dataset and characters were more than the number of taxa (Figure 3a). The Spearman method never successfully detected the pattern with no noise (Figure 3b). In fact, when only one pattern was used, the Spearman method never successfully separated the pattern from the random background noise.

When 100 characters were used, the Pearson method again successfully detected the pattern at the ten and twenty taxa levels when the pattern reached 50% of the total characters. When 200 characters were used, the Pearson method successfully detected the pattern at the 50% mark for the 10, 20, and 50 taxa levels (Figure 4a). It also successfully detected the pattern when the pattern was only 25% strength, and 50 taxa were used. When 500 and 1000 characters were used, the Pearson method always discovered the pattern at the 50% mark, regardless of how many taxa were included. The Spearman method never successfully detected the pattern (Figure 4b).

Two Patterns

For this test, an additional pattern was introduced into the dataset. Taxa C and D were given a pattern that was equal in strength, but completely discontinuous from Taxa A and B's pattern. Again, both methods performed poorly when the number of taxa was greater than or equal to the number of characters. As before, the Spearman method performed much worse in this area than the Pearson method, recording much higher false positives and negatives (Figure 5a and b).

When 50 characters were used, the Pearson method and the Spearman method both found the patterns at the 10 taxa level with 50% strength of pattern and the Spearman method even found discontinuity between the groups (Figure 6a). However, when more taxa were introduced, the Spearman method began producing noise (Figure 6b). The Pearson method however, successfully recovered the pattern at the 20 taxa level when the pattern was 40% of the dataset or stronger. At the 100 character level, the Spearman method does not find either pattern without noise. By contrast, the Pearson method finds both patterns at the 30% range and above when 50 taxa or less are used. At the 200 character level, the Spearman method again failed to detect the patterns without noise. The Pearson method was successful at detecting the pattern at the 50% strength

1 Note that all results are not shown as there are too many to fit in an article. Those selected should serve as examples. If a reader wishes to duplicate these result, they are welcome to contact the author for assistance should it be required.

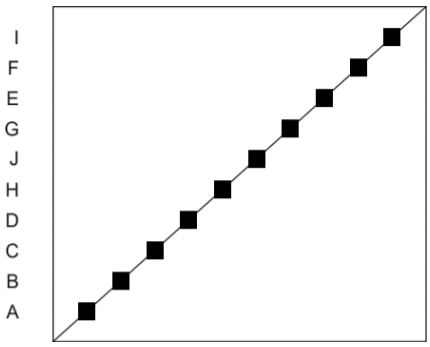

Figure 2A. Pearson coefficient result when presented with randomly generated data. Ten taxa and fifty characters are used for this analysis.

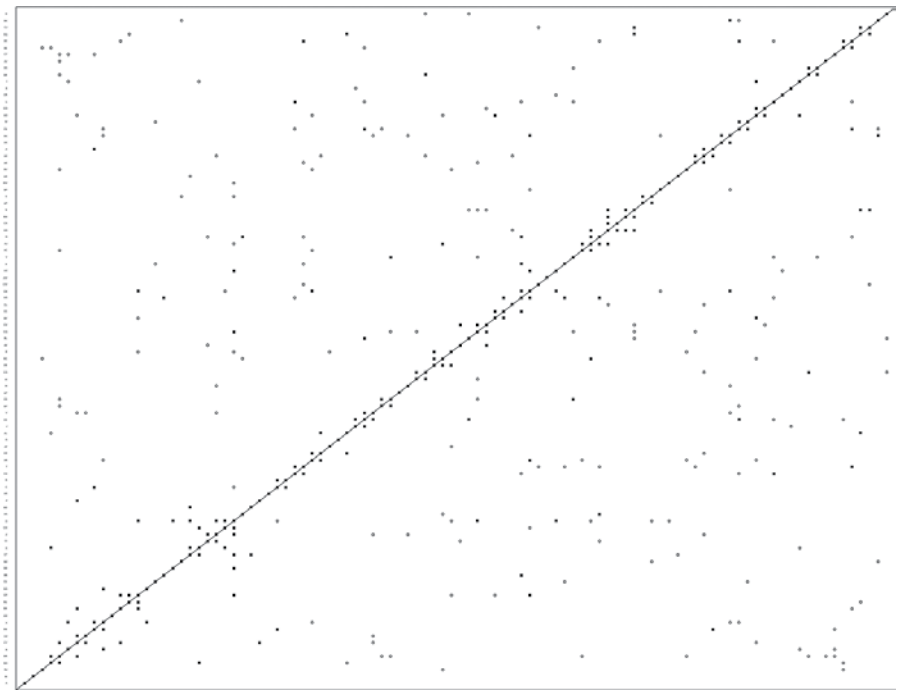

Figure 2B. Pearson coefficient result when presented with randomly generated data. 100 taxa and 1000 characters were used in this analysis.

mark when up to 50 taxa were used and successfully detected the pattern at 25% strength when 50 taxa were used. At the 500 character level, the Spearman method fails to find the patterns through the noise. The Pearson method results are similar to the 200 character level except they now find patterns at the 50 and 100 taxa level with 20% strength and above, and find the patterns at the 40% level no matter what the taxa number. At 40% strength, the Pearson method also sometimes finds appropriate discontinuity between the groups at the 50 taxa and above level. At the 1,000 character level, a very similar pattern was held. The Spearman method could not find the patterns without noise and at the 50% level, the

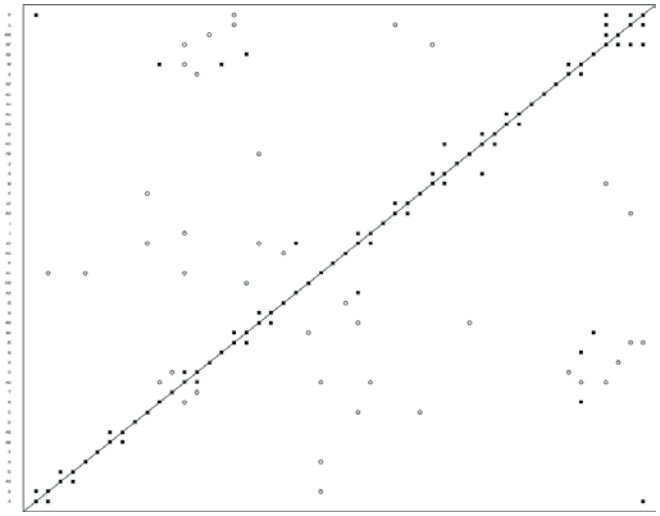

Figure 3A. Pearson coefficient result when presented with a single two taxa pattern. 50 characters and 50 taxa were used for this analysis.

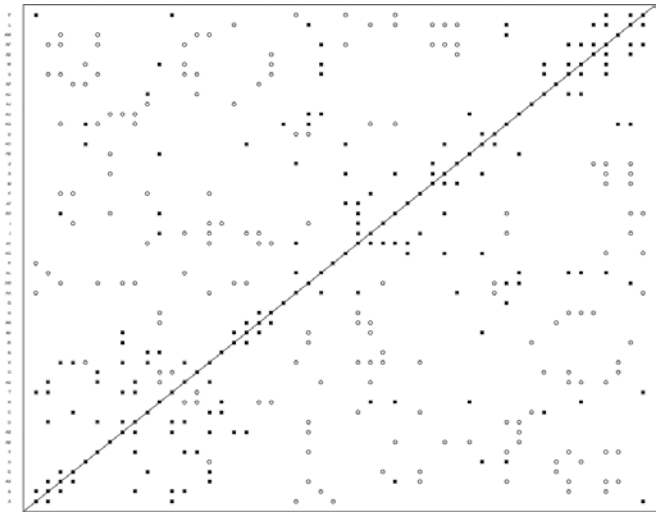

Figure 3B. Spearman coefficient result when presented with a single two taxa pattern. 50 characters and 50 taxa were used for this analysis.

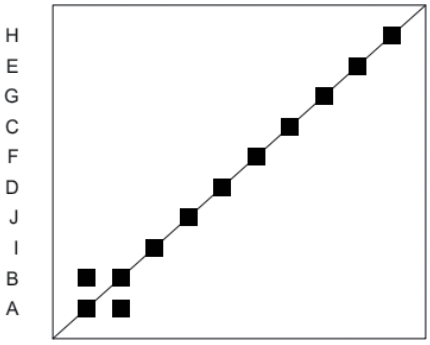

Figure 4. Pearson coefficient result when presented with a single two taxa pattern. 50 characters and 10 taxa were used for this analysis. Strength of pattern was 50%.

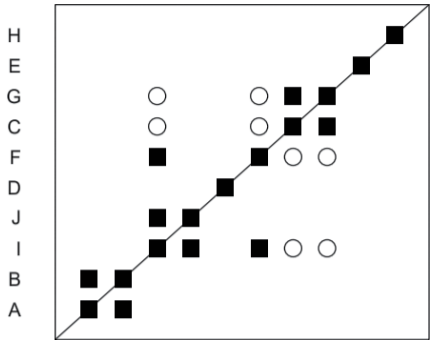

Figure 5. Spearman coefficient result when presented with a single two taxa pattern. 50 characters and 10 taxa were used for this analysis. Strength of pattern was 50%.

Pearson method always was able to detect the pattern. At 50 or more taxa, 20% was enough to detect the pattern.

Three Taxa Pattern

To test whether the prevalence of the pattern had any role in the Pearson method and the Spearman method successfully detecting patterns, a single pattern of three taxa, A, B, and C, was introduced into the dataset. As before, the pattern varied in strength depending both on the number of characters used and the number of taxa tested.

As in the previous single pattern scenario, the Spearman method never successfully detected the pattern without also detecting background noise. In some cases, the Spearman method was all noise, failing to distinguish the pattern at all. This outcome was most common at high numbers of taxa and characters.

The Pearson method performed significantly better. At the 50 character level, the Pearson method detected the pattern at the 50% level when ten and twenty taxa were used, and the 40% level when twenty taxa were used. As before, when characters were at less than 2:1 ratio to taxa, the Pearson method produced statistical noise, though not in the same quantities as the Spearman method.

At the 100 character level, 50% strength of pattern allowed the Pearson method to pick up on the pattern at the 10 and 20 taxa levels. This was also true at the 200 character level, with the pattern also being detected at the 50 taxa level. At the 500 character level, 50% strength of pattern was detected in all taxic levels. At the 20% strength of pattern level, the Pearson method detected the pattern from 20 taxa upwards (Figure 7). As before, 50% strength of pattern allowed for pattern detection for all taxic numbers at the 1,000 character level and 25% strength

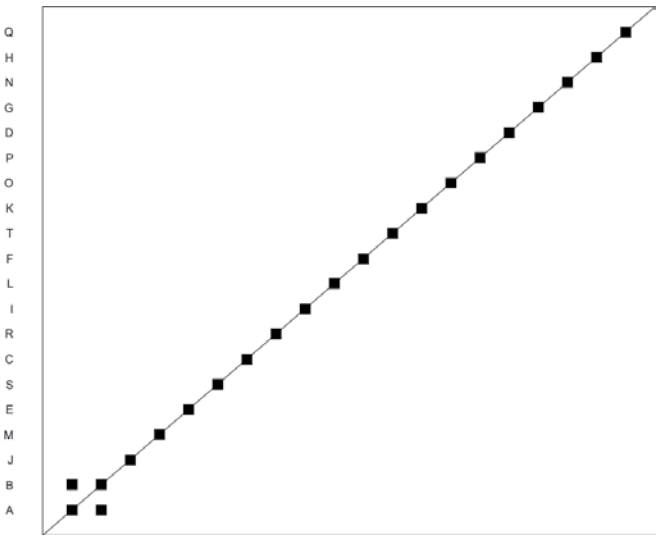

Figure 6A. Pearson coefficient result when presented with a single two taxa pattern. 200 characters and 20 taxa were used for this analysis. Strength of pattern was 50%.

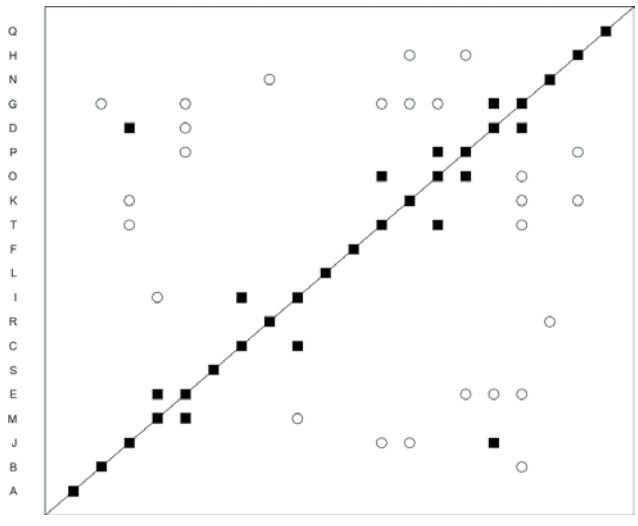

Figure 6B. Spearman coefficient result when presented with a single two taxa pattern. 200 characters and 20 taxa were used for this analysis. Strength of pattern was 50%.

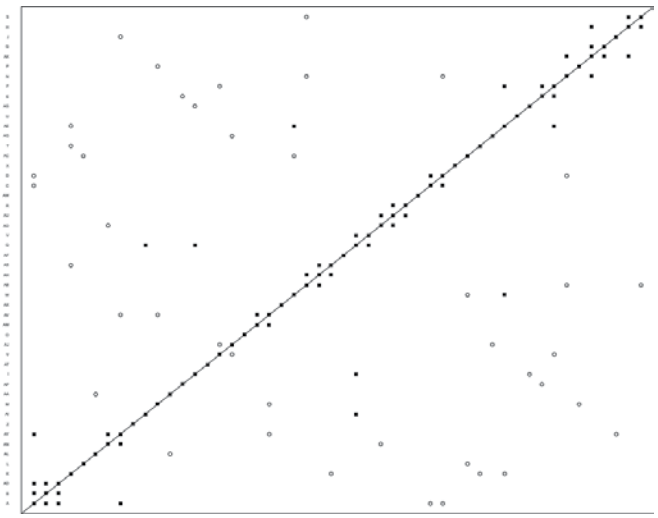

Figure 7A. Pearson coefficient result when presented with two, two-taxa patterns. 50 characters and 50 taxa were used for this analysis. Strength of pattern was 50%.

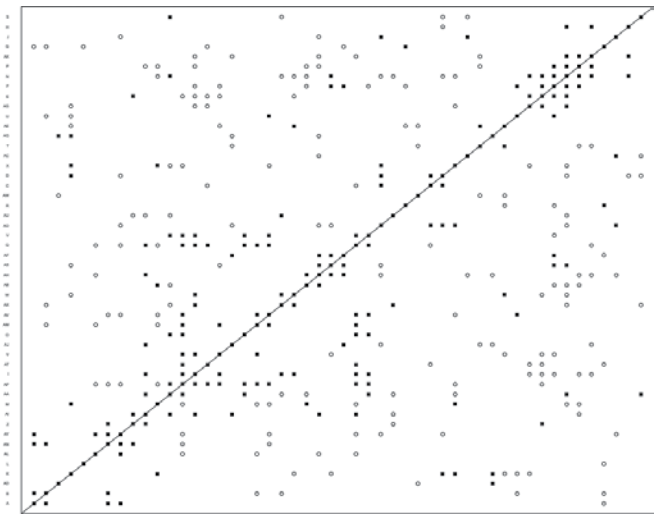

Figure 7B. Spearman coefficient result when presented with two, two-taxa patterns. 50 characters and 50 taxa were used for this analysis. Strength of pattern was 50%.

of pattern was enough at the 50 and 100 taxic levels.

Two 3 Taxa Patterns

To test if prevalence and number of patterns had an effect on the Pearson method and the Spearman method outcomes, two patterns, A, B, C and D, E, F were introduced into the dataset. The introduced patterns were discontinuous with one another and, as before, varied in strength depending on the number of characters and taxa used in the analysis. They are meant to represent two internally continuous, externally discontinuous patterns. They could potentially be holobaramins, but, as discontinuity was ignored (unless it appeared where continuity should be), it cannot be stated definitely.

The Spearman method was able in this scenario to detect the two patterns, but only did so without noise twice out of twenty different scenarios. One time was with 10 taxa, 50 characters, and a 50% pattern strength. In that same scenario, the Pearson method also detected the two patterns, but the Spearman method detected more expected discontinuity (Figure 8a and 8b). The second was at 1,000 characters, 10 taxa, with 25% strength of pattern. Given it failed at the 50% strength of pattern, this result is probably a result of random variation in the dataset as characters randomly changed to strengthen or reduce patterns.

The Pearson method outperformed the Spearman method again in this scenario. At the 50 character level, it correctly determined the patterns at the 50% strength of pattern for the 10 and 20 taxa level and at 40% for the twenty taxa level. Above that, as before, was simply no

At the 100 character level, 50% matching was required for the Pearson method to detect the patterns without noise at the 10 and 20 taxa level. These results carried over into the 200-character level but extended to the 50 taxa level. Further, at the 50 taxa level, 25% strength of pattern was enough for the Pearson method to correctly determine patterns. At the 500-character level, the results were similar. All taxa numbers detected the pattern at 50% strength of pattern and the 50 and 100 taxa levels also detected the pattern at 20% strength of pattern. At the 1,000 taxa level, 50% strength of pattern allowed the pattern to be detected across all taxa numbers tested. Further, 25% strength of pattern was enough from 50 taxa upwards.

3 Patterns 3 Taxa

As a final test, 3 patterns, A,B,C, D,E,F, and G,H,I, were introduced into the dataset. At the ten taxa level, this is equivalent to three groups with an outgroup, something not uncommon in real biological data so this test may be regarded as the closest to an actual dataset. As before, strength of pattern varied with the number of characters and taxa used in the analysis. As before, the Spearman method performed poorly in this test. The Pearson method performed much better as in previous experiments, provided the ratio of character to taxa was kept 2:1 or higher. At the 50 character level, it correctly determined the patterns for the 10 (Figure 9) and 20 taxa levels at 50% strength of pattern, as well as 40%

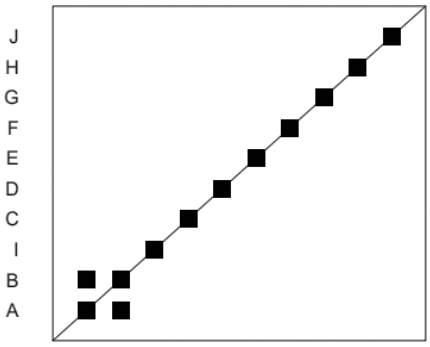

Figure 8A. Pearson coefficient result when presented with two, two-taxa patterns. 50 characters and 10 taxa were used for this analysis. Strength of pattern was 50%.

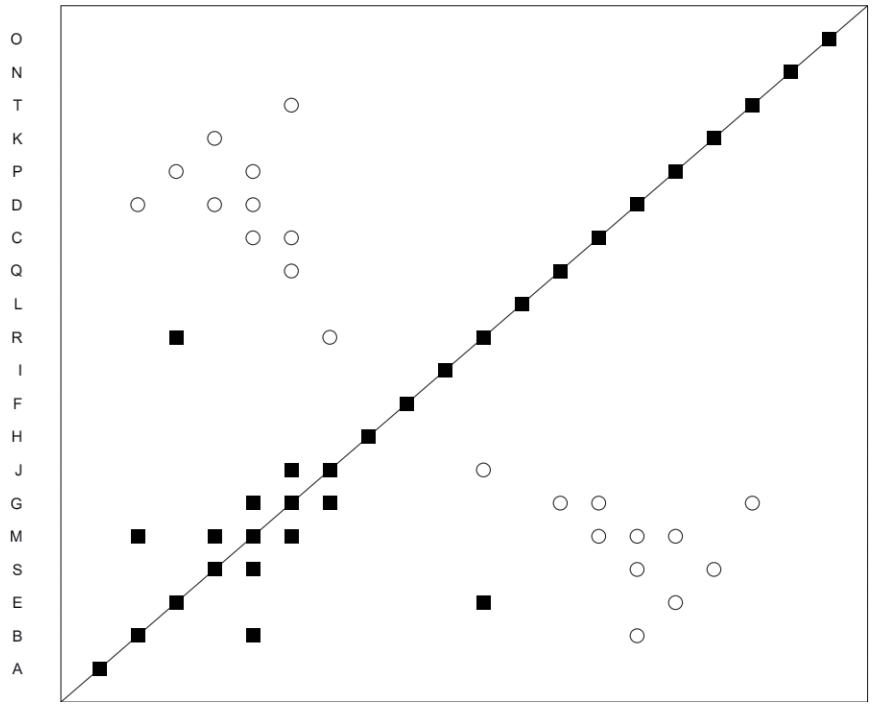

Figure 8B. Spearman coefficient result when presented with two, two-taxa patterns. 50 characters and 20 taxa were used for this analysis. Strength of pattern was 50%.

strength of pattern at the 20 taxa level. The Spearman method includes the outgroup taxa J as part of one of the groups (Figure 10).

At the 100 character level, The Pearson method successfully detected the pattern at 50% strength of pattern up to the 50 taxa level. At 30% strength of pattern, it detected the pattern at the 20 and 50 taxa level. At the 200 character level, 50% strength of pattern was required to detect the pattern up to the 50 taxa level. At 500 characters, 50% strength of pattern was required to detect patterns at all taxic levels. However, 20% was enough at 50 taxa and above. At 1,000 characters, the same was true but, instead of 20%, 25% strength of pattern was enough to detect the pattern when the taxa numbers were 20 and above.

100% strength

Just to ensure that it was possible to get a correct answer, both the Pearson method and the Spearman method were given a 100% strength of pattern for two taxa, two pairs of taxa, three taxa, and two trios of taxa at the ten taxa, 100 character level. The same pat-

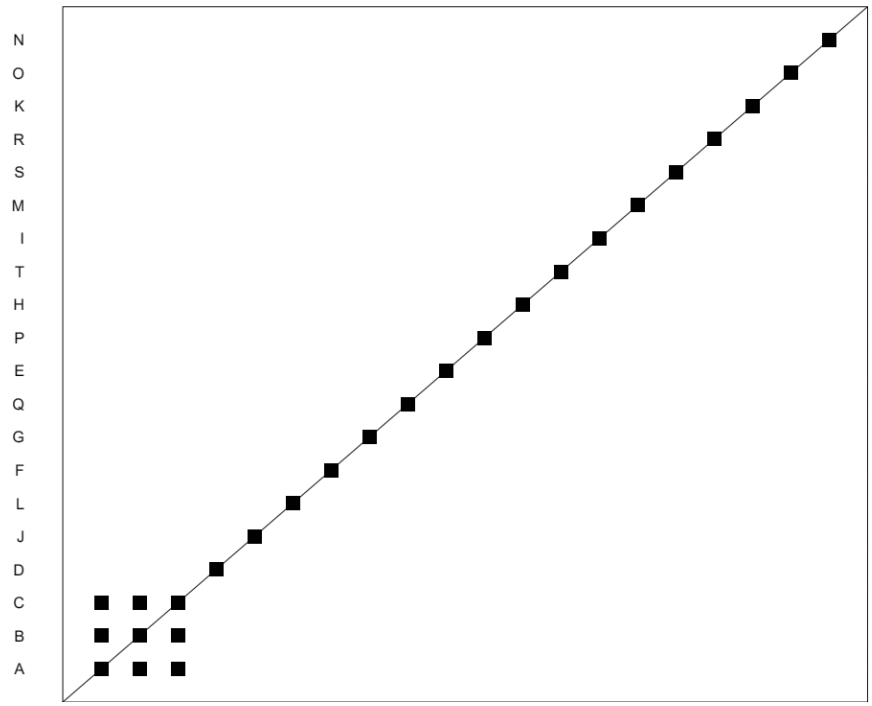

Figure 9. Pearson coefficient result when presented with one three-taxa patterns. 500 characters and 20 taxa were used for this analysis. Strength of pattern was 40%.

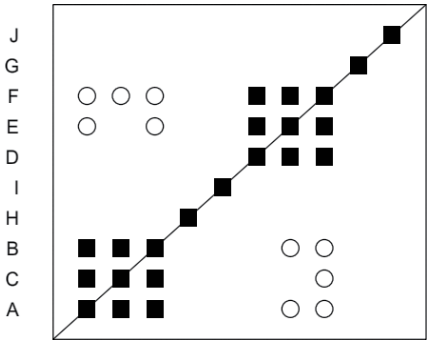

Figure 10A. Pearson coefficient result when presented with two, three-taxa patterns. 50 characters and 10 taxa were used for this analysis. Strength of pattern was 50%.

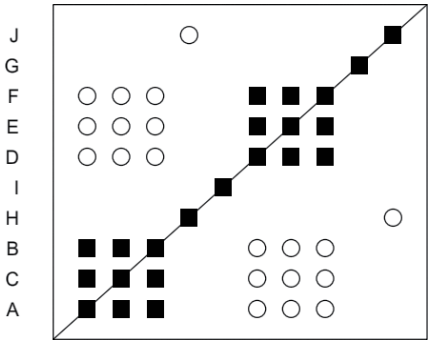

Figure 10B. Spearman coefficient result when presented with two, three-taxa patterns. 50 characters and 10 taxa were used for this analysis. Strength of pattern was 50%.

tern as before was followed. A,B was the first pattern introduced, then C,D was added. For three taxa, the groups were A,B,C and D,E,F. The Pearson method passed every test (Figures 11, 13, 15, 17). The Spearman method failed every test (Figures 12, 14, 16, 18). Even when given a 100% strength of pattern, the Spearman method failed to correctly distinguish pattern from noise. In some cases the Spearman method found whole groups that were not present in the data. In others, it joined outgroups to existing groups. By contrast, the Pearson method successfully found the patterns on every occasion. This evidence alone should be enough to cause concern about the Spearman method coefficient.

Performance Analysis: The Spearman Method

Wood (2020) introduced the Spearman method coefficient into baraminology and performed studies that demonstrated it produced comparable results to the Pearson method. Those results may be correct, but only on a classification level. The actual distance matching between taxa is much different as has been shown above. It is important to point out that the datasets Wood used are unknowns. We do not know the correct answers. That is why simulated data is so useful. The correct answers are known before the tests are run.

The Spearman method performed poorly when attempting work with datasets where correct answers are known. Even when strength of pattern was very weak and matching was not expected (0.5%) (i.e., 5 matching characters per 1,000 characters), the Spearman method always found patterns. Of the 520 tests run during this simulation, the Spearman method correctly reported the patterns without noise, false positives or negatives, or missing connections just 5 times. Every time it did so, ten taxa were in use, along with a small number of characters, usually 50. These facts would seem to indicate that the Spearman method coefficient is inefficient at baraminological analysis and should be immediately withdrawn from use as results obtained using it are likely inaccurate. If use must be made of it, limiting it to small datasets, with few taxa and characters is probably best as it seems to perform best in those circumstances.

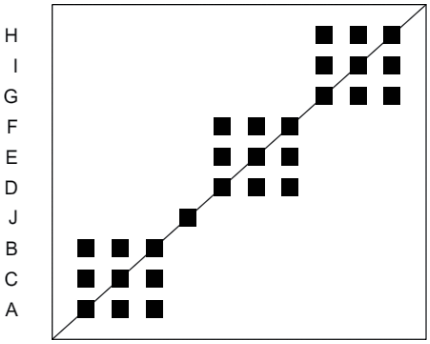

Figure 11. Pearson coefficient result when presented with two three-taxa patterns. 50 characters and 10 taxa were used for this analysis. Strength of pattern was 50%.

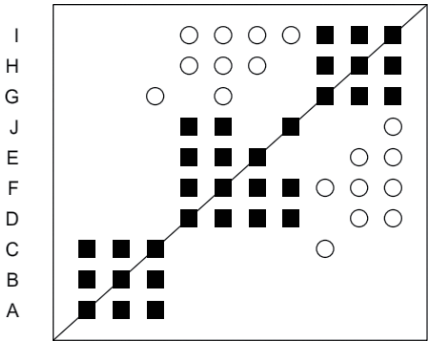

Figure 12. Spearman coefficient result when presented with two three-taxa patterns. 50 characters and 10 taxa were used for this analysis. Strength of pattern was 50%.

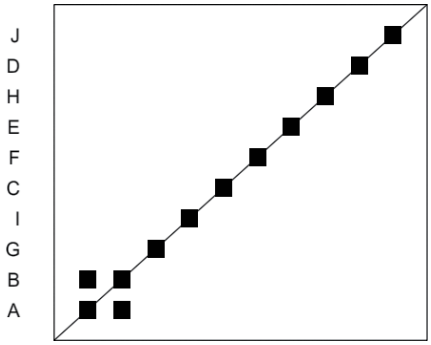

Figure 13. Pearson coefficient result when presented with one, two-taxa pattern. 100 characters and 10 taxa were used for this analysis. Strength of pattern was 100%.

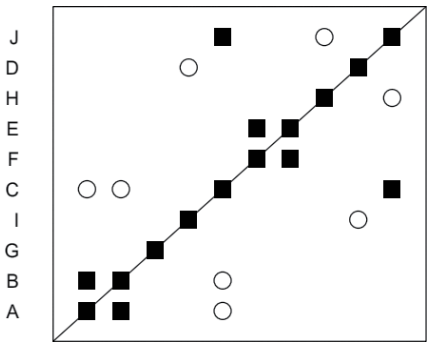

Figure 14. Spearman coefficient result when presented with one, two-taxa pattern. 100 characters and 10 taxa were used for this analysis. Strength of pattern was 100%.

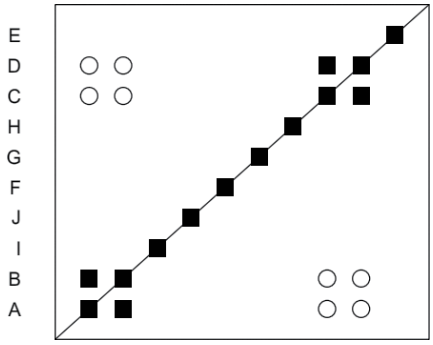

Figure 15. Pearson coefficient result when presented with two, two-taxa patterns. 100 characters and 10 taxa were used for this analysis. Strength of pattern was 100%.

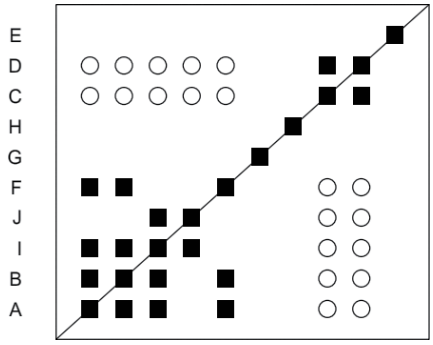

Figure 16. Spearman coefficient result when presented with two, two-taxa patterns. 100 characters and 10 taxa were used for this analysis. Strength of pattern was 100%.

Performance Analysis: The Pearson Method

The Pearson method coefficient (aka the Pearson correlation coefficient) has been criticized recently (Reeves, 2021a, 2021b) which prompted Wood (2020) to release BARCLAY incorporating the Spearman method coefficient. While Reeves's criticisms are fair and well-argued, the proposed cure seems much worse than the disease. Of the 520 tests run in this simulation, 123 times the Pearson method correctly identified the pattern without noise, false positives or negatives or missing connections. That number looks even better if the 15 times (of 20) the Pearson method coefficient correctly found no pattern in purely random data are added in. 138 correct answers out of 520 is much better than 5 out of 520. The strength of pattern both methods could detect was unknown and therefore very weak patterns were used as a baseline and increased up to 50%. Therefore, while 520 tests were done, many of those were expected to not detect patterns and, in many cases, the Pearson method did not produce patterns. In fact, only 126 times of 520 was noise present, compared to 515 times for the Spearman method. Noise was typically only present when the character to taxa ratio dropped below 2:1 in the Pearson method.

Further, the Pearson method correctly determined patterns at all taxic levels and all character counts. However, strength of pattern could be weaker at higher character and taxa counts and still be determined. When taxa counts increased individually, weaker patterns could be detected. This was also true of character counts. Therefore, the Pearson method seems to perform best when character and taxa counts are maximized. However, since no question marks were in the data to simulate absent values, it is impossible to know how the datasets would react to lower character relevance that might be required to increase taxa and character counts. This is an area where further research is required.

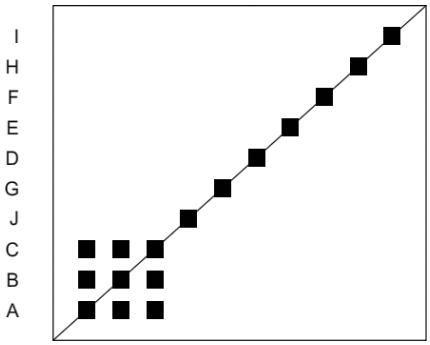

Figure 17. Pearson coefficient result when presented with one, three-taxa pattern. 100 characters and 10 taxa were used for this analysis. Strength of pattern was 100%.

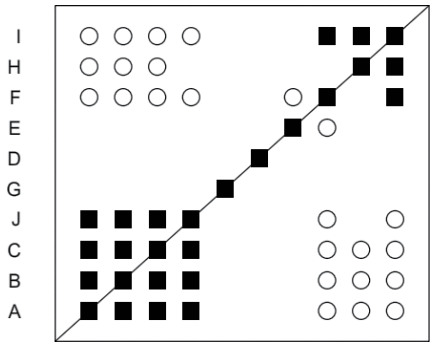

Figure 18. Spearman coefficient result when presented with ones, three-taxa pattern. 100 characters and 10 taxa were used for this analysis. Strength of pattern was 100%.

Future

The Pearson method tests should ensure the character to taxa ratio of 2:1 is used when selecting datasets. If the ratio of characters to taxa is allowed to drop below that level, noise is almost

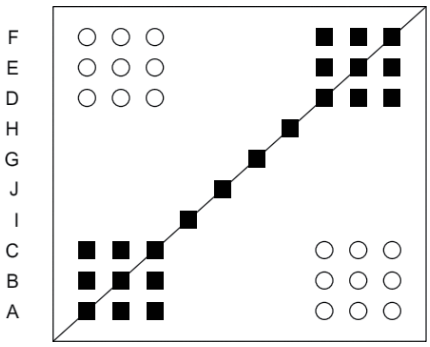

Figure 19. Pearson coefficient result when presented with two, three-taxa patterns. 100 characters and 10 taxa were used for this analysis. Strength of pattern was 100%.

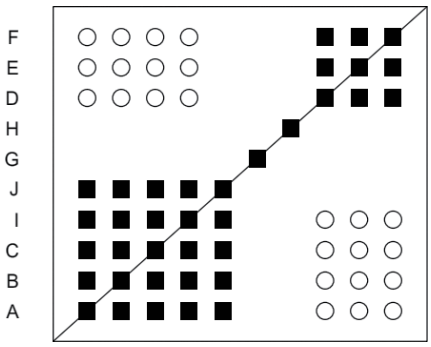

Figure 20. Spearman coefficient result when presented with two, three-taxa patterns. 100 characters and 10 taxa were used for this analysis. Strength of pattern was 100%.

always introduced into the results. Keeping the ratio at 2.5:1 or higher is probably optimal as in some cases even 2:1 produces noise. The 2.5:1 ratio was the lowest ratio that did not produce statistical noise in random data. If the character to taxa ratio is maintained above 2:1, then a strength of pattern of 60% or higher should reveal the correct patterns in most scenarios. However, lower strengths of pattern will work if the character and taxa counts are high enough. Generally, this means 50 taxa and at least 200 characters, which is not always feasible in real datasets. Lower numbers of taxa reduce strength of pattern required, if there are enough characters, usually 500 or more. Importantly, maintaining high levels taxa and characters should be done without lowering taxic or character relevance as neither of these parameters was tested in this study and thus changing them may have unknown effects on study results.

Conclusions

BARCLAY and BDISTMDS are popular with many in the statistical baraminological community because they are easy to use and produce relatively easy to interpret results. However, this basic simulation study produces some concerning results. When using the Spearman method coefficient, statistical baraminology is very unreliable, producing a correct result less than one percent of the time. Because the Spearman method coefficient results are riddled with false continuity and discontinuity, it should be considered unreliable as a method. The Spearman method coefficient, whatever statistical promise it may have brought to the table, must be abandoned. The Pearson method coefficient, however, shows much better results. While the Pearson method coefficient is open to question and may need to be replaced, it is significantly better than the current alternative. For those who wish to practice statistical baraminology, the Pearson method coefficient should be the preferred method for now as the alternative is currently unworkable.

References

Kaufman, L., and P.J. Rousseeuw. 1990. *Finding Groups in Data*. John Wiley & Sons, New York, NY.

Robinson, D.A., and D.P. Cavanaugh. 1998. A quantitative approach to baraminology with examples from the catarrhine primates. *Creation Research Society Quarterly* 34(4):196–208.

Reeves, C.R. 2021a. A critical evaluation of statistical baraminology: Part 1—Statistical principles. *Answers Research Journal* 14:261–269.

Reeves, C.R. 2021b. A critical evaluation of statistical baraminology: Part 2—Alternatives and conceptual and practical issues. *Answers Research Journal* 14:271–282.

Sanders, H., and M. Cserhati. Statistics, baraminology, and interpretations: A critical evaluation of current-morphology-based baraminology methods. *Creation Research Society Quarterly* 58:175–192

Sokal, R.R., and P.H.A. Sneath. 1973. *Numerical Taxonomy*. W.H. Freeman & Co., San Francisco, CA.

Winsor, M.P. 1994. "The Lessons of History." In *Models in Phylogeny Reconstruction*. Scotland, R.W., D.J. Siebert, and D.M. Williams (editors). Clarendon Press, Oxford, UK.

Wood, T.C. 2001. *BDIST Software, v1.0*. Center for Origins Research and Education. Bryan College, Dayton, TN. Distributed by the author.

Wood, T.C. 2005. Visualizing baraminic distances using classical multidimensional scaling. *Origins (GRI)* 57:9–29.

Wood, T.C. 2008. Baraminic Distance, bootstrap, and BDISTMDS. *Occasional Papers of the BSG* 12:1–17.

Wood, T.C. 2011. Baraminology, the image of God, and *Australopithecus sebida*. *Journal of Creation Theology and Science, Series B: Life Science* 1:6–14.

Wood, T.C. 2020. Expanding the toolkit of statistical baraminology with BARCLAY: baraminology and cluster analysis.

Wood, T.C. 2021. Baraminology by cluster analysis: A response to Reeves. *Answers Research Journal* 14:283–302.

Wood, T.C., K.P. Wise, R. Sanders, and N. Doran. 2003. A refined baramin concept. *Occasional Papers of the BSG (Baraminology Study Group)* 3:1–14.

Creation Research Society Quarterly 2024 61:112–132

The North American Midcontinent and the Genesis Flood

Part I: Mapping Surfaces

John K. Reed, Michael J. Oard, Peter Klevberg

Abstract

Maps of diluvial boundaries for the North American midcontinent are presented by state and by sedimentary basin. The upper diluvial boundary is the base of Ice Age sediments. For most of the study area, the basal diluvial boundary is the erosional unconformity between Precambrian crystalline rock and the Phanerozoic sedimentary record. The exceptions are Proterozoic to Cambrian rifts: the Midcontinent, East Continent, Fort Wayne, Reelfoot, Rough Creek Graben, and Rome Trough rifts. These are remnants of severe crustal disruption at the onset of the Flood, with varying ratios of volcanic and sedimentary fill. This paper focuses on the basal marine diluvial boundary and the upper diluvial boundary, excluding the rifts, showing the volume and distribution of sediments of the Ice Age. Deep Proterozoic rifts will be addressed in Part II. Detailed state maps of the basal diluvial boundary are shown in the appendix. Maps of the study area reveal cratonic basins of varying size, show a thickening of diluvial strata toward the south, and show the extent of Ice Age deposition. All these aid in understanding the work of the Flood in this region.

Key Words: Early Flood, Illinois Basin, Michigan Basin, Midcontinent, Precambrian, sedimentary basin, Williston Basin

Introduction

Scripture and science tell us that the Flood was a catastrophic global event. Details of these processes in any given locale are open only to forensic investigation and could include: vertical and horizontal tectonics, overthrusting, the formation of rifts and sedimentary basins, powerful earthquakes, huge tsunamis, volcanism, impacts, and associated erosion, transport, and deposition, which included the burial of trillions of organisms. Many geological questions confront an understanding of the Genesis Flood, and skeptics challenge us on these issues.

One of the most basic products of the Flood is the sedimentary record. Sediments raise may questions. How much sediment exists on the continents

* Accepted for publication May 13, 2024

today? How much sediment is in the oceans? How much ocean sediment was eroded off the continents? How much of the record is from the Flood? How much sediment accumulated on the continents at the peak of the Flood, approximately 150 days (Boyd and Snelling, 2014)? Where did this sediment originate? How was it transported?

The Flood Sediment Research Project

In order to answer the above questions and spur research, we have started the *Flood Sediments Research Project*. This is primarily a mapping project because we consider maps to be the language of geology. Thanks to the GlobSed project, we have a good estimate of the sediments in the oceans (Reed et al, 2022). The GlobSed goal was to map the distribution and thickness of ocean sediments. A rough estimate for the total sediment thickness and volume for the ocean sediments was published in 2003 and in 2013. These two attempts contained uncertainties that were addressed by Straume et al. (2019). Version 3 of GlobSed (Straume et al., 2019) increased the projected volume of oceanic sediments by an astounding 29.7% over earlier versions. New data for the northeast Atlantic, the Mediterranean Sea, and the Arctic and Antarctica continental margins were largely responsible for this change.

The next logical step is to determine the volume and distribution of continental sediments and to link that to continental margin sediments (GlobSed maps stop at the coastlines) to assess Flood runoff. One challenge is to map at a sufficient level of detail relative to the available data. Once complete, we can better estimate the amount of sediment eroded and transported from somewhere onto the continents and try to assess its place in the Flood. Several wide-ranging estimates have been made in the past (Reed et al., 2022). Clarey (2020) has compiled sediment thickness, but he used oceanic sediments from the margin and some Precambrian sediment. Therefore, we have concluded that we need to do our own estimate of continental sediments. We are mapping on a state-by-state level because state sources best provide a sufficient level of detail without becoming overwhelmed by data. States provide well data, some seismic profiles, gravity data, and reports and maps by local experts. Using these data, we compile GIS maps of the lower and upper diluvial boundaries which yield volumes for basins, states, or any other geographic boundary. Colorado served as a pilot study (Reed et al., 2023). Of course, data quantity and quality vary by state. Our ultimate goals are to provide maps and volumes for North America and to develop a GIS mapping method that can easily be applied to other continents. Each state and region also provides more concrete and detailed data to support Flood models.

The Midcontinent Rift and Surrounding States

The North American midcontinent region has been geologically well studied for more than a century. Mining, oil and gas, water resource discovery and conservation, and environmental concerns have driven robust data acquisition and interpretation, and a correspondingly robust understanding of this region's surface and subsurface geology. If maps are the language of geology, then mapping within the diluvial paradigm is of utmost importance. For that reason, we present regional maps showing diluvial boundaries and derivative volumes of diluvial and Ice Age strata, as well as their distribution. The study area (Figure 1) is a broad cratonic surface, punctuated by rifting and large sedimentary basins. The North American Midcontinent Rift is the largest single feature of this study area and one of great interest to geologists. For diluvialists, it illustrates crustal disruption at the beginning of the Flood (Reed, 2000; Clarey, 2020). Though many studies continue to be published (i.e., Miller and Nicholson, 2013; Stein et al., 2015; Woelke and Hinze, 2015; Stein et al., 2016; Fairchild et al., 2017; Stein et al., 2018a, 2018b; Grauch et al., 2020; Hinze and Chandler, 2020), maps of the Midcontinent Rift are limited to its surface or bedrock (sub-glacial) two-dimensional extent, both in terms of volcanism and sedimentation. Horst-top and flanking basins have been characterized (e.g., Anderson, 1990; Jirsa et al., 2011; Woelke and Hinze, 2015), but no map of the base of the rift is available. We will present such a map in Part II, as well as integrating maps of the basement beneath the East Continent Basin, the Reelfoot Rift, the Rough Creek Graben, and the Rome Trough. Three-dimensional maps of the basal diluvial boundary of the entire study area are a prerequisite of any forensic investigation of the Flood. Crystalline basement is exposed in uplifts of the Black Hills of South Dakota and the St. Francois Mountains of Missouri. Proterozoic quartzites (Sioux, Baraboo) are also exposed in South Dakota, Minnesota, and Wisconsin. Both crystalline basement and these quartzites immediately underlie glacial sediments in large parts of Wisconsin, Minnesota, and Michigan. Otherwise, the basement is known from deeper well penetrations, seismic lines, and maps of gravity (Kucks, 1999) and magnetic anomalies (Bankey et al., 2002). In a few parts of the rifts, notably the Rough Creek Graben and Rome Trough, well penetrations are helpful, as are outcrops of the Midcontinent Rift around Lake Superior, but the Midcontinent Rift, the East Continent Basin, the Reelfoot Rift-Rough Creek

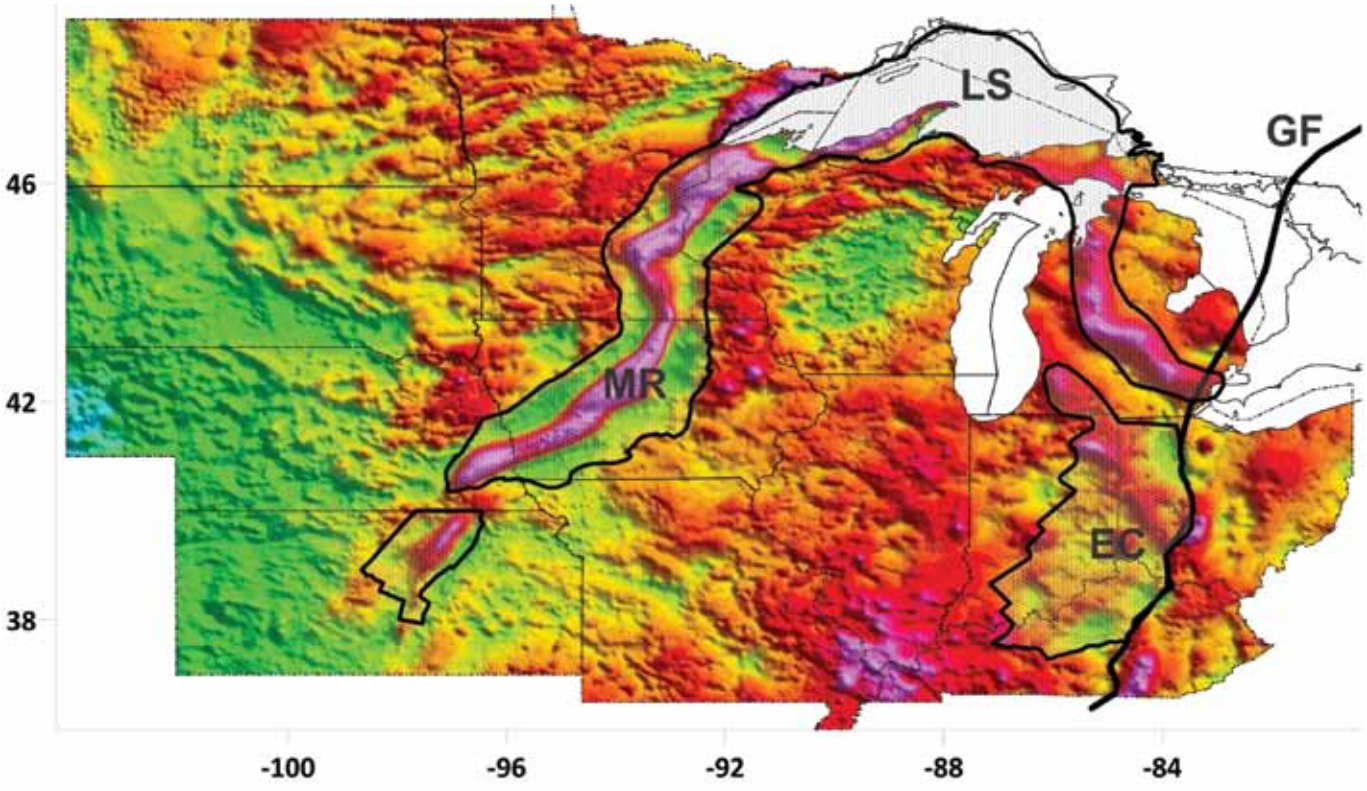

Figure 1. Study area of this paper shown on the Bouguer Gravity Anomaly map (Kucks, 1999), showing the Midcontinent Rift (MR), East Continent Basin (EC), and Grenville Front (GF). The largest, deepest part of the Midcontinent Rift is in the Lake Superior Basin (LS). Pink, purple, and red are positive gravity anomalies, while green colors are negative gravity anomalies. Notice in the MR that high gravity anomalies, representing horsts of uplifted denser rocks, are found in the center. They are surrounded by low gravity anomalies, representing sedimentary basins along the edge.

Graben, the Rome Trough, and even a proposed Illinois Graben (Freiburg et al., 2022)—are known largely by geophysical investigation.

Relationships between these rifts are discounted by secular geologists due to different dates (e.g., Drahovzal and Harris, 1998 vs. Moecher et al., 2018). Although the Midcontinent and East Continent rifts are roughly age equivalent, ~1.1 Ga, southern rifts in the study area are dated nearly 600 million years later, as Early Cambrian, in Ohio, Kentucky, and Indiana (Drahovzal et al., 1992); at the boundary of Missouri, Arkansas, Tennessee, and Kentucky (Dart, 1995; Hickman, 2011, 2013); in eastern Kentucky, West Virginia, and Pennsylvania (Drahovzal and Noger, 1995; Gold et al., 2005). Although outside the study area, the nearby Oklahoma Aulacogen (Reed, 2004) is also dated as Early Cambrian. However, a Biblical paradigm might suggest that large similar tectonic features reflecting a significant disruption of the antediluvian crust would be of similar age and related in their genetic cause.

Method

We mapped a rectangular study area (Figure 1) to show regional context and minimize gridding anomalies. It covers 13 states and a small part of Ontario. Our goal is to define three volumes: (1) Ice Age (and Recent) sediments, (2) diluvial marine strata, and (3) diluvial rift fill. These require four gridded surfaces: (1) a digital elevation model (DEM), to represent surface topography; (2) the base of glacial deposits; (3) the base of the marine diluvial; and (4) the base of the diluvial rifts (Figure 2). The volume and distribution of these stratal packages provides fundamental information about the Flood and Ice Age and facilitates volume and thickness comparisons to other regions. For the study area, diluvial marine strata are those between the Precambrian crystalline basement and the erosional unconformity underlying Ice Age sedi-

ments. Subglacial strata are commonly called "bedrock" to differentiate them from glacial sediments.

It is worth noting that the Ice Age and Recent sediments are probably reworked diluvial deposits. Using regional-scale maps and DEMs, differentiation of very thin sediments draping irregular surfaces can introduce isopach mapping and volume calculation errors. That is why we calculated Ice Age volumes and then subtracted them from the total volumes to derive the Flood totals. As will be shown, the Ice Age volumes are quite small in proportion, especially when factoring in the rift fill. Exceptions are found in Minnesota and Wisconsin, which have thin diluvial and thick Ice Age strata. Our maps (in the appendix) were developed from those published by state geological surveys, supported by publicly-available well data and published geophysical data. To a lesser degree, we use other publications from journals and state surveys, USGS sources, and dissertations. Many of the state maps were modified, often to rectify them with surrounding states.

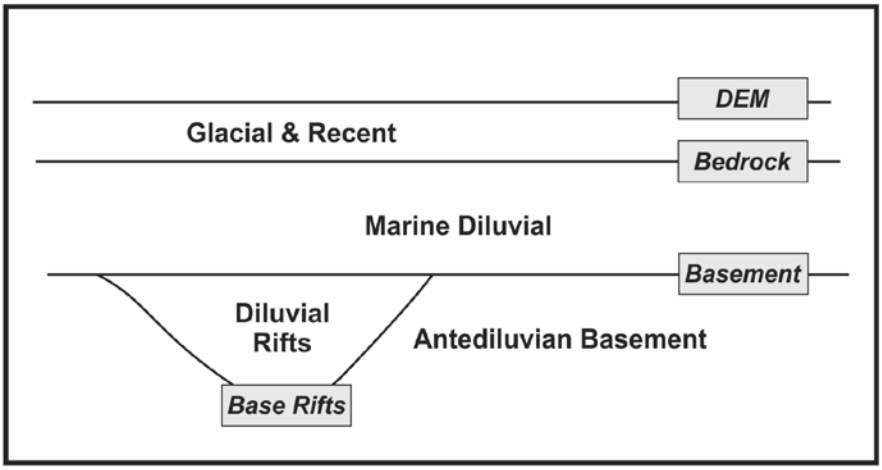

Figure 2. Schematic of three volumes to be assessed and four map horizons to define them. DEM = Digital Elevation Model (representing surface topography).

DEM

The USGS (https://www.usgs.gov/faqs/what-digital-elevation-model-dem) defines a digital elevation model (DEM) as "a representation of the bare ground (bare earth) topographic surface of the Earth excluding trees, buildings, and any other surface objects." Newer DEMs are the product of lidar, or aerial laser pulses bouncing off the ground and back to aerial sensors. These produce detailed, accurate pictures of ground topography. The level of detail is a function of the scale, representing a balance of detail and file size. Detailed DEMs are often available but unworkable at our scale due to computational limits. The extent of current data and their downloads can be found at the National Map downloader at https://apps.nationalmap.gov/downloader/. We tested three workable options: (1) NASA's Shuttle Radar Tomography Mission (SRTM) in 1 arc-second resolution, (2) NOAA's ETOPO global relief model in 15, 30, and 60 arc-second resolutions, and (3) the USGS 3-D Elevation Program (3DEP) dataset. We found that ETOPO provided similar resolution to the slower 3DEP, with fewer problems than SRTM. For finer scale work, we would recommend the 3DEP surface or DEMs from state sources. This is especially true of areas with thin or irregular sediment cover and abrupt topography.

Sub-Glacial Bedrock Surface

During the Ice Age, sediment was transported and deposited by glaciation and by associated processes, such as glacio-fluvial processes (Oard, in press). Their extent has been mapped (Figure 3) and covers much of the study area. Thicknesses rarely exceed a few hundred feet and are thin at the margins. These thicknesses are small compared to the total diluvial sedimentary record. Exceptions are found in Minnesota and Wisconsin, and beneath Lake Superior, where they exceed 1,700 ft. (518 m) per Soller and Garrity (2018) or 2,500 ft. (762 m) per Hamilton (2020). However, the average thickness over all of Minnesota is only 195 ft. (59 m). But the thin marine diluvial record makes the glacial fraction of the total sedimentary record more significant: 57% of the total in Minnesota and 19% in Wisconsin. Other states range from < 1% to 7%. Ice Age thicknesses are significant in Michigan but still small compared to the Michigan Basin fill. Once rift fill is factored in, these percentages drop precipitously. In Minnesota, they drop to 5.48%, Wisconsin, to 1.36%, and Michigan to 0.9%. The other states range from 0.09% to 4.48%. For the study area as a whole, the percentage of Ice Age sediments drops from nearly 2.66% to 1.36%. Even with mapping uncertainties, the Ice Age record is still very small.

The bedrock (Figure 4) is a rough, well-incised erosional surface, probably reflecting the post-Flood, and perhaps even Late Flood, drainage system development. Figure 4 was constructed from a variety of state sources

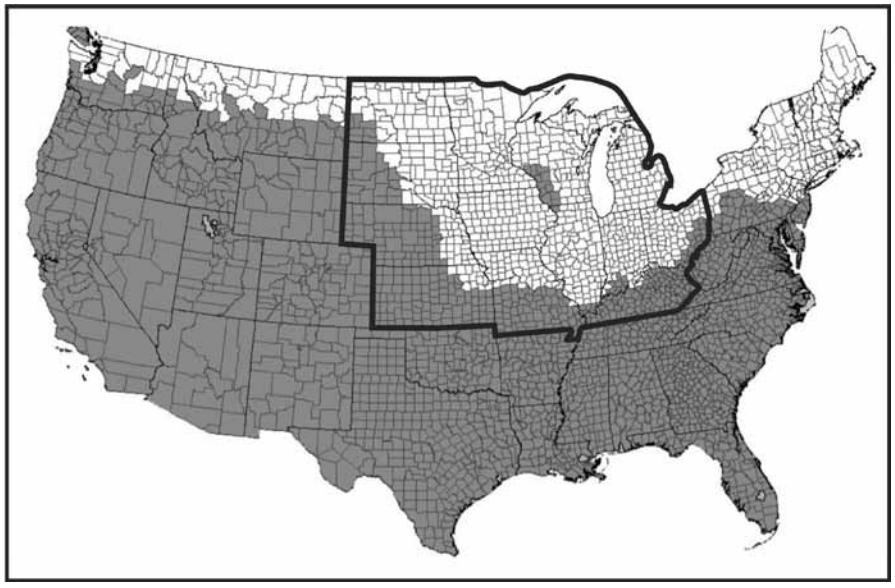

Figure 3. Glacial extent in upper Midwest. Note that every state in the study area has some Ice Age sediments. Modified from https://mapsontheweb.zoom-maps.com/post/78118597495/extent-of-glacial-ice-sheets-in-the-united-states.

(Hansen, 1972, 1973, 1975, 1978, 1985, 1986, 1992; Cagle, 1973; Gray, 1982; Hansen and Runkle, 1986; Herzog et al., 1994; Denne et al., 1998; Tomhave and Schulz, 2004; Hamilton, 2020) and sources from the USGS (Soller, 1997; Soller and Garrity, 2018). Maps from the Minnesota, Illinois, Indiana, Ohio, and South Dakota surveys are the most detailed. Michigan, Nebraska, North Dakota, and Wisconsin offer no maps, though Wisconsin is working on detailed maps at the county scale. For that reason, we used the less detailed contours of Soller and Garrity (2018) to create a unified map of the bedrock topography. A large portion of southwestern Wisconsin has no glacial sediment (note darker gray counties on Figure 3 and white area in Figure 4). The outline of this "driftless region" in Wisconsin, Minnesota, and Iowa is well-defined (Carson et al., 2023).

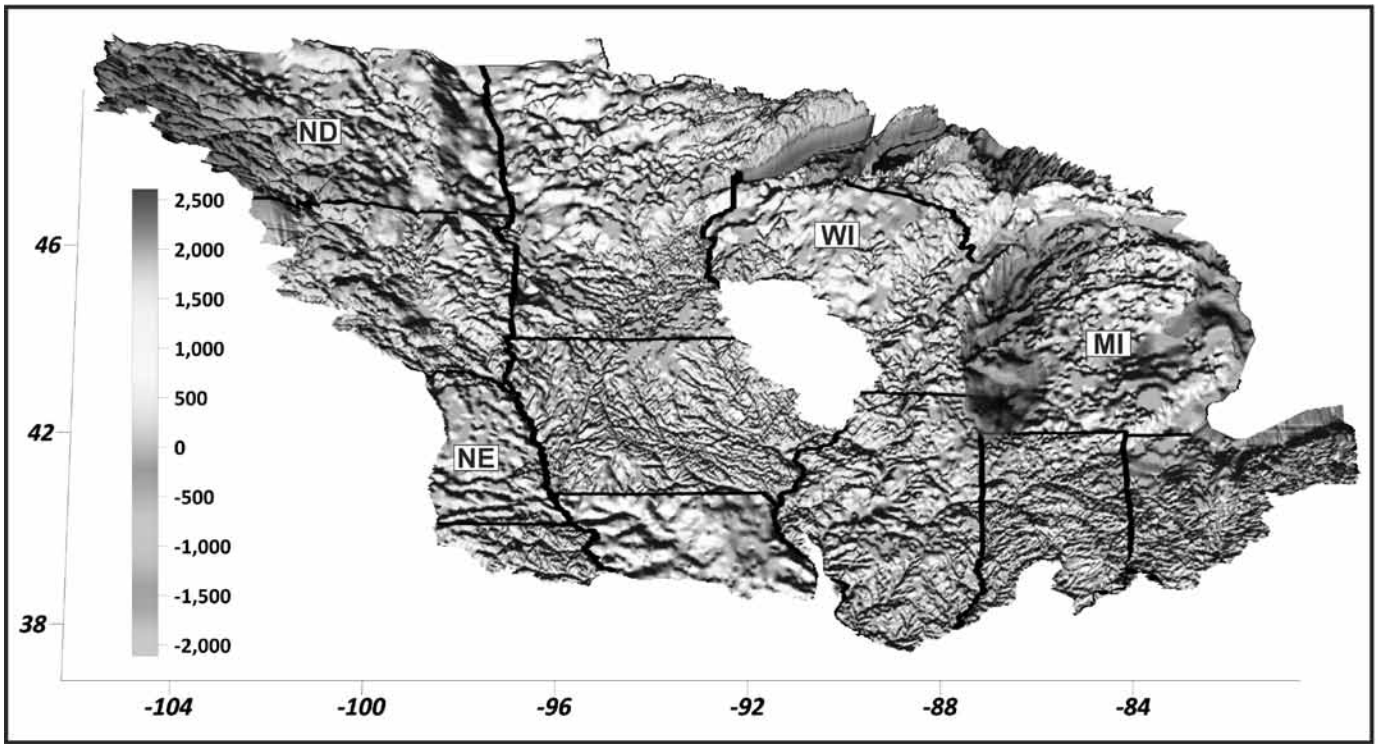

Figure 4. Bedrock topography of study area in feet asl (above sea level). Note irregular topography reflecting channelized erosion and watershed development after the Ice Age. Bedrock maps in labeled states from Soller and Garrity (2018); remainder from state geological surveys. The white area is the driftless area.

To better show the thickness and distribution of Ice Age and Recent sediments (Figure 5), we compared data from state surveys in Ohio, Illinois, Missouri, Minnesota, and North Dakota. Isopach maps of drift thickness were taken from Soller and Garrity (2018) but were compared to state survey maps from Ohio, Illinois, Minnesota, Missouri, and North Dakota. The older USGS Groundwater Atlas maps (Bluemle, 1986, 2003; Olcott, 1992; Lloyd and Lyke, 1995; Soller, 1997; Whitehead, 1997; Grimley, 2015; Hamilton, 2020; Missouri DNR, 2023; Ohio DNR, 2023) are also available for comparison. Thin, patchy glacial sediments in eight counties of northern Kentucky were ignored. Ice Age sediments seldom exceed a few hundred feet. Incised sediment-filled channels reach 800 ft. (244 m) in South Dakota. Thicknesses reach 1,400 ft. (427 m) near Itasca Park, in northwestern Minnesota, and exceed 2,500 ft. (762 m) beneath Lake Superior off Minnesota (Hamilton, 2020). Soller and Garrity (2018) show thick sections in Michigan reaching 1,000 ft. (305 m). Their thicknesses are generally in line with the state surveys, although the newer map in Minnesota (Hamilton, 2020) includes more recent data and shows thicker drift in some areas. The most significant difference was in Missouri, where their Department of Natural Resources map returned a total of 1,814 km^3, while Soller and Garrity's map (2018) only showed 1,141 km^3. The Missouri state map also showed a glaciated *area* approximately 10 percent greater than that of Soller and Garrity (2018). The southern limit of glacial sediments was derived from Soller and Garrity (2018), state survey maps, and the Ground Water Atlas. These limits were simplified in some areas where alluvial sediments stretched south of the main body of glacial sediments in narrow river valleys (e.g., Ohio).

We calculated the volumes by state and for the study area (Table I). The "grid average" is *only* for the areas actually overlain by Ice Age and Recent sediments (cf., Figure 3). That excludes parts of every state. The "state average" is that for the area of the *entire* state. Kansas and Nebraska have very low grid areas, reflecting glacial limits. Michigan and Minnesota have much greater relative coverage. Michigan has the greatest total volume, due to significant thicknesses beneath Lake Superior. The average thickness of Ice Age sediments in the study area is 86 ft. (26 m); that for the states range from 3 ft. (1 m) in Kansas to 195 ft. (59 m) in Minnesota.

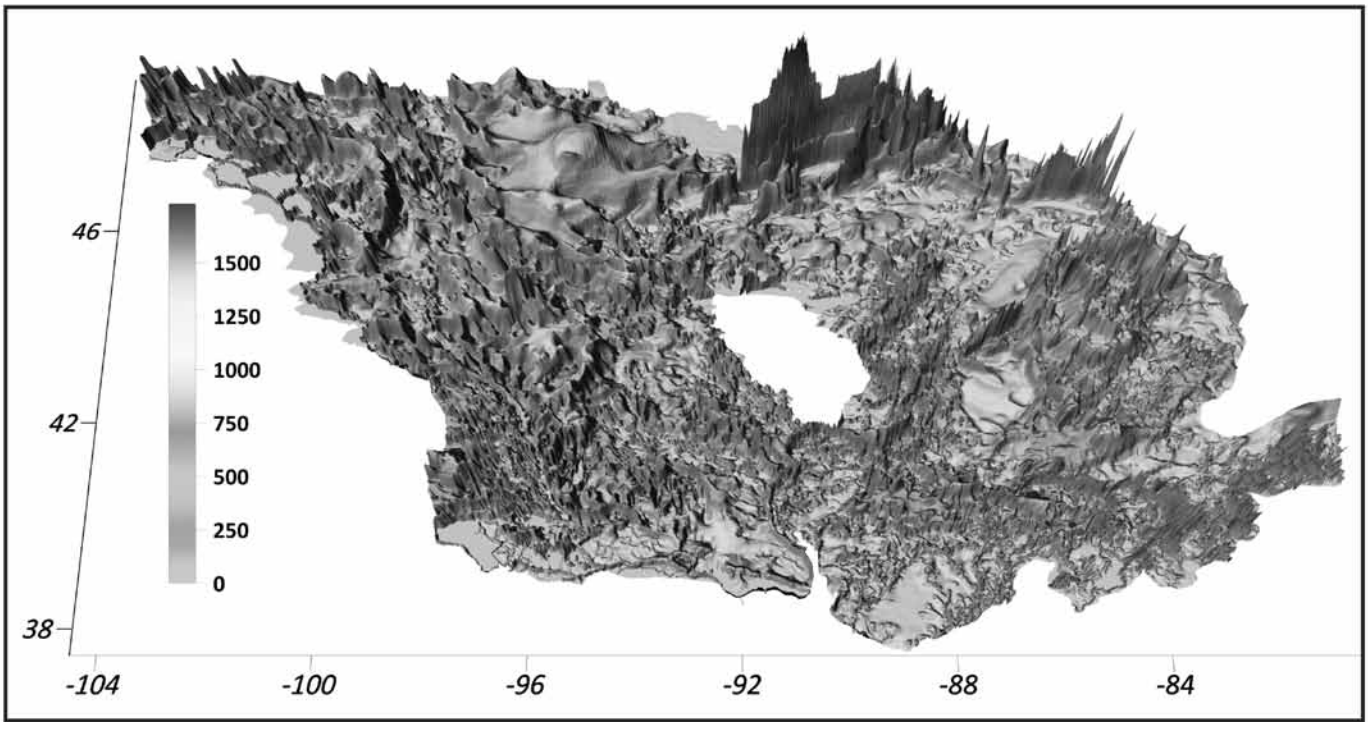

Figure 5. Thickness of glacial and Recent deposits in study area based on Soller and Garrity (2018). State boundaries distorted by overlay on 3D surface. Note maximum thicknesses beneath Lake Superior, in northwestern Minnesota and the northwestern part of Michigan's southern peninsula. For the study area, the thickness averages 86 ft. (26 m). White area is the driftless area that was never glaciated. See Table I.

Table I. Ice Age and Recent sediment volume and average thicknesses of study area. Average thicknesses are divided into the area gridded and the entire extent of the state. From Soller and Garrity (2018).

STATE	TOTAL AREA (km²)	GRID AREA (km²)	VOLUME (km³)	AVG THICKNESS GRID		AVG THICKNESS STATE	
				(M)	(FT)	(M)	(FT)
Illinois	149,995	142,330	3,744	26	86	25	82
Indiana	94,326	78,973	2,758	35	115	29	96
Iowa	145,756	136,254	6,528	48	157	45	147
Kansas	213,100	18,584	178	10	31	1	3
Michigan	250,487	248,214	13,160	53	174	53	172
Minnesota	225,163	214,957	13,378	62	204	59	195
Missouri	180,540	60,620	1,141	19	62	6	21
Nebraska	200,330	45,904	2,163	47	155	11	35
North Dakota	183,108	129,814	5,964	46	151	33	107
Ohio	116,098	87,065	1,899	22	72	16	54
South Dakota	199,729	90,625	5,498	61	199	28	90
Wisconsin	169,635	140,005	3,936	28	92	23	76
Total	2,232,918	1,393,345	60,347	43	142	26	86

The next surface is the base of the marine diluvial package, with its base at the erosional unconformity between Precambrian crystalline rocks/rift fill and the overlying Phanerozoic sedimentary sequence. Due to the irregularity of the bedrock surface (Figure 4), we derive volume and thicknesses for the entire sedimentary sequence and then subtract the Ice Age volume by state. The exception was in Minnesota, where thin, diluvial sediments and irregular topography degraded the grid differencing operation. However, Minnesota has published excellent bedrock topography and drift thickness maps (Hamilton, 2020). We used the bedrock topography map to derive the diluvial thicknesses and added the drift thicknesses of Soller and Garrity (2018) to derive a total sediment volume.

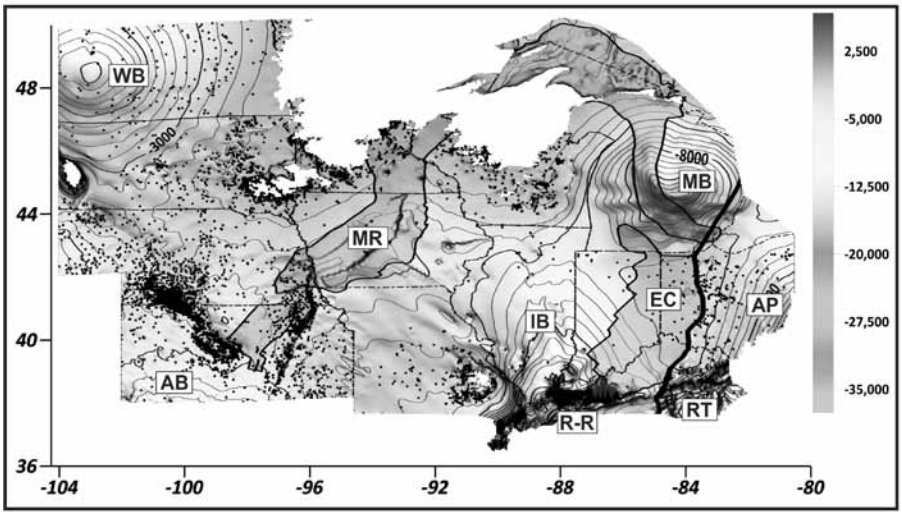

Figure 6. Configuration of the Precambrian surface in the upper midcontinent in feet asl. Contour interval is 1,000 feet. White areas are those of exposed or subglacial Precambrian crystalline and metamorphic rock: the Sioux Ridge in southeastern South Dakota, the Black Hills in southwestern South Dakota, the Baraboo quartzites in Wisconsin, and the St. Francois Mountains in southeastern Missouri. Major sedimentary basins in the study area include the Anadarko (AB), Williston (WB), Illinois (IB), Michigan (MB), and Appalachian (AP) Basins. This surface also forms the top of the Proterozoic Midcontinent Rift (MR) and East Continent Basin (EC), both shaded darker. The Reelfoot Rift-Rough Creek Graben (R-R) and Rome Trough (RT) are deep rift grabens along the southern boundary of the study area; the Rome Trough continues northeast through West Virginia and Pennsylvania. Black dots show well control.

Top Precambrian Surface

For most of the study area, the unconformity atop the Precambrian (Figure 6) is interpreted as forming the lower diluvial boundary because it is an erosional surface atop crystalline basement at the base of the sedimentary record. The Midcontinent Rift, found beneath seven states and part of Ontario, and the East Continent Basin, found beneath Indiana, Kentucky, Michigan, and Ohio are the major exceptions. Other cratonic rifts in the study area are dated as Cambrian, have much less volcanic fill, and contain fossiliferous marine sediments. These include the Reelfoot Rift, the Rough Creek Graben, and Rome Trough, all partly in Kentucky. Lacking any hard data, we did not attempt to map the recently-proposed Illinois Graben (Freiburg et al., 2022).

The North American craton is well known for its large marine sedimentary basins—the Williston, Illinois, and Michigan Basins. Smaller basins include the Salina, Forest City, and

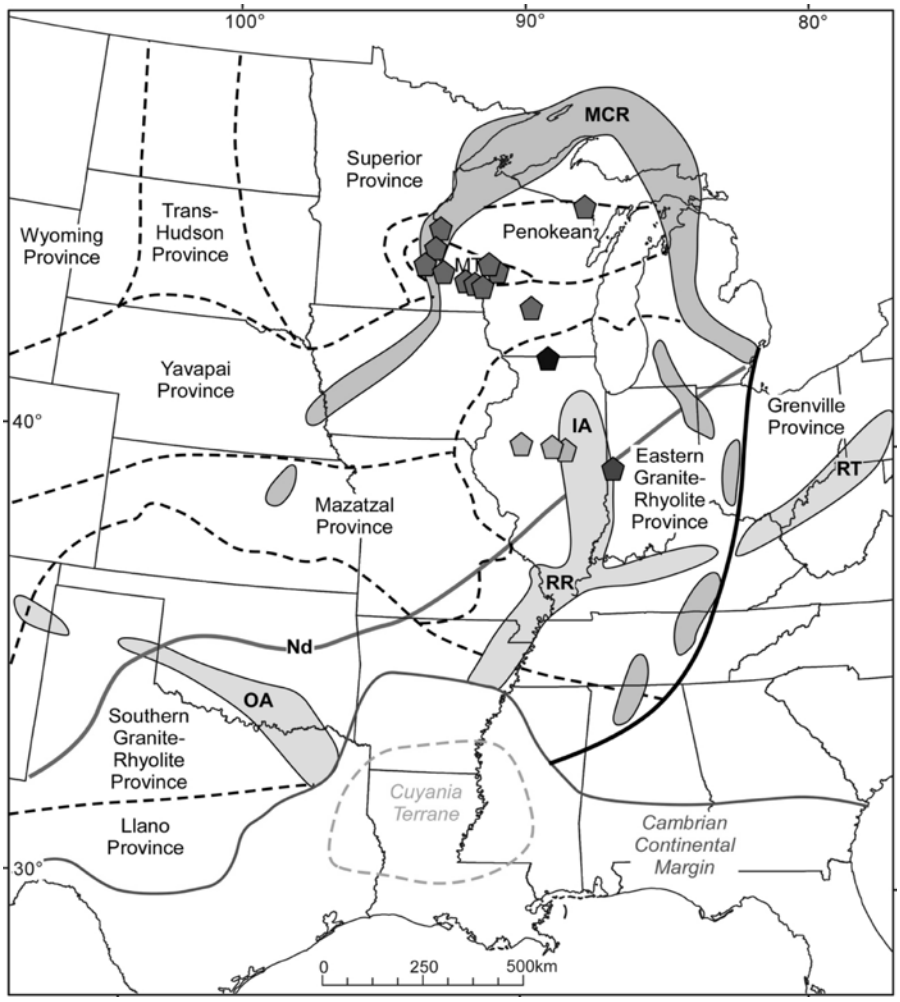

Figure 7. Interpretation of Precambrian basement provinces and features from Freiburg et al. (2022). Pentagons are drill and sample sites discussed in their paper. Cambrian rifts, including the Oklahoma Aulacogen (OA), Illinois Aulacogen (IA), Reelfoot Rift complex (RR), and Rome Trough (RT) are shown in light gray and Proterozoic rifts in darker gray. Terranes are interpreted by gravity and magnetic signatures, limited lithologic samples, and radiometric dating.

Cherokee Basins. The Anadarko and Appalachian Basins are large but lie primarily outside the study area. Marine Phanerozoic strata of the Williston, Illinois, Michigan, and smaller basins are separated stratigraphically from the Midcontinent Rift and East Continent Basin by the Precambrian/Cambrian unconformity. State maps in Figure 6 that comprise this figure are described and shown in the appendix. White areas show where Precambrian crystalline rocks are either exposed at the surface or immediately underlie glacial deposits. The Sioux Quartzite was also blanked. Although we suspect it is an Early Flood deposit (Oard et al., 2023a), there are no available maps of its base. Mapping it and the other Proterozoic quartzites is a separate study, so we mapped the basal diluvial boundary across their tops. Though barely visible in Figure 6, the Baraboo Hills exposures in south-central Wisconsin are likewise blanked. The current uniformitarian interpretation of the underlying Precambrian terranes is shown in Figure 7.

Interpretation of Rifts, Troughs, and Basins

We interpret the Precambrian (and Cambrian) rifts in the study area as products of the Flood (Reed, 2000; Clarey, 2020). The largest two, the Midcontinent Rift and East Continent Basin, dwarf the others. In the study area, there is a clear contrast between north and south. In the south, rifting was less intense, less volcanic, and the rifts were infilled by mostly marine sediments. Farther north, rifts are larger and were filled by volcanics (primarily basalt) and unfossiliferous terrigenous sediments. On top of the rift fills, Phanerozoic marine sediments occur. We created two volumes of diluvial rock in the study area: one for the Phanerozoic and one for the rift fills. We discovered that the top of the Precambrian is a heavily eroded surface. Because of dense well control, we have mapped the presence of interesting large erosional remnants, such as in the Kansas basement (Figure A-4 in the appendix). That 3D surface was then subtracted from NOAA's 2022 30-arc second ETOPO DEM. The resulting volumes (base Phanerozoic to surface) include Flood, Ice Age, and Recent deposits. The Ice Age/Recent sediments, shown in Table I, were subtracted as shown in Table II to yield diluvial volumes outside the Midcontinent Rift and East Continent Basin. Volumes for the Reelfoot Rift, Rough Creek Graben, and Rome Trough are included since they are filled with Phanerozoic marine sediments. Differencing of grids typically returns both "cut" and "fill" volumes and areas. We used the cut volume and area. Uncertainties in estimating volume estimates can be obtained from the lead author. Average

Table II. Volume and average thickness of Phanerozoic strata in the study area. Glacial data from Table I. Average thicknesses exclude areas of exposed or subglacial Precambrian basement. No Ice Age thickness was assigned to Kentucky, which has patchy, thin glacial sediments in only eight counties.

		Base Phanerozoic to Surface			Ice Age and Recent Sediment			Marine Diluvial		
STATE	AREA (km^2)	VOLUME (km^3)	AVG THICK (m)	AVG THICK (ft.)	VOLUME (km^3)	AVG THICK (m)	AVG THICK (ft.)	VOLUME (km^3)	AVG THICK (m)	AVG THICK (ft.)
Illinois	149,995	260,913	1,734	5,688	3,744	25	82	257,169	1,709	5,606
Indiana	94,321	146,479	1,552	5,093	2,758	29	96	143,721	1,523	4,997
Iowa	145,756	97,300	686	2,251	6,528	45	147	90,772	640	2,100
Kansas	213,100	203,523	964	3,162	178	1	3	203,345	963	3,159
Kentucky	104,656	289,485	2,788	9,146	0	0	0	289,485	2,788	9,146
Michigan	250,487	363,527	1,682	5,517	13,160	53	172	350,367	1,621	5,318
Minnesota	225,163	23,382	415	564	13,378	59	195	10,004	177	582
Missouri	180,540	111,913	621	1,361	1,141	6	21	110,772	624	2,046
Nebraska	200,330	127,818	642	2,105	2,163	11	35	125,655	631	2,070
North Dakota	183,108	332,712	1,952	6,405	5,964	33	107	326,748	1,917	6,290
Ohio	116,098	169,096	1,460	4,790	1,899	16	54	167,197	1,444	4,737
South Dakota	199,729	122,714	748	2,452	5,498	28	90	126,538	634	2,079
Wisconsin	169,635	21,216	294	965	3,936	23	76	17,280	240	786
Ontario (SA)	65,833	UNK	–	–	–	–	–	–	–	–
TOTAL	2,295,682	2,270,078	1,212	3,975	60,347	26	86	2,209,731	1,179	3,870

thicknesses were calculated using only the areas without exposed Precambrian (see Appendix). Minnesota and Wisconsin show the greatest proportion of Ice Age and Recent sediments to diluvial marine strata. In addition to higher volumes of Ice Age strata, these states showed lower volumes and thicknesses of diluvial strata. Figure A-6 shows that much of the subglacial area of both states is crystalline basement, resulting in large areas of zero Flood thickness. This suggests that either this area was high during the entire Flood and/or that there was significant erosion during the Recessive Stage of the Flood.

The greatest volumes of Phanerozoic marine diluvial rocks were emplaced in Michigan (Michigan Basin), North Dakota (Williston Basin), Kentucky (Early Cambrian grabens and Appalachian Basin), Illinois (Illinois Basin), and Kansas (Salina and Anadarko Basins). Kentucky has the greatest average thickness of sediments, followed by North Dakota, Illinois, and Michigan. We modified the outline of the Reelfoot Rift and Rough Creek Graben from Coleman and Cahan (2012) based on our own basement map and adopted Coleman and Cahan's (2012) outline of the Rome Trough. Both the Reelfoot Rift and Rome Trough extend beyond the study area, but within the study area, the three features occupy 43,573 km^2. In that area, 187,147 km^3 of sediment were deposited between the basement unconformity and the ground surface. Their average thickness of 14,091 ft. (4,295 m) of fill is predominantly Cambrian to Early Ordovician arkoses to carbonates. Hickman (2013) notes that the maximum thickness of the Late Cambrian/Early Ordovician Knox Group alone exceeds 11,500 ft. (3,505 m) in the Rough Creek Graben. Sediment accumulations are typically characterized by basins, so we calculated the volume and thickness by basin (Table III), with the caveat that some basins extend outside the study area and those volumes were not included. For basin boundaries, we used those of Evenick (2021). However, we found his boundaries very general, and our delineation of his Lake Superior and Midcontinent Basins, based on more detailed mapping, are significantly more accurate (see Part II). For that reason, we compared the results from his outlines (Figure 8) to the more conservative ones of Coleman and Cahan (2012), from the USGS (Table III). Average thicknesses by basins are shown in Figure 9.

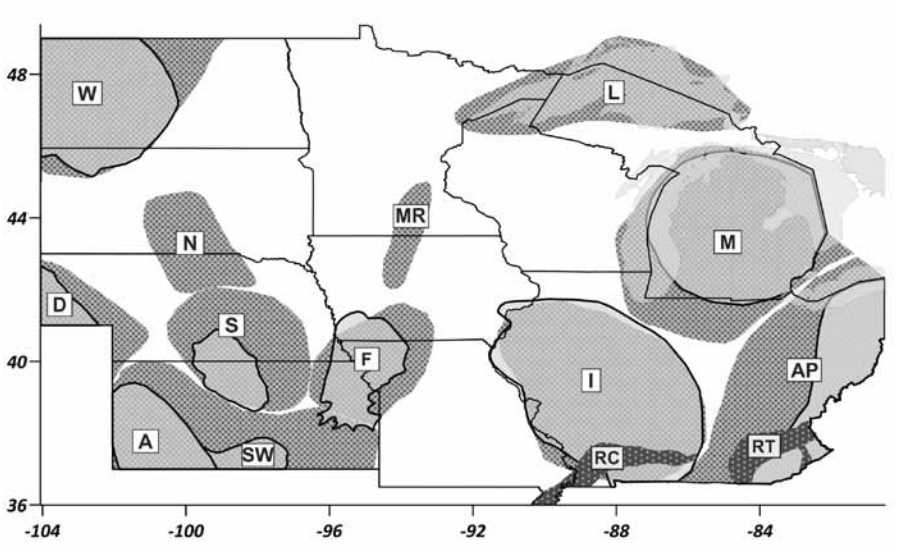

Figure 8. Sedimentary basins in the study area from Evenick (2021) = stippled, and Coleman and Cahan (2012) = lighter gray. RC = Reelfoot Rift/Rough Creek Graben, RT = Rome Trough, AP = Appalachian Basin, I = Illinois Basin, M=Michigan Basin, L = Lake Superior Basin, MR = Midcontinent Basin, F = Forest City Basin, A = Anadarko Basin, S = Salina Basin, SW = Sedgewick Basin, D = Denver Basin, N = Central Nebraska Basin, W = Williston Basin. Evenick's (2021) boundaries are consistently larger than those of Coleman and Cahan (2012). The Lake Superior and Midcontinent Basins are Proterozoic basins.

The basin volumes and average thicknesses show a picture matching that of a regional isopach map (Figure 10). The southern rifts were included on this isopach because they were infilled with mostly Phanerozoic marine fossiliferous sediments rather than unfossiliferous sediments in the East Continent Basin and Midcontinent Rift sedimentary basins. The cratonic basins represented here are sags in the surface relative to the rifts. The Rough Creek Graben reaches more than 38,000 ft. (11,582 m) below sea level. This is comparable to the Appalachian and Anadarko Basins, but much deeper than the Michigan, Illinois, and Williston Basins. The cratonic basins' origins are unclear, although the Michigan Basin, the Anadarko Basin, the Illinois Basin, and the Appalachian Basin all overlie rifts to some extent. The basins with the greatest volume in the study area are the Il-

Table III. Total volume (marine diluvial and Ice Age) and average thickness of sedimentary basins based on boundaries from Figure 8. Basins extending outside the study area were cropped at the study area margin and the volume shown here is *only* that within the study area. No numbers were derived here for the Proterozoic Lake Superior and Midcontinent Basins; they will be done in Part II.

	EVENICK (2021)				COLEMAN AND CAHAN (2012)			
SEDIMENTARY BASIN	AREA (km^2)	VOLUME (km^3)	AVG THICK (m)	AVG THICK (ft.)	AREA (km^2)	VOLUME (km^3)	AVG THICK (m)	AVG THICK (ft.)
Williston	121,576	326,955	2,689	8,823	100,027	294,489	2,944	9,659
Central NE	51,182	19,310	377	1,238	—	—	—	—
Denver	36,108	40,265	1,115	3,659	13,160	19,129	1,454	4,769
Salina	97,025	68,850	710	2,328	27,816	25,149	904	2,966
Anadarko	142,994	153,275	1,072	3,517	45,678	64,800	1,419	4,654
Forest City	73,006	96,623	773	2,537	48,754	38,018	780	2,558
Illinois	202,648	463,243	2,286	7,500	207,129	459,869	2,220	7,284
Appalachian	178,364	304,163	1,705	5,595	70,464	175,888	2,496	8,189
Michigan	222,795	417,905	1,876	6,154	148,459	344,176	2,318	7,606
TOTAL	1,125,698	1,850,410	1,644	5,393	760,471	1,512,702	1,989	6,526

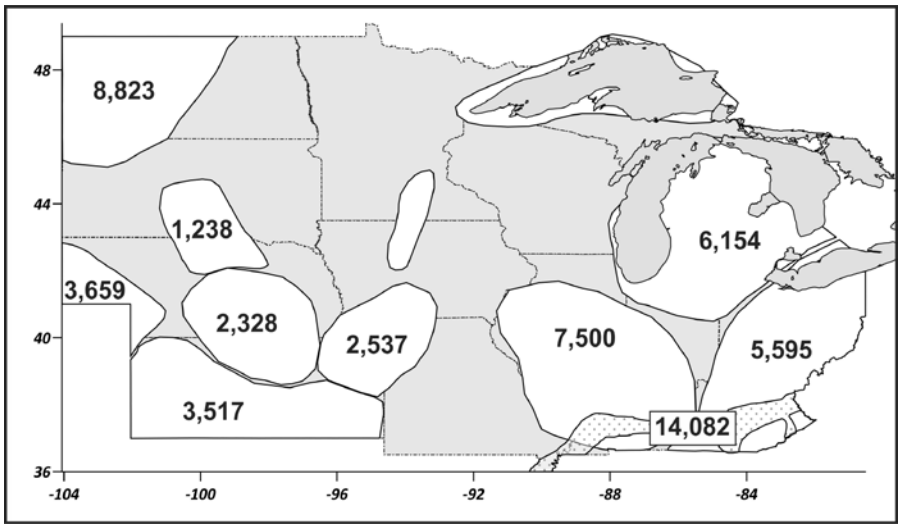

Figure 9. Average thickness in feet of sedimentary basins in the study area based on volumes calculated between our basement map and ETOPO. Outlines and numbers follow Evenick's definitions (2021). See Table III for varying numbers using outlines of Coleman and Cahan (2012). Number for Reelfoot Rift/Rough Creek Graben/Rome Trough (lower right) based on our work.

linois and Michigan Basins, although the Williston, Anadarko, Denver, and Appalachian Basins would be greater if shown in whole.

Discussion

This study seeks to provide basic mapped data as well as investigating some of the mechanics of the Flood.

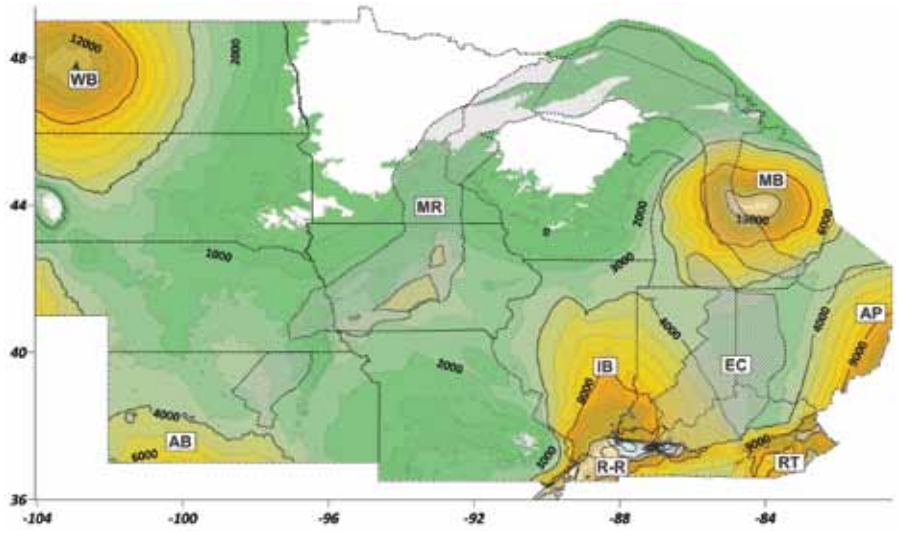

Figure 10. Isopach map of the interval between the ground surface and the unconformity atop crystalline basement for the upper midcontinent region, in feet. Contour interval is 1,000 feet. These thicknesses do not include rift or basin fill in the Midcontinent Rift (MR) and East Continent Basin (EC), shown in outline.

Shape files for the maps used in this study are available to creationist researchers upon request from the lead author. The resulting volume and distribution of sediment therein help explain events of the Early Flood in the northern Midcontinent. Rifting occurred throughout the region. The Oklahoma Aulacogen lies a few hundred miles south of the study area (Figure 7). It is a rift largely containing igneous bimodal rock fill; granite and rhyolite forming over deep and thick mafic gabbros (Reed, 2004). The basement was eroded before being covered by the transgressive sequence of the Timbered Hills Group (Reed, 2005). In this regard, it is similar to the Reelfoot-Rough Creek and Rome Trough structures. The Midcontinent Rift and East Continent Basin rifting have preserved volcanics as predominantly basalt, although significant erosion of these rocks occurred during and after their emplacement. However, the associated large sedimentary basins under Lake Superior and flanking the rift in Minnesota, Iowa, Nebraska, and Kansas are not found in Oklahoma. In the Rough-Creek/Reelfoot Rift/Rome Trough complex, basal Phanerozoic clastic and carbonate sediments dominate over basalt and rhyolite. The characteristics of these rifts will be more closely investigated in Part II, and diluvial explanations of their similarities and differences will be explored. For now, what are we to make of the sequence of the rock record in the study area outside the areas of rifting? Two particular issues arise: (1) the evidence of significant, widespread, and powerful erosion of the crystalline basement, and (2) the evidence of the overwhelming activity of the Flood in shaping the volume and distribution of the rock record in the region. Crystalline basement in the study area was subjected to three episodes of erosion: (1) the Early Flood, (2) the Late Flood regression, and (3) that associated with

glaciation. Since paleotopography appears to have been higher to the north, based on large-scale sediment patterns, erosion in all three episodes would have increased from south to north. Early Flood erosion left impressive erosional remnants (Figure A-4). As water flowed south, the large channels would have combined into sheets—the opposite of the Late Flood transition from sheet flow to channels (Oard, 2013). At some level of energy, those sheets would have created vast planation surfaces with erosional remnants. The study area was covered by diluvial sediments at the height of the Flood. Oard et al. (2023b) estimated that an average of about 2,000 m (6,560 ft.) of sediment was removed from North America during the Late Flood regression. In other words, nearly 40% of the original record was eroded preferentially from the younger Flood record. Those places where Ice Age sediments directly overlie crystalline basement were probably once covered by significant thicknesses of Flood sediment. Their erosional remnants are seen today in patches atop the crystalline basement beneath glacial rocks in Minnesota and well into Canada (Ambrose, 1964; Jirsa et al., 2011). Therefore, the remaining sedimentary rocks and sedimentary basins are much smaller than they would have been at the highstand of the Flood and those that remain disproportionately represent earlier stages of the Flood. Finally, the most significant Ice Age erosion in the study area occurred in Minnesota, Wisconsin, and Michigan. Subglacial crystalline rock is exposed in small patches in eastern North Dakota (Bluemle, 2003) and along the Sioux Ridge in southeastern South Dakota and southwestern Minnesota (McCormick, 2010c). It is currently unclear as to whether those irregular surfaces are the result of Ice Age erosion only or whether they may also exhibit relicts of the Flood.

Conclusion and Summary

The Midcontinent region of the United States is a well-studied area that provides many insights into the Flood. It includes five major rifts and six major cratonic basins. Based on data from state surveys, the USGS, and from other publications, we mapped four key surfaces in order to derive the thickness and distribution of three significant volumes: (1) Ice Age and Recent sediments, (2) Phanerozoic marine diluvial strata, and (3) rift fill. The first two packages are described in this paper; the rift fill will be addressed in Part II. Ice Age and Recent strata average 86 ft. (26 m) across the study area and marine diluvial strata averages 3,870 ft. (1,179 m). The thickest sediments of that volume are found in the Rough Creek Graben in Kentucky, with depths reaching over 38,000 ft. (11,582 m) and sediment averaging over 14,000 ft. (4,267 m) in the Reelfoot Rift/Rough Creek Graben/Rome Trough rifts. Thick sediments are also found in the Michigan, Illinois, Williston, and Appalachian Basins. However, as we will demonstrate in Part II, these thicknesses are dwarfed by those of the Midcontinent Rift.

Acknowledgements

We appreciate the resources and help of the state geological surveys of North Dakota, South Dakota, Nebraska, Kansas, Missouri, Iowa, Minnesota, Wisconsin, Michigan, Illinois, Indiana, Ohio, Kentucky, and Ontario. This work would not have been possible without their efforts over many years. Their employees, when asked specific questions, were always helpful and gracious. Any errors are ours.

References

Albert, C.C., S. Marshak, and T.H. Larson. 2016. Map 8: Structure contours of the top of the Precambrian, In S. Marshak, T.H. Larson, and C.C. Albert (compilers). Geological and geophysical maps of the Illinois Basin–Ozark Dome Region. *Illinois State Geological Survey Map 23–8*, 1:1,500,000.

Ambrose, J.W. 1964. Exhumed paleoplains of the Precambrian shield of North America. *American Journal of Science* 262:817–857.

Anderson, R.R. 1990. The Amoco M.G. Eischeid #1 deep petroleum test, Carroll County, Iowa—preliminary investigations. *Iowa Geological Survey Special Report Series No. 2*.

Anderson, R.R. 1995. Structural configuration of the Precambrian surface of Iowa. *Iowa Geological Survey Open File Report 1995–2*.

Anderson, R.R. 2006. Geology of the Precambrian surface of Iowa and surrounding area. *Iowa Geological Survey Open File Map OFM-06–7*.

Anderson, F.J. 2007. Precambrian basement drillhole map of North Dakota. *North Dakota Geological Survey Geologic Investigations 43*.

Anderson, F.J. 2009. Depth to Precambrian basement in North Dakota. *North Dakota Geological Survey Geologic Investigations 85*.

Anderson, R.R., and R.M. McKay. 1989. Clastic rocks associated with the Midcontinent Rift System in Iowa. In *USGS Bulletin 1989-I*.

Bader, J.W. 2021. Assembling Laurentia: Precambrian compressional tectonics in North Dakota and surrounding areas. *North Dakota Geological Survey Geologic Investigation No. 251*.

Bankey, V. et al. 2002. Digital data grids for the magnetic anomaly map of North America. *U.S. Geological Survey Open-File Report 02–414*. U.S. Geological Survey, Denver, Colorado, USA.

Baranoski, M.T. 2013. Structure contour map on the Precambrian unconformity surface in Ohio and related basement features. *Ohio Geological Survey Map PG-23*.

Baranowski, M.T., S.L. Dean, J.L. Wicks, and V.M Brown. 2009. Unconformity-

bounded seismic reflection sequences define Grenville-age rift system and foreland basins beneath the Phanerozoic in Ohio. *Geosphere* 5(2):140–151. DOI: 10.1130/GES00202.1.

Berendsen P., and K. Blair. 1996a. Structural configuration of the Precambrian basement. *Kansas Geological Survey Map M-45.1*.

Berendsen P., and K. Blair. 1996b. Precambrian subcrop. *Kansas Geological Survey Map M-45.2*.

Bickford, M.E., W.R. Van Schmus, and I. Zietz. 1986. Proterozoic history of the midcontinent region of North America. *Geology* 14(6):492–496.

Bickford, M.E., K.L. Harrower, R.L. Nusbaum, J.J. Thomas, and G.E. Nelson. 1979. Preliminary geologic map of the Precambrian basement rocks of Kansas. *Kansas Geological Survey Map M-9*.

Bluemle, J.P. 1986. Depth to bedrock in North Dakota. *North Dakota Geological Survey Miscellaneous Map MM-26*.

Bluemle, J.P. 2003. Generalized bedrock geology map of North Dakota. *North Dakota Geological Survey Miscellaneous Map MM-36*.

Boerboom, T.J. 2020. Minnesota at a glance: Precambrian geology. *Minnesota Geological Survey*. https://conservancy.umn.edu/bitstream/handle/11299/59424/mn%20glance%20precambrian%204%20page.pdf?sequence=10&isAllowed=y.

Boyd, S.W., and Snelling, A.A. (editors). 2014. *Grappling with the Chronology of the Genesis Flood*. Master Books, Green Forest, AR.

Brown, L., L. Jensen, J. Oliver, S. Kaufman, and D. Steiner. 1982. Rift structure beneath the Michigan Basin from COCORP Profiling. *Geology* 10(12):645–649.

Burchett, R.R., and M.P. Carlson. 1986. *Configuration of Precambrian Surface in Nebraska*. Nebraska Geological Survey, Lincoln NE.

Cagle, J.W. 1973. Bedrock topography of south-central Iowa. *Iowa Geological Survey Miscellaneous Investigation Series Map I-763*.

Carson, E.C., B.B. Curry, P.J. Kerr, and B.A. Lusardi. 2023. The Driftless area: The extent of unglaciated and similar terrains in Wisconsin, Illinois, Iowa, and Minnesota. *Wisconsin Geological and Natural History Survey Educational Series 057, Madison, WI*.

Clarey, T. 2020. *Carved in Stone: Geological Evidence of the Worldwide Flood*. Institute for Creation Research, Dallas, TX.

Cole, V.B. 1976. Configuration of the top of Precambrian rocks in Kansas. *Kansas Geological Survey Map M-7*.

Coleman, Jr., J.L., and S.M. Cahan. 2012. Preliminary catalog of the sedimentary basins of the United States: *U.S. Geological Survey Open-File Report 2012–1111*, 27 pages (plus 4 figures and 1 table available as separate files). Available online at http://pubs.usgs.gov/of/2012/1111/.

Collinson, C., M.L. Sargent, and J.R. Jennings. 1988. "Illinois Basin region." In Sloss, L.L. (editor). *Sedimentary Cover—North American Craton, U.S., Geology of North America, v. D-2*, pp. 383–426. Geological Society of America, Boulder, Colorado,

Csontos, R., R. Van Arsdale, R. Cox, and B. Waldron. 2008. Reelfoot Rift and its impact on Quaternary deformation in the Central Mississippi River valley. *Geosphere* 4(1):145–158.

Dart, R.L. 1995. Maps of Upper Mississippi embayment Paleozoic and Precambrian rocks. *USGS Miscellaneous Field Studies Map MF-2284*.

Dart, R.L., and H.S. Swolfs. 1998. Contour mapping of relic structures in the Precambrian basement of the Reelfoot Rift, North America Midcontinent. *Tectonics* 17(2):235–249.

Denne, J.E., R.E. Miller, L.R. Hathaway, H.G. O'Conner, and W.C. Johnson. 1998. Hydrogeology and geochemistry of glacial deposits in northeastern Kansas. *Bulletin 229*, Kansas Geological Survey, Lawrence, KS.

Drahovzal, J.A., and D.C. Harris. 1998. *The East Continent Rift System: Its Age and Genesis.* AAPG Search and Discovery Article #90930. 1998 AAPG Eastern Section, Columbus, OH.

Drahovzal, J.A., D.C. Harris, L.H. Wickstrom, D. Walker, M.T. Baranowski, B. Keith, and L.C. Furer. 1992. The East Continent Rift Basin: A new discovery. *Ohio Geological Survey Information Circular 57*. Published by Kentucky Geological Survey, Lexington, KY. Also published as *Indiana Geological Survey Special Report 52* and *Kentucky Geological Survey Special Publication 18, Series XI*.

Drahovzal, J.H., and M.C. Noger. 1995. Preliminary map of the structure of the Precambrian surface in eastern Kentucky. *Kentucky Geological Survey Map and Chart Series 8*.

Evenick, J.C. 2021. Glimpses into Earth's history using a revised global sedimentary basin map. *Earth-Science Reviews* 215. https://doi.org/10.1016/j.earscirev.2021.103564.

Fairchild, L.M., N.L. Swanson-Hysell, J. Ramezani, C.J. Sprain, and S.A. Bowring. 2017. The end of Midcontinent Rift magmatism and the paleogeography of Laurentia. *Lithosphere* 9(1):117–133.

Freiberg, J.T., D. Malone, and M. Huisman. 2022. Geochronology of Cambrian sedimentary and volcanic rocks in the Illinois Basin: Defining the Illinois Aulacogen. *The Sedimentary Record* 20(1): 1–7. doi.org/10.2110/001c.37650.

Geiger, C.A., and C.V. Guidotti. 1989. Precambrian metamorphism in the southern Lake Superior region and its bearing on crustal evolution. *Geoscience Wisconsin* 13:1–33.

Gold, D.P., S.S. Alexander, R. Cakir, A.G. Doden, and S.I. Root. 2005. Precambrian basement map of the Appalachian Basin and Piedmont Province in Pennsylvania, version 1.0. *Pennsylvania Geological Survey Open-File General Geology Report OFGGR 05–01.0*.

Grauch, V.J.S., E.D. Anderson, S.J. Heller, E.K. Stewart, and L.G. Woodruff. 2020. Integrated geophysical analysis provides an alternate interpretation of the northern margin of the North American Midcontinent Rift System, Central Lake Superior. *Interpretation*. https://doi.

org/10.1190/INT-2019–0262.1.

Gray, H.H. 1982. Map of Indiana showing topography of the bedrock surface. *Indiana Geological Survey Miscellaneous Map 35*, scale 1:500,000. Digital download available at https://igws.indiana.edu/bookstore/details.cfm?Pub_Num=MM35.

Grimley, D. 2015. Drift thickness of Illinois (data originally from *ISGS Circular 490*, Piskin and Bergstrom, 1975). Illinois Geological Survey. http://isgs.illinois.edu/nsdihome/webdocs/st-geolq.html; accessed February 2022.

Hamilton, J. 2020. Bedrock topography vs. depth to bedrock. *Minnesota Geological Survey Open Data GIS Story*. https://mngs-mn.opendata.arcgis.com/apps/c36a3951cc174e6f9bdee7514b11b7e7/explore.

Hansen, R.E. 1972. Bedrock topography of east-central Iowa. *Miscellaneous Geologic Investigations I-717*, two sheets. Iowa Geological Survey, Iowa City, IA.

Hansen, R.E. 1973. Bedrock topography of southeast Iowa. *Iowa Geological Survey Miscellaneous Investigation Series Map I-808*.

Hansen, R.E. 1975. Bedrock topography of northeast Iowa. *Iowa Geological Survey Miscellaneous Investigation Series Map I-933*.

Hansen, R.E. 1978. Bedrock topography of north-central Iowa. *Iowa Geological Survey Miscellaneous Investigation Series Map I-1080*.

Hansen, R.E. 1985. Bedrock topography of central Iowa. *Iowa Geological Survey Miscellaneous Investigation Series Map I-1609*.

Hansen, R.E. 1986. Bedrock topography of northwest Iowa. *Iowa Geological Survey Miscellaneous Investigation Series Map I-1726*.

Hansen, R.E. 1992. Bedrock topography of southwest Iowa. *Iowa Geological Survey Miscellaneous Investigation Series Map I-2230*.

Hansen, R.E., and D.L. Runkle. 1986. Bedrock topography of west-central Iowa. *Iowa Geological Survey Miscellaneous Investigation Series Map I-1688*.

Heck, T. 1988. Precambrian structure map of North Dakota. *North Dakota Geological Survey Miscellaneous Map 30, Bismarck, ND*.

Hemborg, H.T. 1996. *Basement Structure Map of Colorado with Major Oil and Gas Fields*. Colorado Geological Survey, Denver, CO.

Herzog, B.L., B.J. Stiff, C.A. Chenoweth, K.L. Warner, J.B. Sieverling, and C. Avery. 1994. Buried bedrock surface of Illinois, third edition. *Illinois Map 5*. Illinois State Geological Survey and U.S. Geological Survey.

Hickman, J.C. 2011. *Structural Evolution of an Intracratonic Rift System: Mississippi Valley Graben, Rough Creek Graben, and Rome Trough of Kentucky, USA*. University of Kentucky Doctoral Dissertation (Lexington, KY). https://uknowledge.uky.edu/gradschool_diss/144/. His plate 16 is PC Map 11.

Hickman, J.C. 2013. Rough Creek Graben consortium final report. *Contract Report 55, Series XII*. Kentucky Geological Survey, Lexington, KY.

Hinze, W.J., R.L. Kellogg, and N.W. O'Hara. 1975. Geophysical studies of basement geology of Southern Peninsula of Michigan. *American Association of Petroleum Geologists Bulletin* 59(9):1562–1584.

Hinze, W.J., and V.W. Chandler. 2020. Reviewing the configuration and extent of the Midcontinent Rift System. *Precambrian Research* 342:105688.

Howell, P.D., and B.A. van der Plujim. 1990. Early history of the Michigan Basin: Subsidence and Appalachian tectonics. *Geology* 18(12):1195–1198.

Howell, P.D., and B.A. van der Plujim. 1999. Structural sequences and styles of subsidence in the Michigan Basin. *Geological Society of America Bulletin* 111(7):974–991.

Jirsa, M.A., T.J. Boerboom, V.W. Chandler, John H. Mossler, A.C. Runkel, and D.R. Setterholm. 2011. Geologic map of Minnesota bedrock geology. *Minnesota Geological Survey Map S-21*.

Kisvarsaynyi, E. 1984. Structure contours of the Precambrian surface in Missouri. *Missouri Geological Survey Contribution to Precambrian Geology No. 15, OFM-84–207-GI. Rolla, MO.*

Kucks, R.P. 1999. Bouguer gravity anomaly data grid for the conterminous US. https://mrdata.usgs.gov/services/gravity?request=getcapabilities&service=WMS&version=1.3.0.

Li, J., and I.B. Morozov. 2006. Structural styles of the Precambrian basement underlying the Williston Basin and adjacent regions—An interpretation from geophysical mapping. In *Summary of Investigations 2006*, Volume 1. Saskatchewan Geological Survey, Saskatchewan *Industry Resources, Miscellaneous Report 2006–4.1*, CD-ROM, Paper A-2, 18 pages.

Lloyd, Jr., O.B., and W.L. Lyke. 1995. Segment 10: Illinois, Indiana, Kentucky, Ohio, Tennessee. In *Ground Water Atlas of the United States. USGS Hydrologic Investigations Atlas 730-K. Reston, VA.*

McBride, J.H., E. Hannes, H.E. Leetaru, R.W. Keach II, and E.I. McBride. 2016. Fine-scale structure of the Precambrian beneath the Illinois Basin. *Geosphere* 12(2):585–606.

McCormick, K.A. 2010a. Elevation contour map of the Precambrian surface of South Dakota. *South Dakota Geological Survey Map G-11*.

McCormick, K.A. 2010b. Plate 1: Terrane map of the Precambrian basement of South Dakota. *South Dakota Geological Survey Bulletin 41*.

McCormick, K.A. 2010c. Precambrian basement terrane of South Dakota. *South Dakota Geological Survey Bulletin 41*.

Miller, J., and S. Nicholson. 2013. Geology and mineral deposits of the 1.1 Ga Midcontinent Rift in the Lake Superior Region - An overview. *USGS*.

Missouri Department of Natural Resources. 2020. Top of bedrock elevation. https://gis-modnr.opendata.arcgis.com/search?q=bedrock%20topography, January 2023.

Moecher, D.P., J.R. Bowersox, and J.B. Hickman. 2018. Zircon U-Pb geochronology of two basement cores (Kentucky, USA): Implications for Late Mesopro-

terozoic sedimentation and tectonics in the eastern Midcontinent. *Journal of Geology* 126(1):25–39.

Mudrey, Jr., M.G., B.A. Brown, and J.K. Greenberg. 1982. Bedrock geologic map of Wisconsin, University of Wisconsin. *Extension Geological and Natural History Survey Map*.

Oard, M.J. 2013 (ebook). *Earth's Surface Shaped by Genesis Flood Runoff*. http://Michael.oards.net/GenesisFloodRunoff.htm.

Oard, M.J. *How Noah's Flood Caused a Single Ice Age*. Creation Book Publishers, Powder Springs, GA (in press).

Oard, M.J., J.K. Reed, and P. Klevberg. 2023a. Suggested strategies for fitting Precambrian rocks into Biblical Earth history. *Creation Research Society Quarterly* 60(2):97–111.

Oard, M.J., J.K. Reed, and P. Klevberg. 2023b. Why the sediments are there—Part II: A Flood regression model. *Creation Research Society Quarterly* 59(3):160–175.

Ohio Department of Natural Resources bedrock topography map 1:500,000. https://ohiodnr.gov/business-and-industry/services-to-business-industry/gis-mapping-services/ohio-geology-interactive-map, February 2023.

Olcott, P.G. 1992. Segment 9: Iowa, Michigan, Minnesota, Wisconsin, In *Groundwater Atlas of the United States. USGS Hydrologic Investigations Atlas 730-J. Reston, VA*.

Reed, J.K. 2000. *The North American Midcontinent Rift System: An Interpretation Within the Biblical Worldview*. Creation Research Society, Glendale, AZ.

Reed, J.K. 2003. The geology of the Kansas Basement—Part I. *Creation Research Society Quarterly* 40(3):151–163.

Reed, J.K. 2004. The geology of the Oklahoma basement. *Creation Research Society Quarterly* 41(2):156–167.

Reed, J.K. 2005. Geology of the Timbered Hills Group in Oklahoma. *Creation Research Society Quarterly* 42(1):39–66.

Sims, P.K., R.W. Saltus, and E.D. Anderson. 2008. Precambrian basement structure map of the continental United States—An interpretation of geologic and aeromagnetic data. *U.S. Geological Survey Scientific Investigations Map 3012*, scale: 1:8,000,000.

Sleep, N.H., and L.L. Sloss. 1978. A deep borehole in the Michigan Basin. *Journal of Geophysical Research* 45:125–154.

Soller, D.R. 1997. Map showing the thickness and character of Quaternary sediments in the glaciated United States, east of the Rocky Mountains: Northern and Central Plains states (90 to 102 West Longitude). *Miscellaneous Investigations Series I-1970-C*. USGS, Reston, VA.

Soller, D.R., and C.P. Garrity. 2018, Quaternary sediment thickness and bedrock topography of the glaciated United States east of the Rocky Mountains: *U.S. Geological Survey Scientific Investigations Map 3392*, 2 sheets, scale 1:5,000,000. https://doi.org/10.3133/sim3392.

Stein, C.A., J. Kley, S. Stein, D. Hindle, and G.R. Keller. 2015. North America's Midcontinent Rift: When rift met LIP. *Geosphere* 11(5):1607–1616, doi:10.1130/GES01183.1

Stein, C.A., S. Stein, R. Elling, G.R. Keller, and J. Kley. 2018a. Is the "Grenville Front" in the central United States really the Midcontinent Rift? *GSA Today* 28. doi: 10.1130/GSATG357.

Stein, S., C. Stein, R. Elling, J. Kley, R. Keller, M. Wysession, T. Rooney, A. Frederiksen, and R. Moucha. 2018b. Insights from North America's failed Midcontinent Rift into the evolution of continental rifts and passive continental margins. *Tectonophysics*. DOI: 10.1016/j.tecto.2018.07.021.

Stein, S., et al. 2016. New insights into North America's Midcontinent Rift. *Eos* 97. https://doi.org/10.1029/2016EO056659.

Stewart, E.K., J. Rasmussen, and S.W. Mauel. 2022. Elevation contours of the Precambrian surface of south-central Wisconsin. *Wisconsin Geological and Natural History Survey Data Series DS001*-dataset01 and supplemental report.

Tomhave, D.W., and L.D. Schulz. 2004. Bedrock geologic map showing configuration of the bedrock surface in South Dakota east of the Missouri River. *General Map 9*, South Dakota Geological Survey, Rapid City, SD. Digital data from https://opendata2017–09–18t192802468z-sdbit.opendata.arcgis.com/maps/2b6e7a4a12ab4e188c595e0fb7dc7b65/explore, January 2023.

Whitehead, R.L. 1996. Segment 8: Montana, North Dakota, South Dakota, Wyoming. In *Ground Water Atlas of the United States. USGS Hydrologic Investigations Atlas 730-I, Reston, VA*.

Woelke, T.S., and W.J. Hinze. 2015. Midcontinent Rift System in Northeastern Kansas. *Kansas Geological Survey Bulletin 237*.

Appendix: Basement of the Upper Midcontinent by State

North Dakota

We obtained well picks of the top Precambrian from 331 wells from the North Dakota Geological Survey. The survey has also produced two maps of the Precambrian surface (Heck, 1988; Anderson, 2009). More deep wells exist (Anderson, 2007); however, not all were available. In addition, Bluemle (2003) provided a map of bedrock geology, showing small areas of subglacial Precambrian rock in eastern North Dakota, which were blanked in gridding and volumetric calculations. The Precambrian surface of North Dakota (Figure A-1) is reasonably well constrained, especially in the Williston Basin, which occupies most of the western part of the state. Precambrian rocks under North Dakota are classed into three provinces. The Superior Province of the Canadian Shield underlies the eastern part of the state. The Wyoming Province underlies only a very small portion of the southwestern corner of

North Dakota, but it occupies a salient portion of South Dakota (Figure A-2) and is notably visible in the Black Hills. Between the Superior and Wyoming Provinces is the Trans-Hudson Province, thought to be an ancient convergence zone (Bader, 2021). Each of these can be subdivided into numerous sub-provinces or tectonic zones, based primarily on geophysical data (e.g., Li and Morozov, 2006) and lithology from deep well samples.

South Dakota

In 2010, the South Dakota Geological Survey published a map of the Precambrian surface (McCormick, 2010a), supported by picks from 4,828 wells and core holes. The Sioux Quartzite, in southeastern South Dakota, forms the Sioux Ridge, elevated some hundreds of feet above the surrounding basement (Figure A-1). Perhaps the most interesting feature (thanks to dense well control) is the clarity of erosional channeling on the Sioux Ridge (Figure A-2). The Sioux Quartzite, an especially indurated metamorphic unit, extends into Minnesota and a short distance into Iowa. Where mapped in detail in those states, it shows the same erosional patterns. Its unusual hardness, formed by silica cement, is distinctive and related to diagenetic/metamorphic processes, perhaps associated with volcanism of the nearby Midcontinent Rift. South Dakota is underlain by several granitic terranes (McCormick, 2010b, 2010c), including the Yavapai Province, part of the Wyoming Province, the Trans-Hudson Province, and the Sioux block. Precambrian granite is exposed in southwestern South Dakota in the Black Hills. It is possible that the Sioux (and other Baraboo) quartzites were deposited early in the Flood, but little work has been done to map their base, and though their two-dimensional expression has been well mapped (McCormick, 2010b, 2010c), thickness maps await new data. For this study, exposed (or subglacial) Precambrian quartzites were omitted in gridding and volumetric calculations.

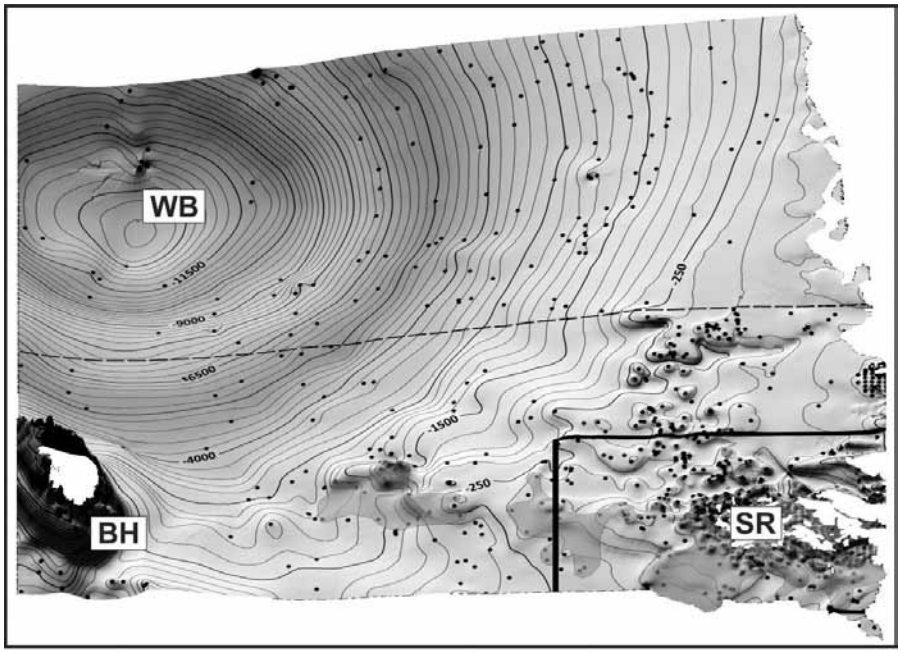

Figure A-1. Configuration of the North Dakota and South Dakota basement in feet asl. Contour interval is 250 feet. Exposed Precambrian is seen as granites in the Black Hills (BH) and far eastern North Dakota, and as subglacial and exposed Sioux Quartzite on the Sioux Ridge (SR). These areas were blanked for gridding. Dots show well control (wells in blanked areas not visible). Basement slopes into the Williston Basin (WB). Darker gray patches in southeastern South Dakota show the extent of the subcrop of the Sioux Quartzite, which extends into Minnesota, Nebraska, and Iowa (Figure A-2).

Nebraska

The Nebraska basement (Figure A-3) is based on Burchett and Carlson (1986). We also obtained tops from 1,997 wells. Most were included in Burchett and Carlson's (1986) map, though some were drilled afterward. We revised their map based on that well control and rectified its contours with newer maps from South Dakota, Colorado, and Kansas. Nebraska is largely underlain by the granitic Yavapai Province (Figure 7), with the Iowa segment of the Midcontinent Rift terminating just into southeastern Nebraska. Basement topographic features include the Central Kansas Uplift, which runs as a broad ridge from the Black Hills into Kansas, dividing the Denver Basin to the west from the Salina and Central Nebraska Basins (Evenick, 2021) to the east. The Nemaha Uplift begins in southeastern Nebraska, extending south through Kansas.

Kansas

The Precambrian surface of Kansas (Figure A-3) is well constrained by data from 3,981 wells. Maps of the Precambrian surface were made by Cole (1976) and Berendsen and Blair (1996a). They also created a map of the Precambrian subcrop (1996b). Their revision was based on Cole (1976) but extrapolated fault patterns from

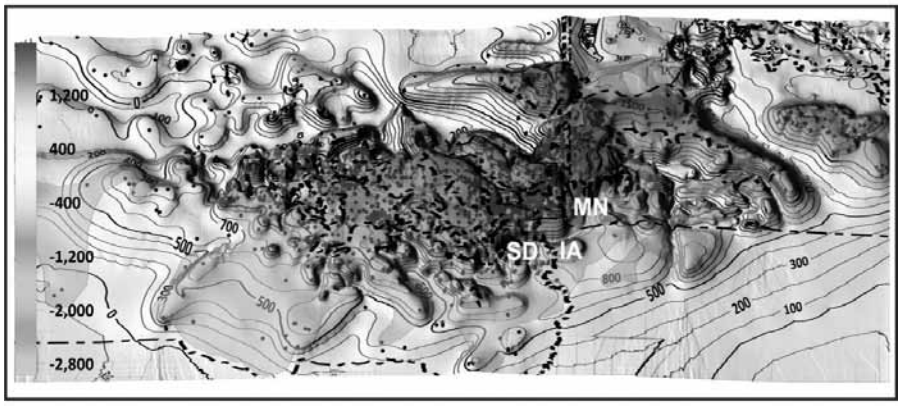

Figure A-2. Detail of the Sioux Ridge erosional patterns in feet asl. Contour Interval is 100 feet. Well control shown by black dots. Sioux subcrop from McCormick (2010b) shown in darker pattern. Dense well control allows detailed mapping of the surface. Similar erosional features and channeling occur throughout Minnesota's Precambrian surface, also visible due to significant well control. Large gullies in the Sioux Ridge exhibit up to 1,000 feet (305 m) of relief.

better studied segments of the Midcontinent Rift. However, Cole (1976) was quite detailed, using not only the Precambrian wells as control, but also many deep Cambrian wells. His work demonstrated the reality of erosional remnants scattered across the basement surface (Figure A-4), some hundreds of feet high, with control from multiple wells.

The basement in Kansas is formed by granite of the Mazatzal and Southern Granite-Rhyolite provinces (Figure 7). It is elevated at the Central Kansas and Nemaha uplifts. Between them is the Salina Basin, overlying the southern segment of the Midcontinent Rift. The western Kansas basement dips south into the Anadarko Basin. Reed (2003, 2004b) described the Kansas basement in more detail. Precambrian lithologies were plotted in Berendsen and Blair (1996b) and Bickford et al. (1979).

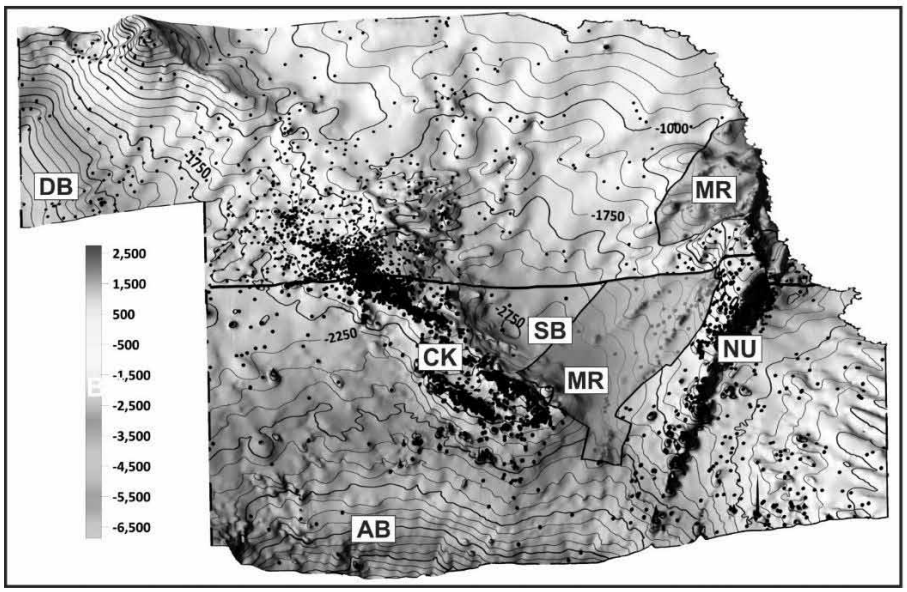

Figure A-3. Configuration of Kansas and Nebraska Basin in feet asl. Contour interval is 250 feet. Black dots show well control. Features include the eastern edge of the Denver Basin (DB), Central Kansas Uplift (CK), Salina Basin (SB), Nemaha Uplift (NU), and the northern part of the Anadarko Basin (AB). The Midcontinent Rift (solid and dashed lines and darker gray) underlies the Salina Basin.

Missouri

The Precambrian surface in Missouri (Figure A-5) was mapped by Kisvarsaynyi (1984) using well control from 898 wells for the top of the Precambrian and several hundred other wells that reached total depth in the Precambrian but with no specific pick. The basement is exposed in the southeast corner of the state in the St. Francois Mountains, which exhibit granite, rhyolite, felsite, ignimbrite, and volcanics. The area is well known for its iron and lead mines. Overall, the Missouri basement is granitic, with parts of the Mazatzal, Yavapai, Southern Granite-Rhyolite and Eastern Granite-Rhyolite provinces underlying the state (Figure 7). At the southeastern tip of Missouri, the basement dives southeast from the surface exposure of the St. Francois Mountains into the Reelfoot Rift (also called the Mississippi Valley Graben), which reaches depths exceeding 38,000 ft. (11,582 m) below sea level in Kentucky (Hickman, 2011, 2013).

Iowa

Iowa's basement surface (Figure A-5) dips from the Sioux Quartzite in the far northwestern corner down to the south and east. In addition to the Sioux,

the northwestern part of the state is underlain by Archean rocks of the Superior Province. Moving southeast, the Yavapai Province is cut by the Midcontinent Rift (Figure 7). Granitic rocks of the Eastern Granite-Rhyolite Province underlie the southeastern part of Iowa (Anderson, 2006). The Midcontinent Rift is, by far, the most dramatic feature of Iowa's basement. Reverse faults form a central volcanic horst (visible in Figure 1) bounded on both sides by sedimentary basins (Anderson, 1990). Anderson (1995, 2006) mapped the Precambrian surface, and we obtained depths from 46 wells, including one deep test, the Amoco M.G. Eischeid #1, on the flank of the Midcontinent Rift (Anderson, 1990). Anderson and McKay (1989) also described the sediments in the flanking basins of the Midcontinent Rift in some detail, summarized in Reed (2000).

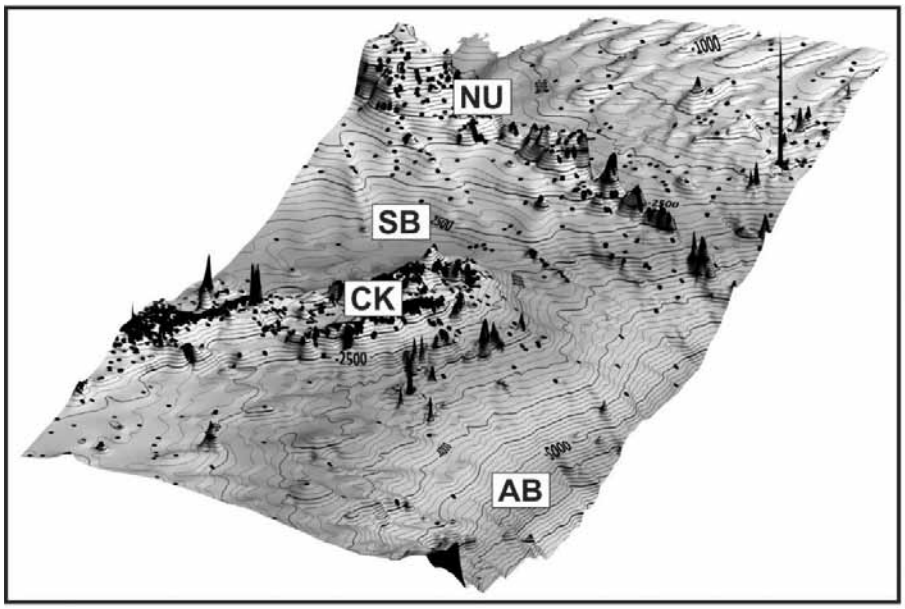

Figure A-4. Erosional remnants on Kansas basement surface, as mapped by Cole (1976), and with significant vertical exaggeration, looking east from Colorado. Most are controlled by multiple wells (black dots). Labels as in Figure A-3.

Minnesota

The Precambrian surface of Minnesota (Figure A-6) is well constrained by data from 40,369 wells with top Precambrian picks, 3,223 additional wells that reach total depth in the Precambrian with no stratigraphic pick, and 2,807 wells that reached total depth in the overlying Mt. Simon Sandstone. This is by far the best constrained Precambrian surface in the study area, made possible in large part by the large areas of shallow Precambrian crystalline rock immediately underlying glacial deposits. In addition, more detailed maps of the Precambrian surface exist in the Minnesota Geological Survey County Atlases (45 out of 87 counties as of this paper). These are not cited individually but can be found at the home page of the survey (https://cse.umn.edu/mgs). Almost all of these Atlas maps were used to help constrain Figure A-6. This surface was a combination of County Atlas Maps, well data points, and control from surrounding states. The well control and careful mapping by Minnesota survey geologists has produced a picture of a deeply eroded basement surface as shown in Figure A-7, which does not blank out areas of exposed or subglacial Precambrian basement. Minnesota occupies part

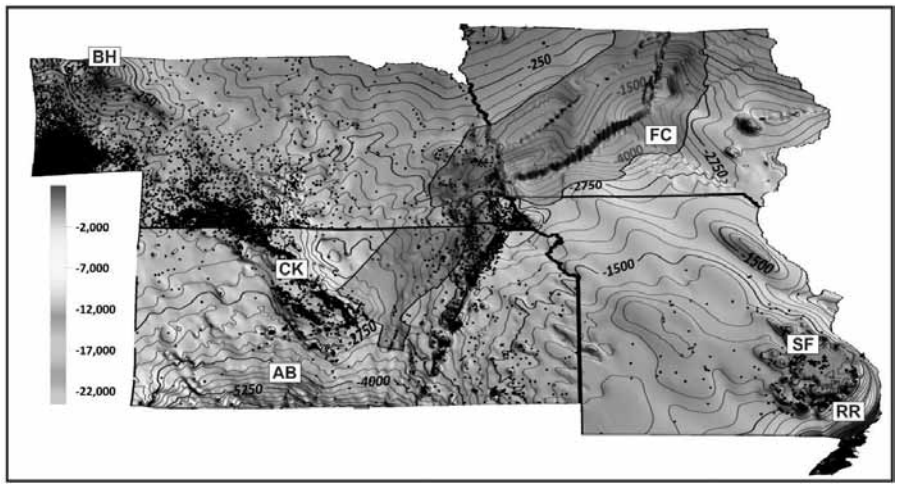

Figure A-5. Configuration of the basement of Nebraska, Kansas, Missouri, and Iowa in feet asl. Contour Interval is 250 feet. Dots show well control. Outline of the Midcontinent Rift shown in darker gray inside dashed line. Features include the Reelfoot Rift (RR), St. Francois Mountains (SF), Nemaha Uplift (NU), Salina Basin (SB), Anadarko Basin, (AB), Forest City Basin (FC), Central Kansas Uplift (CK), and Black Hills (BH). See Figure 7 for Precambrian provinces.

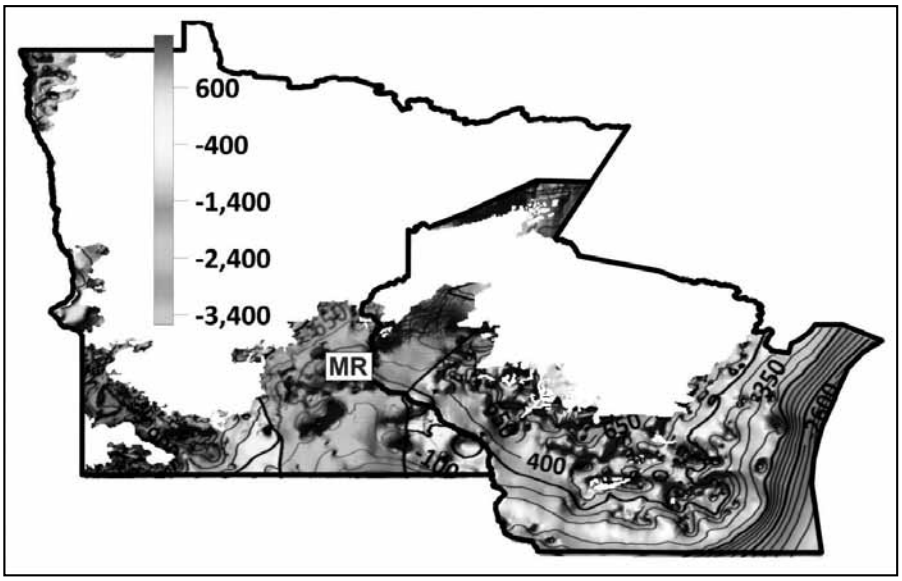

Figure A-6. Configuration of the basement of Minnesota and Wisconsin in feet asl. Contour interval is 200 feet. Blanked areas show subglacial exposed Precambrian crystalline rock. The size of these areas, combined with the thin Phanerozoic sediments results in very low volumes of sediments and with a much higher ratio of Ice Age to marine diluvial strata, though the ratios change significantly when the fill of the Midcontinent Rift is added.

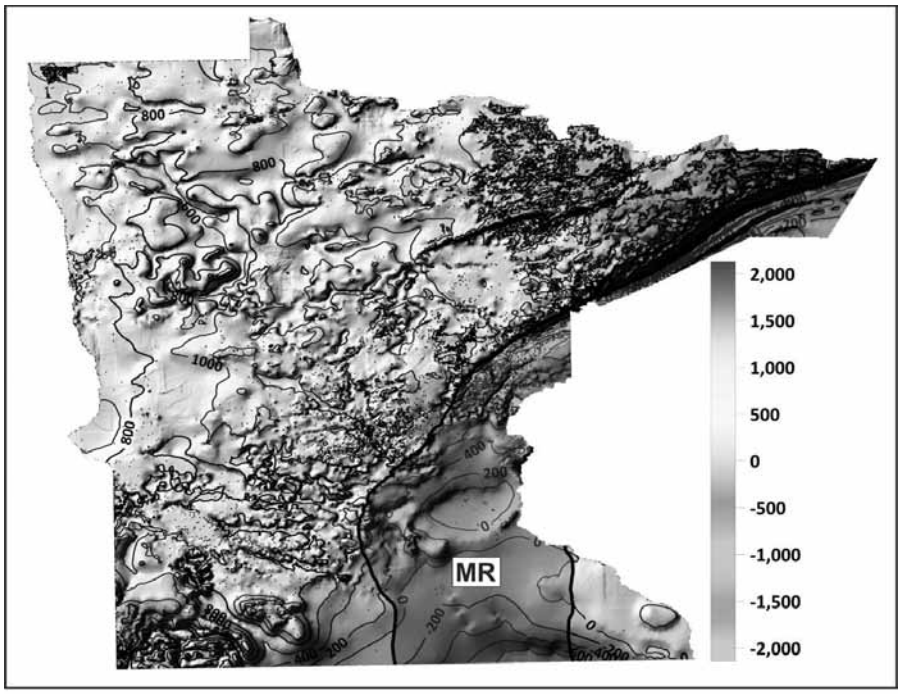

Figure A-7. Precambrian surface of Minnesota with no blanking. Contour Interval is 200 feet. Black dots show well control and abundant well control allows more detailed mapping of the erosion surface. Erosion could date from Early Flood or Late Flood, but it is likely Ice Age. Fewer wells over the Midcontinent Rift surface (MR) smooths contouring there, unlike the detailed picture on the Sioux Ridge (SR) in the southwest corner of the state.

of the southern edge of the Canadian Shield (Boerboom, 2020). Rocks classified as Archean belong to the Superior Province, with several sub-provinces defined and described. These are usually grouped by purported age, with the gneisses of the Minnesota River valley thought to be the oldest, followed by Greenstone-Granite Terrane, followed by metamorphic rocks of the Penokean Orogen in east-central Minnesota (Figure 7). Proterozoic rocks include a Paleoproterozoic terrane of metamorphosed sedimentary and volcanic rocks, including slate, graywacke, quartzite, iron formation, and patches of the Sioux Quartzite. The youngest Precambrian rocks are the Mesoproterozoic volcanic and sedimentary rocks of the Midcontinent Rift. There is abundant copper mined from these rocks, as well as copper, nickel, gold, platinum, and palladium from the Duluth Complex, an intrusive unit associated with the rift on the northwest shore of Lake Superior.

Wisconsin

The Precambrian surface of Wisconsin (Figure A-6) is well constrained by data from 3,190 wells. The only available map of the Precambrian surface was an old USGS map of the upper midcontinent. So we contoured the well data following the general lines of the USGS map and clipped in a recent detailed map of south-central Wisconsin (Stewart et al., 2022). Contours were also constrained by maps from surrounding states, though not at the expense of clear well control. The basement surface, like Kansas and South Dakota, shows evidence of erosion in the form of erosional remnants and channels. That pattern is clearest in the Baraboo Hills (Stewart et al., 2022). A Precambrian geologic map (Mudrey et al., 1982) provides a general picture of the Wisconsin Precambrian. The eastern area is occu-

pied by the Midcontinent Rift, cutting Archean and Proterozoic terranes of the southern Lake Superior Province (Geiger and Guidotti, 1989). These are interpreted to have a long history of igneous and metamorphic activity, particularly the Penokean orogeny. Of some interest are the patches of Baraboo quartzites, which are considered to be of the same middle Proterozoic stratigraphic interval but thought to vary widely in their time and temperature of metamorphism (Geiger and Guidotti, 1989).

Michigan

Michigan lies at the junction of several prominent Precambrian provinces. The Yavapai and Mazatzal Provinces (Figure 7) underlie western and southwestern Michigan, and the Grenville Province underlies the southeastern part of the state. Sims et al. (2008) show boundaries in the central U.S. for the Penokean orogen. However, the Midcontinent Rift forms the most dramatic Precambrian feature of Michigan, extending from the eastern end of Lake Superior through the middle of the state beneath the Michigan Basin (Figure A-8). Though there are limited available seismic data showing details of the rift, COCORP lines (Sleep and Sloss, 1978; Brown et al., 1982) reveal a structure similar to that in the rest of the rift, as expected from the continuity of the linear gravity anomaly from Lake Superior to the Grenville Front (Hinze, 1975; Kucks, 1999) or beyond (Stein et al., 2018).

Aside from the Midcontinent Rift, the most dramatic feature of the Michigan basement is the Michigan Basin. Its subsidence has been stretched by uniformitarian geologists over more than 100 million years, and ultimately tied to episodic crustal weakness linked to the Appalachian Basin development and thermal trends in the crust (Howell and van der Pluijm, 1990, 1999).

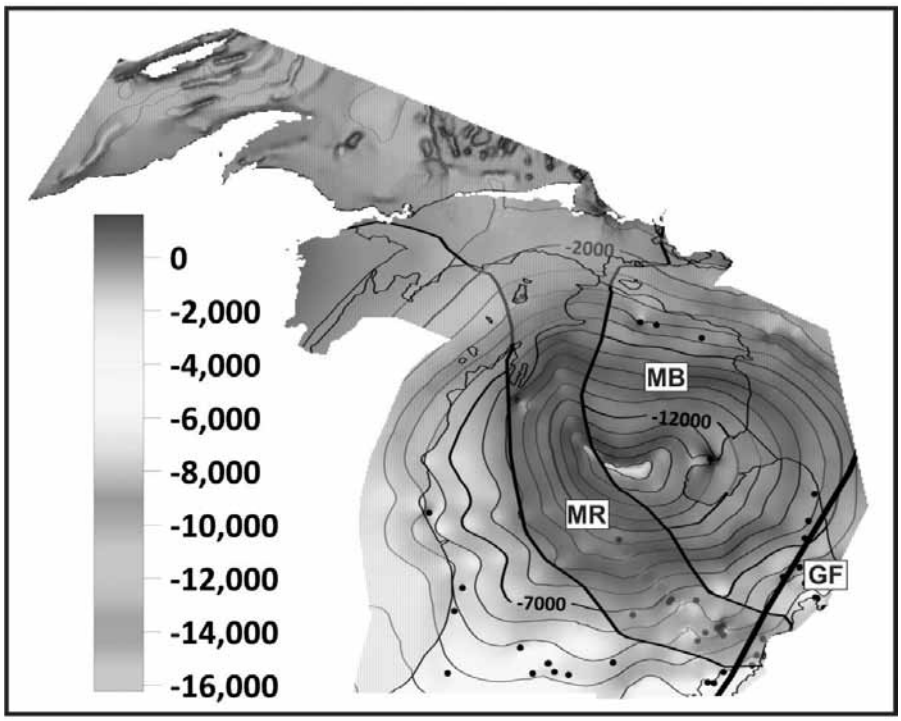

Figure A-8. Configuration of the basement of Michigan in feet asl. Contour interval is 1,000 feet. The Michigan Basin (MB) is underlain by the Midcontinent Rift (MR), shown by the darker gray outline. Parts of the Northern Peninsula are blanked where exposed Precambrian crystalline rock directly underlies glacial sediments, although the bedrock surface beneath Lake Superior is shown.

Illinois

The Precambrian surface of Illinois (Figure A-9) was taken from maps (Collinson et al., 1988; Albert et al., 2016) and constrained by 46 deep wells and seismic data. COCORP lines are publicly available, and private lines are published in some articles (e.g., McBride et al., 2016). The Illinois Basin is a heavily drilled basin, and features are well known in the subsurface, though less so at the Precambrian surface. The state is underlain by the Eastern Granite-Rhyolite Province, although McBride et al. (2016) suggest that small dish structures, a few km across, seen on more detailed seismic data, were created by mafic sills. The deepest part of the Illinois Basin is found in Kentucky, in the Rough Creek Graben (Hickman, 2011, 2013). Freiburg et al. (2022) proposed a Proterozoic Illinois Graben in the eastern part of the state (Figure 7) but evidence is limited. The Rough Creek Graben is bounded by normal faults and largely infilled with Paleozoic sediments, especially thick, Early Cambrian to early Ordovician (Knox Group) sandstones, siltstones, and carbonates. Rifting is interrupted by a basement high just west of the Grenville Front (Figure 7).

Indiana

The Precambrian surface of Indiana is largely underlain by the Illinois Basin (Figure A-9), contoured by Albert et al. (2016) and constrained by 28 wells. It is underlain by the Eastern Granite-Rhyolite Province and cut by the Fort Wayne Rift in the northeastern part

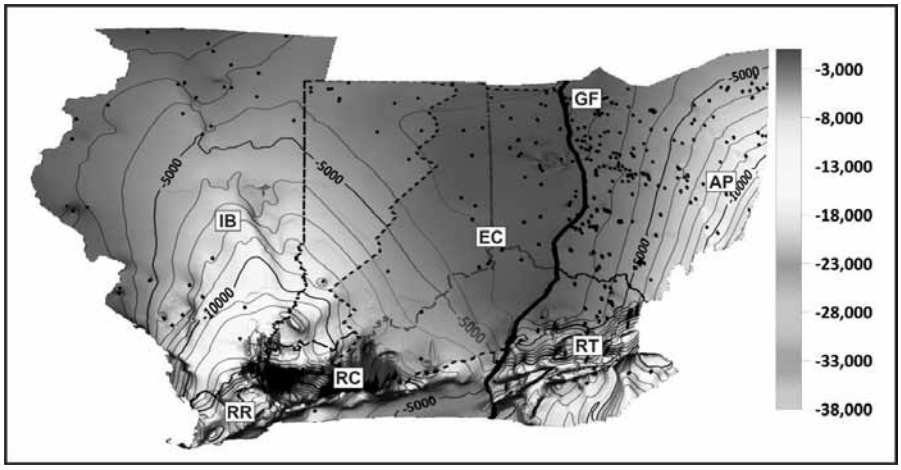

Figure A-9. Configuration of the basement of Kentucky, Ohio, Indiana, and Illinois in feet asl. Contour interval is 1,000 feet. The East Continent Basin (EC, dashed and shaded) is bounded on the east by westward thrusting along the Grenville Front (GF). The Reelfoot Rift (RR), Rough Creek Graben (RC), and Rome Trough (RT) show deep Cambrian rifting, and the trend bends north into the Appalachian Basin (AP) out of the figure.

of the state. The East Continent Basin continues from western Ohio into eastern Indiana and is infilled by volcanics and unfossiliferous red and gray clastic sediments of the Middle Run Formation (Moecher et al., 2018).

Ohio

The Precambrian surface of Ohio (Figure A-9) was mapped by the Ohio Geological Survey (Baranowski, 2013). It is divided north to south by the Grenville Front (Figure 7), separating the Grenville Province from the Eastern Granite-Rhyolite Province. The Precambrian surface in the western part of the state is underlain by sedimentary rocks of the East Continent Basin (Figure 1), and the eastern Ohio basement dips into the Appalachian Basin, with the Cincinnati Arch forming a high in early marine diluvial deposition between the Illinois, Michigan, and Appalachian Basins (Figures 6 and 7).

We obtained data from 205 wells from the Ohio Geological Survey, although Baranowski's (2013) map shows significant additional well control. He also used seismic lines, not publicly available, that provide detailed coverage in some areas (see his map insets). Baranowski contoured the top of the Precambrian surface, which included the Middle Run Formation of the East Continent Basin. The Grenville Front is considered the southward extension of the Canadian Grenville Province (e.g., Bickford et al., 1986), although Stein et al. (2018) used gravity data to propose that it is a southern extension of the Midcontinent Rift. However, seismic data (Baranowski, 2009) show the Grenville Front as an extensive thrust-faulted terrane pushing west over the East Continent Basin, making that debate unclear at present.

Kentucky

The basement surface in Kentucky (Figure A-9) is constrained by 55 wells to the Precambrian, by a number of local seismic lines, and by maps and cross sections published by the Kentucky Geological Survey. Its most dramatic features are the Reelfoot Rift/Rough Creek Graben (Dart and Swolfs, 1998; Csontos et al., 2008; Hickman, 2011, 2013) in the western part of the state and the Rome Trough in eastern Kentucky (Drahovzal and Noger, 1995). These features form deep basement grabens in two distinct segments but do not exhibit the vast basalt flows or dominant terrestrial sedimentation of the Midcontinent Rift. There are thick accumulations of Cambrian sandstones, siltstones, and carbonates (Hickman, 2011, 2013) indicating very rapid sedimentation coinciding with rifting. The Grenville Front runs through central Kentucky and forms the eastern edge of the East Continent Basin, which Drahovzal et al. (1992) extended into Tennessee, although Moecher et al. (2018) terminate it at the edge of the Rough Creek and Rome grabens. Abutting the Grenville Front in Ohio and Kentucky, this basin reaches over 24,000 ft. (7,500 m) (Drahovzal, 1992).

The Horse Evolution Icon Exposed

Jerry Bergman

Abstract

The "horse series" icon of evolution was one of the most commonly cited "proofs" of evolution for over 150 years (Janis, 2008, p. 251). Due to new research and newer discoveries, the popular horse series diagram used in many science textbooks to document straight-line (orthogenetic) horse evolution is now widely acknowledged as inaccurate. It is now recognized that the fossil record documents only that an enormous amount of morphological variety exists in horses, not their gradual evolution from a common ancestor (see Figure 1). Although gradual Darwinian evolution has been rejected, horse evolution has been revised in an attempt to document a scenario more similar to Gould's Punctuated Equilibrium theory and/or Mayr's saltation theory.

Key Words: evolution, fossil record, horse evolution, horses, mammal evolution

Introduction

The many examples of bias and even fraud used to document human evolution have included Piltdown Man, *Hesperopithecus* (Nebraska Man), and Java Man (*Pithecanthropus erectus*). One other often-ignored example of bias that has misled many people relates to horse fossils. Beginning in the 19th century, presentations pictured a simple, gradual, and progressive straight-line horse evolution from the small mammal *Hyracotherium* to the modern *Equus* (see Figure 1). *Hyracotherium,* also once known as *Eohippus* (meaning 'dawn horse') was a small, cat-size mammal, 10–20 inches at the shoulder (Paselk and Lindguist, 2005). So different was *Hyracotherium* from the horse family that *w*hen the "fossils were discovered, *Hyracotherium* was thought to be a monkey" (Jones, 2023). Soon other ideas of what it was surfaced; so many that "scientists in the nineteenth century fought very bitter battles with each other over horse evolution in general. Paleontological disagreements could be nasty, and understanding the evolution of the horse was particularly vexing to European researchers" (Williams, 2015, p. 62). Eventually, *the ladder model* dominated which postulated a steady, gradual evolutionary progression from a "small cat-sized animal" to the modern horse. As will be discussed, the evidence is that *Hyracotherium* was not a horse ancestor due to the enormous morphological difference between *Hyracotherium* and the horses in the ladder model. All, or most, of the other claimed horses that are classified as part of the horse family, illustrate the enormous horse diversity; diversity similar to that of dogs and cats.

The horse family was an important icon because "the so-called progression of horses was considered for a very long time the prime example of evolutionary biology.…'for the truth of evolution,' as George Gaylord Simpson once phrased it" (Franzen, 2010, p. 100). As late as 1997, this progressive evolution claim was still in some textbooks: "The horse provides one of the best examples of evolutionary his-

Accepted for publication June 13, 2024

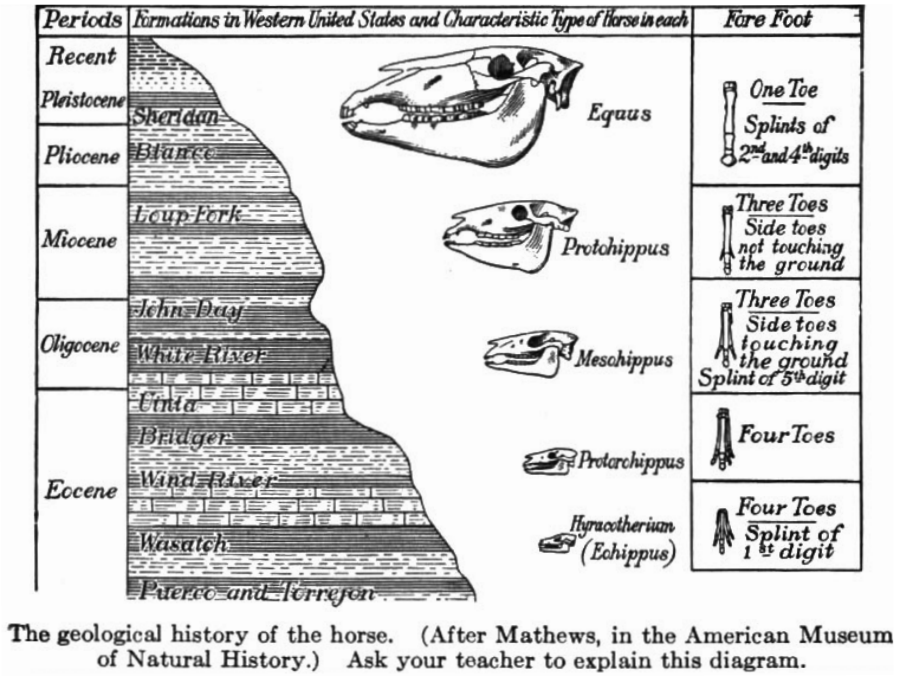

Figure 1. From: Hunter, William. 1914. *A Civic Biology: Presented in Problems*. American Book Company, New York, NY, p. 193. This was the same book that was at issue in the 1925 Scopes Trial. This 1903 diagram by William Diller Matthew was part of a 1920s display at the American Museum of Natural History in New York City. Although widely reproduced, it displayed a "misleading linearity" (Clark, 2008, pp. 28, 145).

tory (phylogeny) based on an almost complete fossil record found in North American sedimentary deposits from the early Eocene to the present" (Soper, 1997, p. 890).

In a chapter titled, "*The Bizarre Course of the Horse* [evolution]," Professor Von Fange observed that these drawings were "copied with some variation in the sequence in museums everywhere as a prize exhibit of evolutionists 'proving' their theory" (Von Fange, 2006, p. 183). The dean of paleontologists, George Gaylord Simpson, wrote that the "beautiful series of ancient and modern horses displayed in many museums are still the simplest way to convince any open-minded person that evolution is a fact. You can see it with your own eyes" (Simpson, 1961, p. xxxiii).

One major problem with horse evolution was the claim that its evolution consisted of a gradual, progressively increased body size. Most horse evolution illustrations show both a steady increase in body size and the alteration of various traits, including the forefoot, hindfoot, forearm, leg, and upper and lower molars (Mather and Chubb, 1924). The gradual increase of horse body size claim was evaluated by Bruce MacFadden of the Department of Vertebrate Paleontology at The American Museum of Natural History. His team analyzed dental and skeletal traits of 40 fossil horses to determine the horses' size changes. The MacFadden study concluded that

> for horses, the traditional interpretation of gradual increase in body size through time is oversimplified because: (1) although the exception to the rule, 5 of 24 species lineages studied are characterized by dwarfism; and (2) the general trend seems to have been a long period (32 ma) of relative stasis followed by 25 ma of diversification and progressive (although not necessarily gradual) change in body size. (MacFadden, 2016, p. 355)

His 32 ma and 25 ma (millions of years) dates were based on several evolutionary assumptions. Nonetheless, it supports my point that a long period of stasis occurred.

Creationists Challenged

The horse evolution icon was also touted as a "nightmare for creationists" by evolutionists as recently as 2016 (Yalmaz, 2016, p. 148). Ex-creationist Aaron Yalmaz even claimed that "The fossil record of horse evolution is by far the most complete of any animal, with almost all of the intermediate species linking the primitive *Hyracotherium* to modern *Equus* known through an excellent series of fossils" (Yalmaz, 2016, p. 148). Ruse, after admitting that the "fossil record has many gaps," added: "It would be nice to see the creationists take on the question of the horse, which is one of the best documented cases of evolutionary change" (Ruse, 1982, p. 311). This review does just that.

The History of the Horse Evolution Story

The horse evolution series was born when Yale professor Othniel Charles Marsh, "one of America's greatest paleontologists, set out to confirm Charles Darwin's evolutionary hypothesis by working out the evolution of the horse" (Milner, 1990, p. 222). To do this he

> collected a magnificent set of American fossil horses and published a paper in 1874 tracing its development from a small three-toed

> animal "the size of a fox" through larger animals with progressively larger hooves, developed from the middle toe. Darwin thought Marsh's sequence from little *Eohippus* ("Dawn horse") to the modern *Equus* was the best evolutionary demonstration anyone had produced in the 15 years since the *Origin of Species* (1859) was published. (Milner, 1990, p. 222)

Inspired by Marsh, the parade of horses from the cat-sized *Hyracotherium* to the modern horse (*Equus caballus*) soon became one of the most well-known textbook examples used to document evolution for almost a century. It has been featured for decades not only in science textbooks, but also in popular mass-market books, and even children's books (Self, 1961, pp. 4–5). This, the "most widely reproduced of all illustrations showing the evolution of horses," was drawn early in the last century for The American Museum of Natural History (AMNH) in New York City, and has been "reproduced hundreds of times since then" (Gould, 1991, p. 174). See Figure 1.

Several leading textbooks used the horse example to illustrate the "slow changes through slight variations" process of evolution to trace the straight-line horse evolution from the simple, primitive, small cat-sized horse to the modern, highly evolved horse (Curtis et al., 1934, p. 615). One textbook described the horse as having

> descended in gradual stages from a creature which existed some sixty million years ago called the *Eohippus*. Within the last hundred years it has been proved that the development of *Equus caballus* took place in what is now North America. (Edwards and Geddes, 1973, p. 14)

Even the book used by the teacher who was prosecuted in the Scopes Trial contained the horse progression illustration (Figure 1) by W.D. Matthew (Hunter, 1914, p. 193). Below the now-infamous horse series drawing, the caption tells students to "Ask your teacher to explain the diagram" (Hunter, 1914, p. 193).

When British scientist Thomas Henry Huxley toured America, he visited Marsh at Yale University and was "mightily impressed with his progressive series of fossil horses" (Milner, 1990, p. 222). When he returned home, Huxley spread the horse progression claim to Europe. Horse evolution supporters claimed that horse phylogeny stretched back over 55 million years,

> From *Orohippus* (Eocene) to *Mesohippus* (Oligocene), to *Miohippus*… (Miocene), to *Protohippus* (Hipparion) and *Pliohippus* (both from the Pliocene), and finally to the Pleistocene and modern day *Equus*. (Franzen, 2010, p. 104)

This was important because the horse family fossil collection was then claimed to show a direct line of evolutionary descent from its precursor animal to the modern horse. To produce an illustration representing his assumption of slow gradual progressive evolution, Marsh selected from a large number of fossils found today in both America and Europe, *some that lived contemporaneously*, to create the illusion of a direct line of evolutionary descent (Chapman, 1992, p. 50).

Although descendants that share common ancestry can live alongside one another, such as the wolf and domestic dog, both are dogs. Marsh selected examples that we now know lived contemporaneously which he dated as having lived, not contemporaneously, but many tens of thousands of years apart. Nonetheless, the success of Marsh's horse example of gradualism evolution made him one of the most prominent paleontologists in the 1870s until his death in 1899.

In 1879, Marsh's work on fossil horses even prompted a letter from Charles Darwin, praising his work as one of the best illustrations of gradualism (continuous progressive evolution) since his [Darwin's] own book, *On the Origin of Species*. Marsh was also one of the first American scientists to embrace Darwin's theory of natural selection and evolutionary gradualism. In turn, Marsh promoted horse evolution to justify his acceptance of Darwinian evolution in contrast to the other theories of evolution, such as Larmarkian evolution, which postulated that organisms altered their behavior in response to environmental changes. Their changed behavior, in turn, modified their body organs, and their offspring inherited these improved structures.

Although Marsh's pictures give the illusion that a slow, gradual evolution of the horse exists from *Hyracotherium* to *Equus*, in fact each of the animals in the illustration abruptly appears in the fossil record, lacking physical evidence of any gradual transitional species. The required evidence which was not found would consist of changes that documented a gradual physical blending from one horse example to the next horse example (see Figure 2, the most recent diagram of horse evolution, discussed below).

Hoof and Toe Evolution

Aside from size, from small to large, one of the changes often used to document horse evolution has been the claimed change of its toe digits from four to the single toe called a hoof. The claimed early horse ancestor, the 'Eocene' *Hyracotherium*, had four front toes, like the modern tapir, compared to the modern horse which has only one (Vincelette, 2023). The horse lineage exhibits the most extreme digit reduction known, from four metacarpals to one, resulting in the *Equus* monodactyl forelimb. The importance of horse-hoof issue was because it was a major part of "evidence" for equine evolution for the reason that the

> traditional story of the evolution of the horse (family Equidae) has been in large part about the evolution of their feet. How did modern horses come to have a single toe (digit III), with the hoof bearing a characteristic V-shaped keratinous frog on the sole, and what happened to the other digits? (Vincelette, 2023)

This change did not involve the evolution of a new trait as required by evolution, but involved the *loss* of its two pairs of side digits. Evidence now exists that they were not lost, but are simply vestigial. Thus the claim that "hooved toes vanished over time, thanks to evolution" (Waugh, 2023). The four toes that are lost in certain non-horse mammals also supports the vestigial theory. Toes vanishing does not support evolution, but rather supports the degeneration theory. Furthermore, because the explanations are driven by an evolutionary ideology, other options are not seriously considered. One such option is that a variety of now-extinct horses once existed in the past, some with several digits, including one with four front toes.

Specifically, the vestigial claim is that the proximal portions of digits II and IV were retained as splint bones and the distal portion was retained as part of the frog. The frog is a tough, thick, V-shaped structure pointing down from the heels which functions to protect the distal cushion beneath it. It also acts as a shock absorber when the horse runs, and aids in both traction and blood circulation in the hoof.

The researchers, by an analysis of the osteology, joint articulations, and both nerve and vessel distribution of the distal forelimb, theorized that

> the *Equus* manus maintains remnants of the 'missing' digits. While it is already known that digits II and IV persist proximally as the splint metacarpals, we propose that digits I and V are also present proximally and that components of all five digits are found distally within the manus. (Solounias et al., 2018)

Professor Solounias et al. concluded that, although "Digit reduction is common among mammals… The horse lineage exhibits the most extreme digit reduction, resulting in the monodactyl" design (Solounias et al., 2018). Furthermore, anatomical and embryological evidence exists for the proximal portions of all the accessory digits (i.e., I and V, as well as II and IV) being retained in the feet of modern horses. Solounias et al. concluded that,

> the evolutionary change to monodactyly is not as dramatic as previously thought and that the horse forelimb is more similar to that of its pentadactyl, tetradactyl and tridactyl ancestors. Although the modern horse maintains only one complete digit, the identities of all five digits are preserved in both the skeletal and soft anatomy as embedded elements into the dominant digit, and the digit positions are consistent with horses in earlier stages of evolution. (Solounias et al., 2018)

Typical of the controversy common in evolution, other paleontologists have marshaled evidence *rejecting* Solounias et al.'s conclusion which was originally published as a paper in the 2018 journal *Royal Society Open Science.* They supported the view that these toes were completely lost in evolution (Vincelette, 2023), and were not retained within the hoof as proposed by Solounias et al. These detractors based their conclusions on their own evaluations of the osteology and metacarpal articulations of the horse and several extinct equids using specimens from the American Museum of Natural History, the Yale Peabody Museum, and the Museum of Comparative Zoology at Harvard.

Their evaluations supported the view that the distant ancestors of modern horses had multiple-hoofed toes which, over time, were lost—leaving the singular hoof existing in modern horses. The advantages of the monodactyly design were detailed by Solounias et al. as follows:

> The reduction of digits in the horse is accompanied by an increase in overall limb length, therefore increasing the distance of each stride. Monodactyly evolves to allow the trot gait characteristic of the modern horse. The limb adapted for the faster trot gait facilitates locomotion in the grassland habitat, as horses are known grazers. The horse limb evolved to move primarily in flexion and extension, and the overall limb structure prevents supination and pronation. In addition, the simplification of the horse hand into a single complete digit stabilizes the limb by reducing the total number of joints. (Solounias et al., 2018)

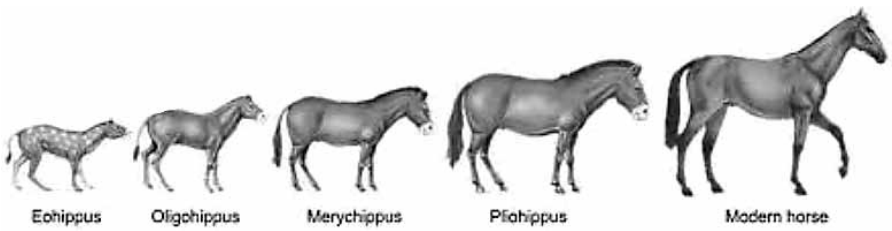

Figure 2. The gradual model of horse evolution. From Wikimedia Commons; https://www.google.com/search?q=modern+horse+evolution+wikimedia+commons.

One of the most extensive studies of horse evolution by George Gaylord Simpson concluded that "the old idea of a steady, uninterrupted reduction in number of toes is, as has lately become clear, not only over-simplified but also essentially false" (Simpson, 1951, p. 193). The reason is because "the reduction was not universal, or constant, and simply counting the toes gives hardly any idea of what is going on in regard to the functioning foot in the animals." In other words, the fossil record of the horse does *not* show a consistent progression from a small, fox terrier-size horse to a modern-size horse, but a great deal of variety. Likewise, the fossil record of the feet does *not* show a consistent progression from three toes to one toe, but a great deal of variety. (Simpson, 1951, p. 193). Modern horses also exist in an enormous amount of variety, as do dogs and cats, but hardly any other modern animal.

There is no agreement among paleontologists on why the loss of toes in modern horses occurred. As described by evolutionary researcher and Harvard graduate, Dr. Brianna McHorse, horses are a classic example of the evolution of "three major traits—large body size, tall-crowned teeth (hypsodonty), and a single toe (monodactyly)—but how and why monodactyly evolved is still poorly understood" (McHorse, 2019). As one headline proclaimed, the evolution of monodactyly is a mystery (Baisas, 2023).

Modern horses have had 3 hooves at least until the 20th century and they are just as much a horse as the 1-hooved majority. This adaptation is thus clearly a microevolutionary change, aka, a variation within their Genesis kind. Furthermore, historically, farmers and ranchers have for centuries surgically removed "extra" toes and selectively bred single-toed horses (Carstanjen, 2007). The reason why is that one big toe provided more resistance to bone stress than many smaller toes, and for this reason were better work horses (McHorse et al., 2017, p. 1).

Of note are the prized horses of Alexander the Great (his horse was named Bucephalus) and Julius Caesar which both had extra toes, indicating that the trait existed for many decades. Neither process is "evolution," and evolutionists appear to be unaware of this human-centric history. The fact that the modern horse hoof provided several advantages supports the view that a variety of designs existed in the past, and horses with multiple digits became extinct for the same reason(s) that many other animals have become extinct.

Harvard's Gould, a Vocal Critic of the Horse Evolution Icon

This staple, ladder-model "proof" for the entire evolutionary theory was described by Gould as the "most common scenario of horse evolution used by Darwinists for decades." He explains that the ladder model was actually "a twisted and tortuous excursion from one branch to another… the path proceeds not by continuous transformation but by lateral stepping with geological suddenness" (Gould, 1991, p. 175).

The horse series that Gould condemned, was the classic *Hyracotherium*, evolving into the three-toed *Mesohippus* (with only one toe touching the ground) which then evolved into the one-toed *Pliohippus*, and lastly ended with the modern horse. The major problem is that the "first chapter in the evolution of the horse—during which all of these developments took place—is missing" (Franzen, 2010, p. 179). In other words, the question of what *Hyracotherium* evolved from was unknown. As University of Chicago paleontologist David M. Raup wrote:

> 120 years after Darwin...the knowledge of the fossil record has been greatly expanded. We now have a quarter of a million fossil species but the situation hasn't changed much.…ironically, we have even fewer examples of evolutionary transitions than we had in Darwin's time. (Raup, 1979, p. 25)

Furthermore, problems also beset the rest of the horse-evolution steps. A specific example is that

> some of the classic cases of Darwinian change in the fossil record, such as the evolution of the horse in North America, have had to be discarded or modified as a result of more detailed information—what appeared to be a nice simple progression when relatively few data were available now appears to be much more complex and much less gradualistic. So Darwin's problem has not been alleviated in the last 120 years and we still have a record which does show change but one that can hardly be looked upon as the most reasonable consequence of natural selection. (Raup, 1979, p. 25)

This problem is not due to lack of research. Bruce MacFadden documented that more research has been completed on horse evolution than all other areas of evolution except human evolution (MacFadden, 1992). Many "new discoveries and reinterpretation of existing museum fossil horse collections have added to the known diversity of extinct forms." For this reason, except *Hyracotherium*, the other examples illustrate the enormous diversity of horses, not its evolution as Darwinists claim (MacFadden, 2005, p. 1729).

The idea of a smooth progression was increasingly called into question as more research was completed. *Pliohippus* (the earliest one-toed horse), was found buried together with *Merychippus* (a three-toed horse from which it supposedly evolved), proving they

lived contemporaneously (Voorheis, 1981, p. 74). Depending on the reference, one or more major links must have existed between *Pliohippus* and *Merychippus*. The reason paleontologists made this judgment was the morphological difference between the two animals was considered too large to bridge the gap between the two horses. This gap was illustrated in the ubiquitous line drawings of horse evolution (see Figure 1) and those based on it (Figure 2).

The Genus *Hyracotherium*

At the base of the evolutionary tree is the animal claimed to be the progenitor of all living and extinct horses, now called *Hyracotherium.* First described by the "great British anatomist" Richard Owen in 1841, Owen named it a hyrax because it "looked" like a cross between a hyrax and pig or *Hyracoidea* (Gould, 1991, p. 60). Owen was a creationist, and therefore did not attempt to link the hyrax animal to horses. Hyraxes were small, rabbit-sized terrestrial or arboreal ungulate mammals. Their blunt heads, short ears and legs, and stubby tails made them look much more like a guinea pig than a horse. Hyraxes, or "rock badgers," still live today in the wild.

Later, Yale paleontology professor Othniel Charles Marsh renamed the hyrax *Eohippus*, meaning "dawn horse," or the "first horse." *Hyracotherium* replaced the term *Eohippus* when the evidence convinced many paleontologists that it was not the progenitor of modern horses, nor a horse ancestor, or even a horse, but a small animal, the specifics of which are still being debated (Gould, 1991 p. 160).

Enormous differences exist between a modern horse and the *Hyracotherium*, not just body size. The *Hyracotherium* was about the size of a house cat, requiring massive changes to evolve to the size of a horse. The changes were from an animal about eight inches tall to one with a height of 1.5 to 2 meters (4.5 to 6 feet), and from an average weight of around 10 pounds to a weight of from 900 to 2,000 pounds (450 to 1200 kg) (Floyd, 2007, p. 102). This weight difference requires a very different skeletal *design* than that of a house cat, specifically one that is strong enough to carry the weight of a 50 to a 180-pound rider (McHorse, 2019, p. 638). Furthermore, *Hyracotherium* had a "primitive," short face, with eye sockets halfway between the back of the skull and the tip of the snout in *Hyracotherium* while in modern *Equus* the eyes are closer to the back.

Paleontologists have many examples to guide them in determining *Hyracotherium* traits because *Hyracotherium* fossils have been found in many Eocene localities both in the western United States and Europe (Solounias et al., 2018). Unfortunately, evolutionary presuppositions dominate the interpretation of the fossil record, distorting the interpretation of the evidence. An example where evolution has been assumed before demonstrated is the following claim: "As the taxa evolved, the forefoot (manus) changed from being tetradactyl to tridactyl and ultimately becoming monodactyl" (Solounias et al., 2018). With the assumption of creation, however, these differences (tetradactyl to tridactyl to monodactyl) are easily explained by designed variations in different animals, as exists today. Furthermore, excluding *Eohippus*, the difference is from tridactyl to monodactyl.

Horse Evolution Not Linear

As illustrated in Figures 2 and 3, what the horse fossil record documents is not linear evolution, but instead an enormous amount of variety, as is true in both horses and dogs today. Nor do the diagrams show an evolutionary tree with connecting branches, but horizontal lines to indicate *possible* or proposed branches. As Gould wrote, the ladder model "is much more than merely wrong. It never could provide the promised illustration of evolution, progressive and triumphant" (1991, p. 180). When the eminent "paleontologist George Gaylord Simpson reexamined horse evolution and concluded that generations of students had been misled.…he showed that there was no simple, gradual unilineal development at all" (Milner, 1990, p. 222).

The Flaws in Gradual Horse Evolution Exposed

In his survey of biology textbooks, Gould wrote that he "found the beam in our own [meaning fellow evolutionists'] eye" and became more distressed by the commonly illustrated parade of horses from a small, dog-sized animal to the modern horse (*Equus caballus*) "than by any capitulation to the yahoos [referring to the creationists]." Gould concluded that the problem with the acceptance of evolution is not based in

> what others are doing to us, but in what we are doing to ourselves. In book after book, the evolution section is virtually cloned. Almost all authors treat the same topics, usually in the same sequence, and often with illustrations changed only enough to avoid suits for plagiarism. Obviously, authors of textbooks are copying material on a massive scale and passing along to students an ill-considered and virtually Xeroxed version with a rationale lost in the mists of time. (Gould, 1991, p. 156)

Gould then discussed in detail what he judged as the most common example of textbook cloning, the section on horse evolution. When textbooks "illustrate evolution with an example from the fossil record, they almost invariably trot out that great-

est warhorse among case studies—the history of horses themselves." Gould adds that the

> standard story begins with an animal informally called *Eohippus* (the dawn horse), or more properly, *Hyracotherium.* Since evolutionary increase in size is a major component of the traditional tale, all texts report the diminutive stature of ancestral *Hyracotherium.* A few give actual estimates or measurements, but most rely upon a simile with some modern organism. For years, I have been much amused (and mildly bothered) that the great majority of texts report *Hyracotherium* as "like a fox-terrier" in size. (Gould, 1991, pp. 158–159)

Even this claim is probably inaccurate—that the average *Hyracotherium* was closer to the size of a house cat. The horse evolution example, although for many decades the primary illustration used to support evolution in high school textbooks, came to an inglorious end. Under the subtitle of horse evolution, "Saddled with Errors," Gould's close colleague and lifetime friend Richard Milner wrote:

> Marsh's classic unilineal (straight-line) development of the horse became enshrined in every biology textbook and in a famous exhibit at the American Museum of Natural History. It showed a sequence of mounted skeletons, each one larger and with a more well-developed hoof than the last. (The exhibit is now hidden from public view as an outdated embarrassment.) (Milner, 1990, p. 222; the statement in parentheses is in the original.)

In 2008 The New York museum totally revised the horse exhibit in an attempt to make it more accurate. However, a search of their website for "*Eohippus*" revealed that the museum continued to teach *Eohippus* as an early pre-horse for decades.

The Enormous Variety of Modern Horses

Horses, like dogs, display enormous morphological variety that is revealed in both living horses and in the fossil record. In size alone, living horses range from the miniature horse, which is about the size of a full-grown German Shepherd and weighs around 200 pounds, to the Shire, which weighs up to 2,300 pounds and stands 68 inches high, close to the size of a small elephant. The world records for size are held by a miniature sorrel brown mare that is only 17.5 inches tall and a Belgian draft horse that is 6 feet 6 inches tall (Campbell et al., 2008).

External morphological differences, including color and hair traits, are other examples of horse variety. The many different horse varieties known today include Fjords, Belgians, and Quarter horses. According to the Swedish University of Agricultural Science, a total of 784 horse breeds exist in the Food and Agriculture database (Horse Breeds, 2022). However, most equine experts recognize close to 200 distinct horse breeds. As far as is known, all are able to interbreed, thus all are part of the horse kind (Moore and Slusher, 2004, pp. 296–297). In short, the pattern of horse evolution "depends to a large extent upon who is telling it." This is because the pattern is

> as chaotic as that proposed by Osborn for the evolution of the Proboscidea [the elephant 'kind'], where, "in almost no instance is any known form considered to be a descendant from any other known form; every subordinate grouping is assumed to have sprung, quite separately and without any known intermediate stage, from some hypothetical common ancestors in the Early Eocene or Late Cretaceous." (Kerkut, 1960, pp. 144, 149)

This same conclusion is still largely valid today. Simpson's study that refuted the ladder theory is still, even now, one of the most authoritative debunkings of the classical horse evolution theory (Simpson, 1951). He showed that some horse types in the series that are now extinct *overlap* in the geological record with other extinct horse kinds that were supposedly their evolutionary precursors. Although they can both have a common ancestor, an animal that lives contemporaneously with another cannot be its ancient ancestor. Gould wrote that each horse genus is actually a

> bush of several related species, not a rung on a ladder of progress. These species often lived and interacted in the same area at the same time (as different species of zebra do in Africa today). One set of strata in Wyoming, for example, has yielded three species of *Mesohippus* and two of *Miohippus*, all contemporaries. (Gould, 1991, p. 179)

A major reason why the multi-branching "bush" view is now the dominant picture of horse history is that the enormous number of horse fossils does *not* show any recognizable pattern supporting gradual straight-line evolution. The bush 'tree' in some ways is remarkably similar to the modern dog family tree. One difference is that the dog "bush" is modern, whilst the source of the horse "bush" is based largely on fossils.

The Extinction Theory

Another position, in horse evolution that is well supported, is that the Eocene *Hyracotherium* was *not an extinct horse* as commonly assumed by evolutionists. Rather, it was an extinct animal that had feet like those of a modern tapir: four toes in front and three behind (Waugh, 2023). Each toe was individually hooved with an underlying foot pad. The extinction theory is supported by the fact that the equid fossil record includes an estimated 50 genera and hundreds

of species, in addition to the extinct Eocene *Hyracotherium*. Thus, the oldest known horse from this view was just another extinct horse-like animal (McHorse, 2019, p. 638). Supporting this view is the finding that many fully modern mammals were found in the same geological strata in which *Hyracotherium* was buried (MacFadden, 1976). If these mammals have not changed since then, why would we expect the *Hyracotherium* to have evolved into a very different animal during the same time?

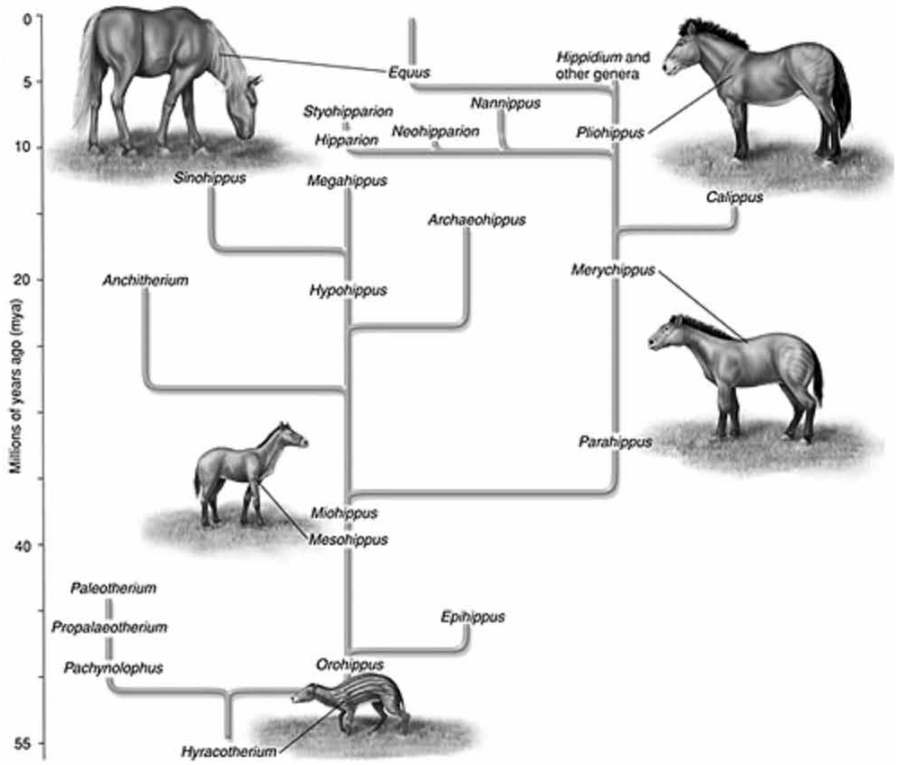

Figure 3. Yet another theoretical horse-evolution tree used in science classes showing these crazy horse fossils. Note again the hypothetical horizontal lines. https://calaski.wordpress.com/science-units/biological-evolution-unit/natural-selection/horse-evolution-tree/.

The Fossil Record

An enormous number of fossil horses exist. An estimated collection of 50,000 are housed in the American Museum of Natural History alone, in addition to the extensive collections of the Smithsonian Institution and several other American and European museums (Janis, 2008, p. 253). A key conclusion of the horse fossil record is that the species that make up these bushes "tend to arise with geological suddenness, and then to persist with little change for long periods" in the fossil record (Gould, 1991, p. 180). The fact that the horse fossil record shows abrupt appearance and stasis, not gradual evolution, is reflected in newer diagrams used to illustrate horse evolution (Janis, 2008, p. 259).

This same existing problem today bothered Darwin. Specifically, the erratic behavior of the horse fossil record "gave Charles Darwin a serious headache. For Darwin, the process of evolution was gentle and even-paced, like a soft English summer rain. Darwin didn't care much for perturbation—when the stress was too great he retired to his favorite health spa… And yet—here were these crazy horse fossils" (Williams, 2015, p. 62–63).

One modern example of these crazy horse fossils is the illustration used in science classes (Figure 3) and the updated horse-evolution tree diagram used at the University of Texas (Figure 4). Note also that the diagram in Figure 6, in dramatic contrast to George Gaylord Simpson's phylogenetic tree (Figure 5), attempts to show horse evolution from a common ancestor. Figure 6 shows 22 different horse-like animals, all of which appeared and disappeared in the fossil record, (shown in black), with no lines showing one ancestral horse evolving into the several new horse varieties via imaginary phylogeny. When the hypothetical horizontal lines are removed, the creationists' "lawn" or "orchard," which is produced strictly by fossil data, is readily apparent. Furthermore, there exists

> no evidence of long-term changes within these well-defined species [of *Mesohippus* and *Miohippus*] through time. Instead, they are strikingly static through millions of years. Such stasis is apparent in most Neogene [later] horses as well, and in *Hyracotherium*. This is contrary to the widely-held myth about horse species as gradualistically-varying parts of a continuum, with no real distinctions between species. Throughout the history of horses, the species are well-marked and static over millions of years. At high resolution, the gradualistic picture of horse evolution becomes a complex bush of overlapping, closely related species. (Prothero quoted in Gould, 1991, p. 180)

Given the standard geological time scale, the fact that many of the animals

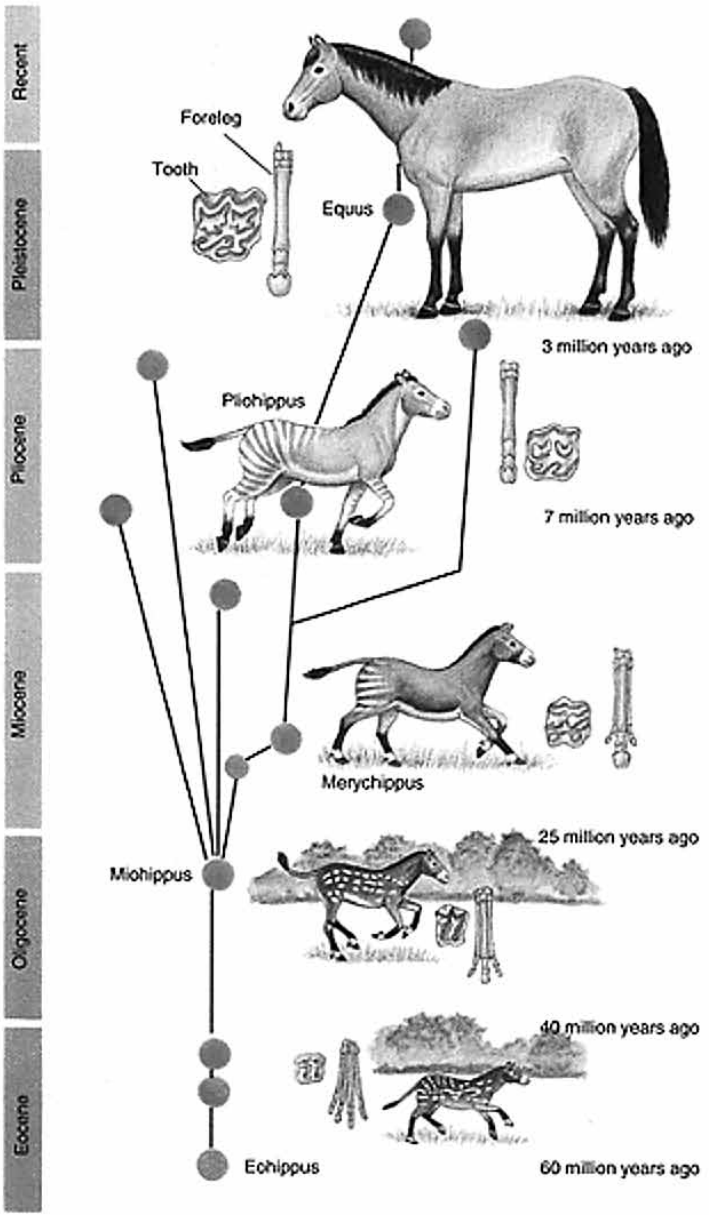

Figure 4. The horse evolution chart used at the University of Texas to teach macroevolution in their Integrative Biology Class. The modern horses are shown to all have evolved from the *Miohippus*. The coloration is conjectural. Note how this is a modification of the now infamous, disproven, 1903 diagram by William Matthew. http://www.sbs.utexas.edu/levin/bio213/evolution/evol.proc.html.

in the horse fossil series are found *in the same strata* is evidence that they lived *at the same general time*, and in the same, or a similar, environment, thus bringing into question whether some were evolutionary ancestors to the other contemporaneous horses in the series. In spite of much speculation, there exists about modern horses

> no unanimity of opinion even among experts concerning the origins of the domestic horse. Debate about it has so far lasted for about 150 years. Even before Darwin's new theories…of evolution, the immense diversity of size, form and color of horses had led inquiring minds to explore the possibility of various primitive races of horse being extinct before the domestication of *Equus caballus*. However, most of these 'primitive races' were supposed to differ from each other in color, and the theorists have therefore been able to draw little support from archaeological remains. (Edwards and Geddes, 1973, p. 14)

Debate on Horse Origins Continues Today

The debate on horse origins continues today, but no dispute remains among experts regarding the fact that the classic horse evolution picture used in the textbooks for the last century is clearly wrong (MacFadden, 1992). See Janis (2008, p. 250) for another conclusion. The main problem

> is the failure of paleontologists to find convincing phylogenies or sequences of organisms demonstrating major evolutionary change. Naturally many will have escaped fossilization or have been subsequently destroyed, but surely one or two should survive? The horse is often cited as the only fully worked-out example. But the fact is that the line from *Eohippus* to *Equus* is very erratic. It is alleged to show a continual increase in size, but the truth is that some of the variants were smaller than *Eohippus*, not larger. Specimens from different sources can be brought together in a convincing-looking sequence, but there is no evidence that they were actually arranged in this order in time. 'Phylogeny is still biology's major unfinished task,' admits Professor Hanson. (Taylor, 1983, p. 230)

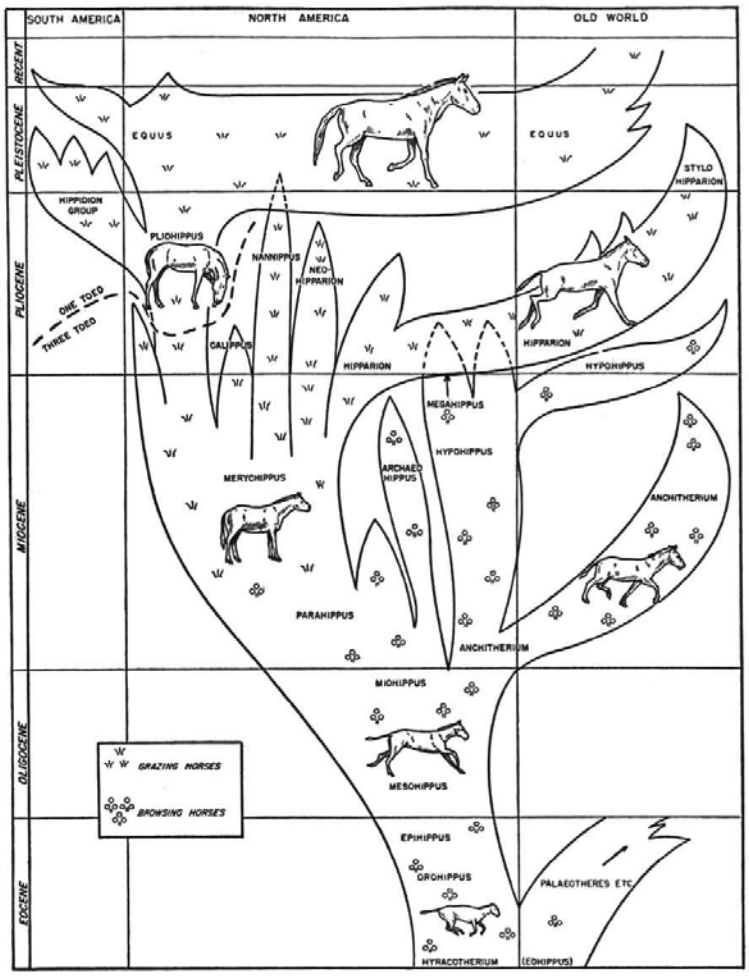

13. The lineages of the horse family. The main lines of horse descent and relationships of the more important genera treated in the text. The restorations are to scale.

Figure 5. Diagram showing the evolution tree from the alleged ancestor of all horses, *Hyracotherium*. From: Simpson, George Gaylord. 1951. *Horses: The Story of the Horse Family in the Modern World and Through Sixty Million Years of History*. Oxford University Press, New York, NY, p. 114.

This conclusion is quite in contrast to the paleontological opinion expressed in 1926 which declared: "evolution…from the simple Eocene ancestor to the large and specialized horse of today [demonstrates] a progressive series leading to the living horse" (Loomis, 1926, p. 218). The main cause for this evolution was "apparently…natural selection and mutation" (Loomis, 1926, pp. 218, 224). American paleontologist Frederic B. Loomis concluded that "paleontology proves the fact of evolutionary progress in the horse line…but, as of yet, we know almost nothing about how new mutant types originate" (Loomis, 1926, p. 228).

As early as 1923, George McCready Price concluded that the now infamous 1903 diagram by William Diller Matthew consisted of an arrangement "not found in nature—this is a purely artificial arrangement made up from widely scattered formations with nothing whatever of actual fact." He added that, all these so-called 'horses' may have once been living contemporaneously (Price, 1923, p. 562).

The major well-documented problems of the horse series were reviewed back in 1954 by University of Lund professor Heribert-Nilsson (Cousins, 1971). In 1943, Heribert-Nilsson was elected a member of the Royal Swedish Academy of Sciences, the organization that awards the Nobel Prizes. Nilsson concluded that "The family tree of the horse is…continuous only in the textbooks" (Heribert-Nilsson, 1954).

Evolutionists Deal with the Loss of the Horse Progression Theory

Specifically, evolutionists rejected the "straight shot," "ladder-like," "orthogenic," gradual "Darwinian view" of horse evolution. Consequently, they reject Darwin's theory of evolution by natural selection which taught the gradualistic model whereby "natural selection acts solely by accumulating slight, successive, favorable variations, [and therefore] it can produce no great or sudden modifications; it can act only by very short and slow steps" (Darwin, 1859, p. 471).

Nonetheless, due to the overwhelming evidence against the gradualists' model leading to the rejection of the Darwinian gradualistic model of horse evolution, most committed evolutionists reject creation, and therefore must accept the belief that horses evolved from some hypothetical *Eohippus*-like creature. One alternative that came after rejecting Darwin's view was to replace straight-line, horse evolution with the punctuated-equilibrium evolutionary model.

The Punctuated Model

Over 110 years after Darwin introduced the natural selection theory,

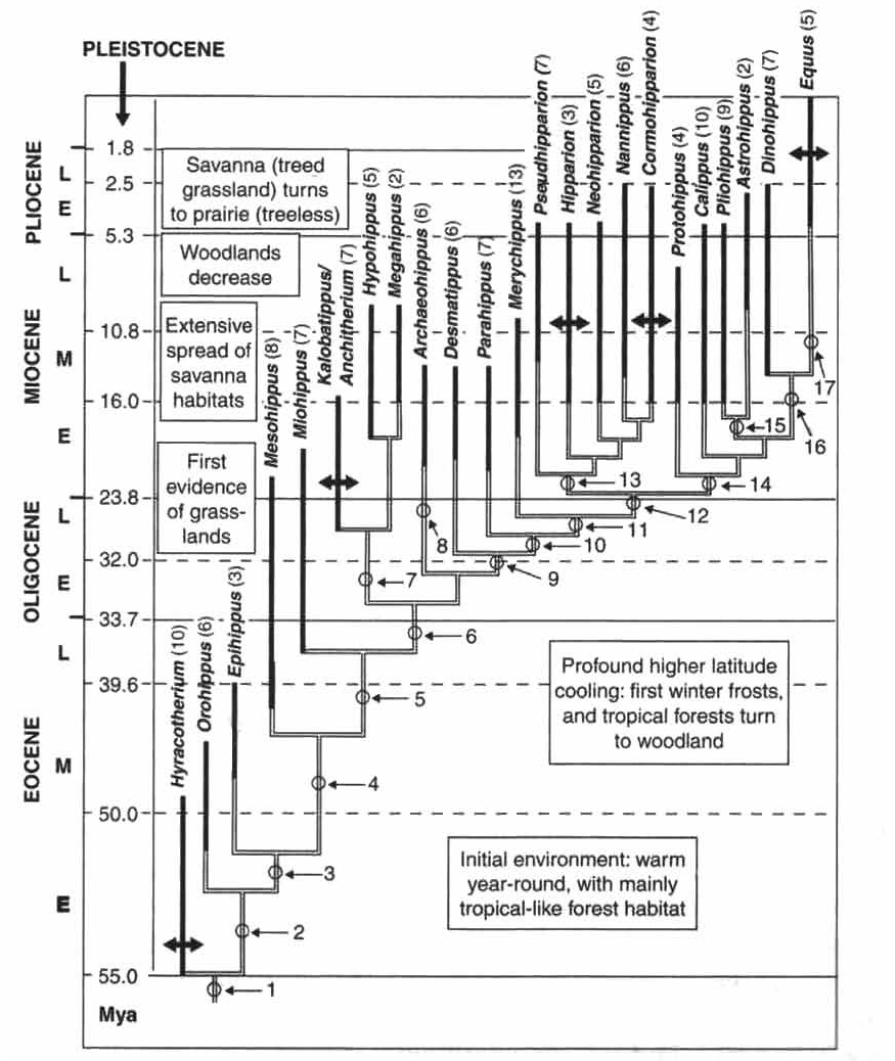

Figure 6. The most detailed horse diagram showing horses appearing in the fossil record and some that became extinct. It does not even attempt to show the tree diagram in contrast to the Simpson diagram (Figure 5). The dark black lines are based on actual fossil data and the light double lines are hypothetical evolutionary lineages. The figure shows 22 different horse kinds. From: Janis, Christine. 2008. "The Horse Series." In *Icons of Evolution: An Encyclopedia of People, Evidence, and Controversies*, pp. 251–280, p. 259. Brian Regal (editor). Greenwood Press, Westport, CN.

Niles Eldredge and Stephen Jay Gould introduced the theory of Punctuated Equilibria to replace Darwin's gradualistic account of evolution. They observed that very little change occurred between speciation events—a phenomenon they referred to as evolutionary stasis. The fossil record often showed rapid bursts of change followed by longer periods in which little or no change occurred. After documenting the problems with the gradualistic model, Eldredge argued that the Punctuated Equilibria model was superior. Referring to the horse-evolution display at the American Museum in the 1920s, based on the 1903 diagram by Matthew, Eldredge observed that

> Undoubtedly one message the exhibit intends to convey is the gradual and even directional nature of horse evolution…the message comes through loud and clear: anyone looking at the exhibit is bound to come away with the notion that evolution is a matter of gradual, or progressive change through time…. [In fact] each specimen represents an entire species that was but one of several species alive at any one time, and when we further recognize that each species tended to remain stable for [at] least a million years, we get the alternative, more 'punctuated' picture of evolutionary change. (Eldredge, 1987, pp. 221–222)

More than 40 years after Gould and Eldredge proposed their theory, "the theory of punctuated equilibria remains controversial, with many biologists still unconvinced as to the value of the theory as a description of how evolution proceeds" (Venditti and Pagel, 2008, pp. 274–275).

Conclusions

The focus of this review has been on the horse evolution "ladder" illustration that was once prominently displayed in the textbooks to prove "molecules-to-man" evolution. This idea, along with the illustration that supports this view, has now been carefully refuted by many prominent paleontologists. Its importance is illustrated by the fact that in the past "apart from human evolution, horse evolution represents the only "classic" example [of evolution] from the mammals" (Janis, 2008).

The fact is "Fossil horses have since become one of the exemplars of evolu-

tion as displayed in the fossil record, endlessly repeated and recycled in textbooks and museum displays (but often with outdated or incorrect information)" (Prothero, 2009, p. 290). As Milner concluded, the history of horse evolution is "saddled with errors" and the gradualism model is only one example (Milner, 1990, p. 222).

What the fossil record shows is an enormous variety in the horse kind similar to what we find in the dog and cat kinds. Likewise, little agreement exists on the evolution-based, phylogenetic trees, as illustrated in Figures 3 to 6. The modern horse kind displays enormous variety, and because, as far as is known, most of the numerous horse species can hybridize, they are a single family. The fact is that the

> evolutionary sequence of fossil horses was the prime example of straight-line evolution, or—more scientifically—orthogenetic or orthoselective evolution. We know today that this concept is wrong. It was based on the few fossil finds known from the end of the nineteenth century….We are still a long way from tracing evolutionary development from species to species. Considering the gaps in the fossil record, it is questionable whether we will ever achieve this aim. (Franzen, 2010, p. 179)

In other words, in spite of over two centuries of research, we have no convincing evidence of the evolution of horses from non-horses, which is the central concern of evolutionists. In contrast, we have a great deal of evidence for genetic stasis and an enormous variety within the horse kind.

Nonetheless, the peer-reviewed literature on this topic is often irresponsible, such as the claim by W.D. Matthew that the horse "fossil record is the most complete among the larger animals" (Matthew, 1926, p. 139). In his 1926 article, Matthew strongly argued against creation, concluding that the evidence is unequivocal: evolution is fact, and creation has been disproved based on the evidence for horse evolution (Matthew, 1926, p. 176).

Christine Janis uses an entire chapter in an attempt to discredit the creation/intelligent design position on horse evolution. Her faith in Darwinism remains intransigent in spite of her inability to document horse evolution from some hypothetical, non-horse ancestor. The late Harvard professor Ernst Mayr wrote:

> one would expect the fossils to document a gradual steady change from ancestral forms to the descendants. But this is not what the paleontologist finds. Instead, he or she finds gaps in just about every phyletic series. New types often appear quite suddenly, and their immediate ancestors are absent in the earlier geological strata… the fossil record is one of discontinuities, seemingly documenting jumps (saltations) from one type of organism to a different type." (Mayr, 2001, p. 14)

History has shown that Matthew's now infamous horse-evolution chart is misleading if not fraudulent (Matthew, 1926, p. 172). Unfortunately, the horse series idea still lives on in the textbooks in spite of its exposure as a myth (Morris, 2008, p. 13). It has to live on because, if creation is wrong, evolution *must* be true. No other option exists. Evolutionists believe that all life has evolved from some simple life-form. Consequently, they have attempted to produce a horse series from the current bush 'horse-tree' to support their view. The attempts proposed are very different and contradictory, being subject at times to the directive whims of a single, horse-series textbook author.

References

CRSQ: Creation Research Society Quarterly

Baisas, L. 2023. Horses once had multiple hoofed toes. What happened to them is still a bit of a mystery. *Popular Science*. https://www.popsci.com/science/horse-hooves-toes-feet-evolution/.

Blakely, R.L. 1985. Miniature horses. *National Geographic* 167(3):384–393.

Campbell, N.A., J.B. Reece, and E.J. Simon. 2008. *Essential Biology*. Benjamin Cummings, New York, NY.

Carstanjen, B., et al. 2007. Bilateral polydactyly in a foal. *Journal of Veterinary Science* 8(2): 201–203.

Cavanaugh, D.P., T.C. Wood, and K.P. Wise. 2003. Fossil equidae: A monobaraminic, stratomorphic Series. *Proceedings of the Fifth International Conference on Creationism* 5(11):143–155. Creation Science Fellowship, Pittsburgh, PA.

Chapman, G. 1992. Horse nonsense. *Creation Ex Nihilo* 14(1):50.

Clark, C.S. 2008. *God or Gorilla: Images of Evolution in the Jazz Age*. Johns Hopkins University Press, Baltimore, MD.

Cousins, F. 1971. A note on the unsatisfactory nature of the horse series of fossils as evidence for evolution. *CRSQ* 8(2):99–108.

Curtis, F.D., O.W. Caldwell, and N.H. Sherman. 1934. *Biology for Today.* Ginn and Company New York, NY.

Edwards, E., and C. Geddes. 1973. *The Complete Book of the Horse*. Arco Publishing Company, New York, NY.

Eldredge, N. 1987. *Life Pulse: Episodes from the Story of the Fossil Record*. Facts On File, New York, NY.

Floyd, A.E. 2007. "Evolution of the Equine Digit and Its Relevance to the Modern Horse." Chapter 7 in *Equine Podiatry*. A.E. Floyd and R.A. Mansmann (editors). W.B. Saunders Company, New York, NY (Elsevier, Health Sciences Division, St. Louis, MO).

Franzen, J. 2010. *The Rise of Horses: 55 Million Years of Evolution*. Johns Hopkins University Press, Baltimore, MD.

Gould, S.J. 1991. *Bully for Brontosaurus.* W.W. Norton & Company, New York, NY.

Heribert-Nilsson, N. 1953. *Synthetische Artbildung: Grundlinien einer exakten Bi-*

ologie. C.W.K. Gleerup, Lund, Sweden.

Horse Breeds. 2022. How many horse breeds are there in the world? https://horseracingsense.com/how-many-horse-breeds-are-there-world/.

Hunter, G.W. 1914. *A Civic Biology: Presented in Problems.* American Book Company, New York, NY.

Janis, C. 2008. "The Horse Series." In *Icons of Evolution: An Encyclopedia of People, Evidence, and Controversies*, pp. 251–280. Brian Regal (editor). Greenwood Press, Westport, CN.

Jones, D. 2023. Hyracotherium. https://www.floridamuseum.ufl.edu/fossil-horses/gallery/hyracotherium/.

Keen, C. 2005. Ideas about fossil has undergo evolution in thinking. *Florida Museum of Natural History*. https://www.floridamuseum.ufl.edu/science/ideas-about-fossil-horses-undergo-evolution-in-thinking/.

Kerkut, G.A. 1960. *Implications of Evolution*. Pergamum Press, New York, NY.

Loomis, F.B. 1926. *The Evolution of the Horse*. Marshall Jones Company, Boston, MA.

MacFadden, B. 1992. *Fossil Horses: Systematics, Paleobiology, and Evolution of the Family Equidae.* Cambridge University Press, New York, NY.

_____. 2016. Fossil horses from "Eohippus" (*Hyracotherium*) to *Equus*: Scaling, Cope's Law, and the evolution of body size. *Paleobiology* 12(4):355–369.

MacFadden, B. 2005. Fossil horses—Evidence for evolution. *Science* 307(5716):1728–1730.

Matthew, W.D. 1926. The evolution of the horse: A record and its interpretation. *The Quarterly Review of Biology* 1(2):139–185.

Matthew, W.D., and S.H. Chubb. 1921. *Evolution of the Horse.* American Museum of Natural History, New York, NY.

MacFadden, B.J. 1976. Cladistic analysis of primitive equids, with notes on other perissodactyls. *Systematic Zoology* 25(1):1–14.

McHorse, B. 2019. Mechanics of evolutionary digit reduction in fossil horses. *Proceedings of the Royal Society B* 284(1861):20171174. http://dx.doi.org/10.1098/rspb.2017.1174.

McHorse, B., et al. 2019. The evolution of a single toe in horses: Causes, consequences, and the way forward. *Integrative and Comparative Biology* 59(3):638–655.

Milner, R. 1990. *The Encyclopedia of Evolution.* Facts on File, New York, NY.

Molen, M. 2009. The evolution of the horse. *Journal of Creation* 23(2):59–63.

Moore, J.N., and H. Slusher. 2004. *Biology: A Search for Order in Complexity*, Second Edition. Christian Liberty Press, Arlington Heights, IL.

Morris, J. 2008. The mythical horse series. *Acts & Facts* 37(9):13.

Nilsson, H. 1954. *Synthetische Artbildung*. Verlag CWE Gleerup, Lund, Sweden.

Paselk, R., and M. Lindguist. 2005. https://natmus.humboldt.edu/exhibits/prehistoric-mammals/horses.

Pendragon, B. 2015. Phylogeny of the horse—From tapir-like hyracotheres or from equine anchitheres? *Journal of Creation* 29(3):87–96.

Price, G.M. 1923. *The New Geology*. Pacific Press, Mountain View, CA.

Prothero, D. 2009. Evolutionary transitions in the fossil record of terrestrial hoofed mammals. *Evolution Education Outreach* 2:289–302.

Raup, D. 1979. Conflicts Between Darwin and Paleontology. *Field Museum of Natural History Bulletin* 50(1):22–29.

Reeves, C.R. 2021a. A critical evaluation of statistical baraminology: Part 1—Statistical principles. *Answers Research Journal* 14:261–269. https://answersresearchjournal.org/statistical-baraminology-principles/.

Reeves, C.R. 2021b. A critical evaluation of statistical baraminology: Part 2—Alternatives and conceptual and practical issues. *Answers Research Journal* 14:271–282.https://answersresearchjournal.org/statistical-baraminology-alternatives-issues/.

Ruse, M. 1982. *Darwinism Defended*. Addison-Wesley, Reading, MA.

Self, M.C. 1961. *The How and Why Wonder Book of Horses*. Wonder Book (and C.E. Merrill), New York, NY.

Simpson, G.G. 1951. *Horses.* Oxford University Press, New York, NY.

Simpson, G.G. 1961. *Horses.* Doubleday Anchor, New York, NY.

Solounias, N., et al. 2018. The evolution and anatomy of the horse manus with an emphasis on digit reduction. *Royal Society Open Science* 5(1). https://royalsocietypublishing.org/doi/10.1098/rsos.171782.

Soper, R. (editor). 1997. *Biological Science 1 and 2*, Third Edition. Cambridge University Press, Cambridge, England.

Taylor, G.R. 1983. *The Great Evolution Mystery*. Harper & Row, New York, NY.

Venditti, C., and M. Pagel. 2008. Speciation and bursts of evolution. *Evolution: Education and Outreach* 1:274–280.

Vincelette, A.R. 2023. Hipparion tracks and horses' toes: The evolution of the equid single hoof. *Royal Society Open Science* 10(6). https://royalsocietypublishing.org/doi/full/10.1098/rsos.230358.

Von Fange, E.A. 2006. *In Search of the Genesis World: Debunking the Evolution Myth*. Concordia Publishing House, Saint Louis, MO.

Voorheis, M. 1981. Ancient ashfall creates Pompeii of prehistoric animals. *National Geographic* 59(1):66–75.

Waugh, R. 2023. Horses 'used to have toes,' new study shows. *yahoo!news*. https://www.yahoo.com/news/horses-used-to-have-toes-new-study-shows.

Wells, J. 2000. *Icons of Evolution: Science or Myth? Why Much of What We Teach About Evolution Is Wrong*. Regnery Publishing, Washington, D.C.

Williams, Windy. 2015. *The Horse. The Epic History of Our Noble Companion*. Scientific American, New York, NY.

Yilmaz, A. 2016. *Deliver Us From Evolution? A Christian Biologist's In-Depth Look at the Evidence Reveals a Surprising Harmony Between Science and God*. Sehnsucht Publishing Company, Hamburg, Germany.

Creation Research Society Quarterly 2024 61:146–157

Sternberg's Law Statistical Study of Surficial Gravels in North Central Montana— Part II: Analysis and Conclusions

Peter Klevberg

Abstract

As was shown in Part I of this paper, a simple application of Sternberg's Law of downstream fining does not accommodate all the data included in this study. The study area includes the low-relief Great Plains and the high relief of the Rocky Mountains, good overall terrain for application of Sternberg's Law, but with some complications from isolated mountain ranges. Most of the study area exhibits evidence of glaciation, but diluvial planation surfaces are also present. Channelized flow, transport by ice, and sheet flow are all candidate processes for transport of gravel. Results from statistical analysis of 5,839 sieve analysis reports indicate a complex history for the surficial gravel deposits.

Key Words: geostatistics, grain size distribution, gravel, paleohydrology, Sternberg's Law

Background

As shown in Part I (Klevberg, 2024), Sternberg's Law (Sternberg, 1875) relationships are evident in the data from the study area (Figure 1), but the data do not show a simple Sternberg's Law relationship (Figure 2). Maximum and mean particle sizes decrease from the mountain front toward the Great Plains in a generally exponential manner, though effects from the mountain ranges are imprinted on the general fining-eastward trend.

The relationship between mean size and sorting is weak. Various scenarios could explain this:

- Transport from a given source is not reflected in the data, i.e., they are unrelated deposits.
- Transport from a given source is reflected in the data but not the source itself, i.e., they are similarly deposited ("all at once").
- A significant portion of the data resulted from Case IV.
- Glacial transport was involved; ice was too viscous for sorting to occur.

As shown in Table I, positive skewness coincides with Cases II–IV of McLaren (1981) and is not diagnostic. The relationship between mean and skewness does not appear to be significant. The skewness could be explained by a mixture of Case I and the other cases per Table I.

Accepted for publication November 28, 2023

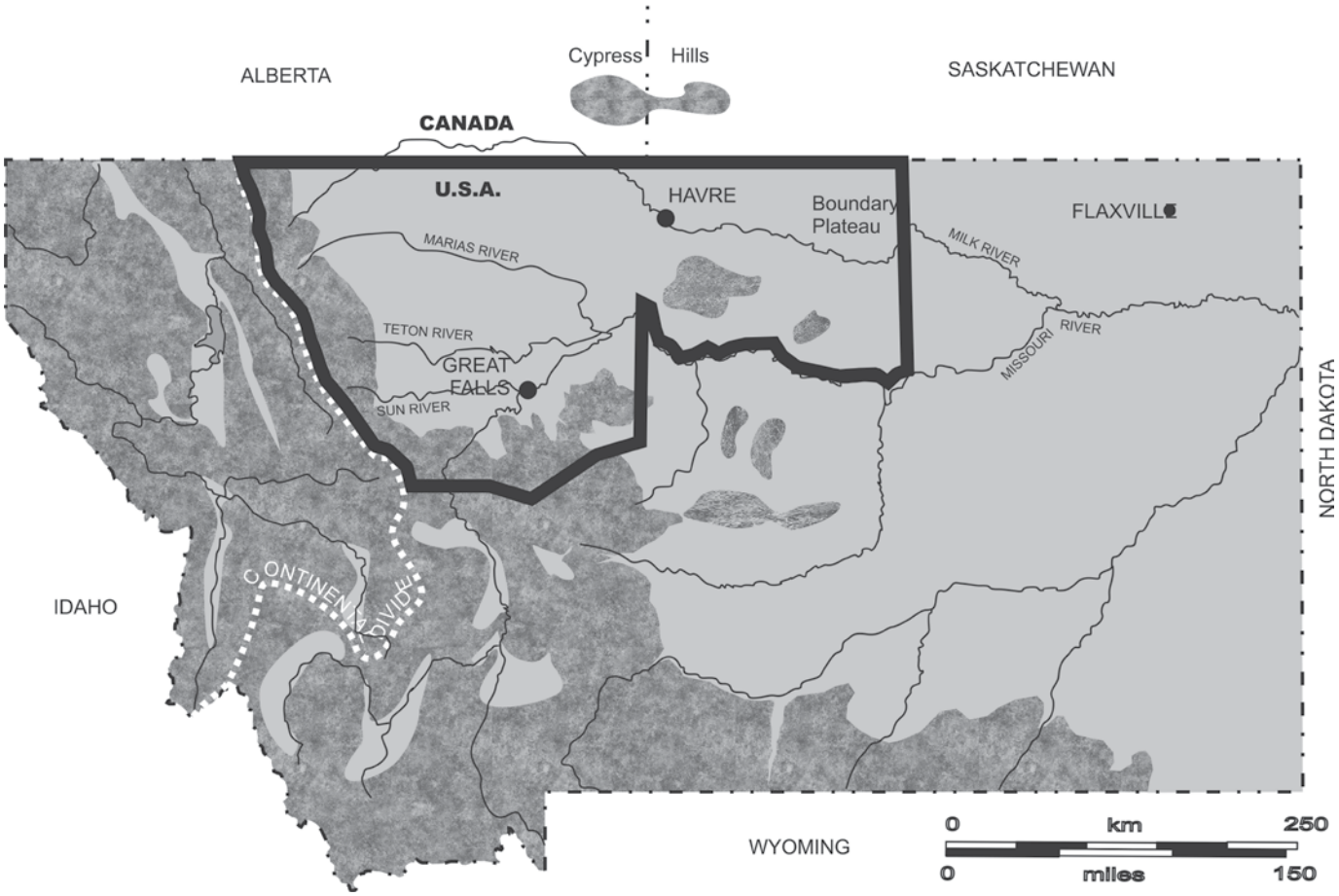

Figure 1. Study area in North Central Montana indicated by outline.

Data plotted on a C-M diagram (Figure 3) generally fit the river-terrace gravel region with a small percentage in the beach gravel region. Very few samples fell in the till region, and then only in the part of that region abutting the river-terrace gravel region.

Analysis

Predictions from fluvial, glacial, and diluvial hypotheses are compared to the statistical analysis of the study area gravels in Table II. While Sternberg's Law is straightforward for a single stream reach, it is complicated by the size and topography of the study area. Portions of the study area long recog-

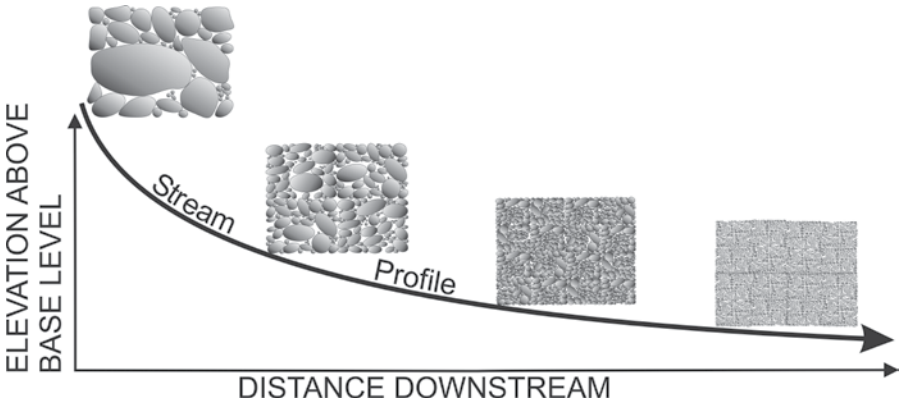

Figure 2. Idealized map showing expected change in particle size based on Sternberg's Law and topography (dashed lines) superimposed on measured mean grain size isopleths (solid lines) based on Trask definition. Only rough correspondence is evident.

Table I. Effects of Transport Sequence (after McLaren, 1981).

Case	Process	Mean	Sorting	Skewness
I	Erosion incapable of removing largest clasts from source, transport, total deposition	smaller	better	negative
	Erosion capable of removing all clasts, segregation in transport, total deposition following lag deposition (segregation)			
II	Erosion incapable of removing largest clasts from source, then lag deposition	coarser	better	positive
	Erosion capable of removing all clasts, then lag deposition			
IIIA	Erosion incapable of removing largest clasts from source, transport, selective deposition	finer	better	positive
IIIB	Erosion capable of removing all clasts, transport, then selective deposition	coarser		
IVA	Current with excess capacity erodes into bed, wanes, selective deposition	fining*	poorer	positive*
IVB	Current with excess capacity erodes into bed, wanes, total deposition			uncertain*

Cases I–III from McLaren (1981); Case IV added.

*Constant changes to mean and skewness with constant incorporation of material and deposition.

nized as unglaciated (Alden, 1932) display characteristics of diluvial rather than the fluvial/alluvial deposition that uniformitarians posit (Klevberg and Oard, 1998). Figure 4 grants the benefit of the doubt to uniformitarians by including potentially diluvial deposits as "braid plain" deposits from streams. When superimposed on maps of project data (Figures 4 and 5), there is a degree of correspondence, along with differences. Figure 6 shows somewhat less correspondence. As the D_{95} value is linked to competence, there is a definite mountains-to-plains fining in the D_{95} data.

Sorting is the standard deviation of the population and the inverse of grading. Differential transport increases sorting and uniformity of the sediment. In modern streams, especially gravel-bedded rivers, channel geometry can complicate and confuse this (Buffington and Montgomery, 1999; Mohtar et al., 2017). Sorting is simplest in sheet, beach, and uniform channel

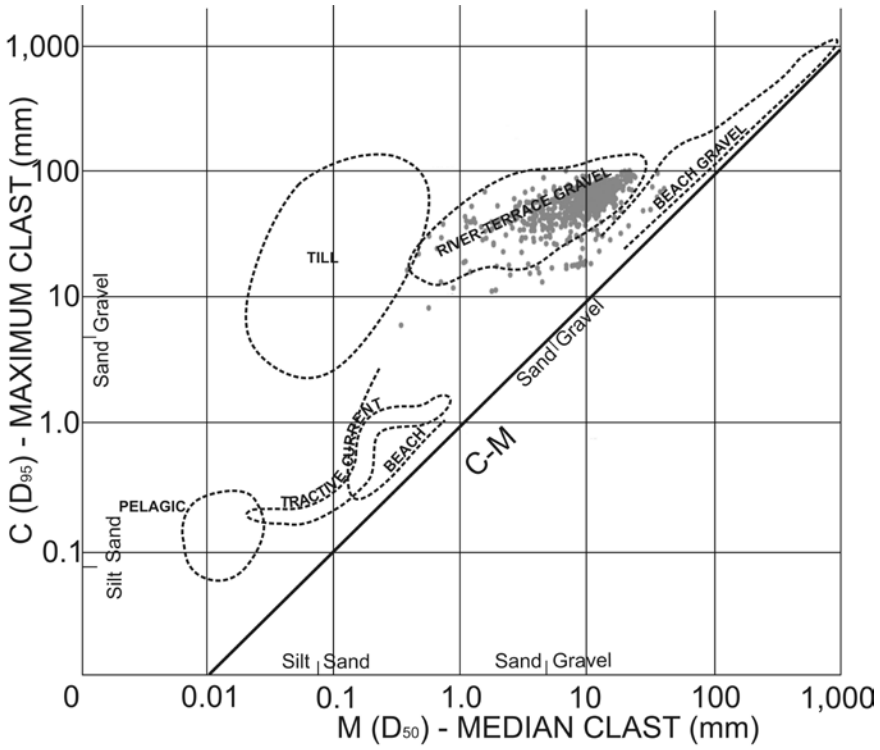

Figure 3. Plot of maximum (C) vs. mean (M) clast size. Maximum is normally defined as D_{99}, but D_{95} substituted here, shifting points very slightly down. Fields corresponding to transport mechanisms are shown by dashed lines as modified from Passega (1964) and Schlee (1973).

Table II. Analysis of Statistical Results.

Parameter	Process	Prediction	Observation
Mean and Largest Clast Sizes	Fluvial	Exponential, rapid reduction in maximum and mean downstream per Sternberg on a reach basis between tributaries	Fining from west to east and from mountain front on south to northeast is evident for all methods, though most obscure with Inman and clearest with Kondolf & Wolman and Trask methods. General reflection of topography.
	Glacial	Very large boulders possible, including many angular rocks, mean size may be unrelated	
	Diluvial	Potentially very large clasts, mean may be related to maximum via flattened Sternberg relationship, rocks rounded	
Sorting	Fluvial	Consistent increase in sorting downstream per reach between tributaries likely	No clear regional pattern; mapping of Kondolf & Wolman and Inman sorting may show weak local patterns; a few locations on rivers seem to have poorer sorting.
	Glacial	No evident sorting	
	Diluvial	None (maximum sheet flow) to increased sorting with distance for waning, channelized flow	
Skewness	Fluvial	More negative with strong (winnowing) current, more positive downstream when all deposited by waning current	The four methods do not show consistent patterns; skewness is more often positive than negative.
	Glacial	May be positive or negative depending on nature of drift	
	Diluvial	More likely to be negative unless fine-grained substrata eroded and incorporated into bed material	
Kurtosis	Fluvial	Should decrease downstream with better sorting	The four methods vary only slightly; kurtosis is generally slightly higher eastward or away from mountains, higher along Great Falls of the Missouri River and canyon through Big Belt Mountains.
	Glacial	Expected to be very high, especially where erratics are present with fine-grained matrix	
	Diluvial	May decrease gradually downstream, especially waning, channelized flow	

deposits. It is a very useful statistic but not diagnostic. The lack of a clear sorting signal is evident in Figure 6. Since mean should vary downstream per Sternberg's Law, and sorting should improve, comparing these statistics via a scatter plot is very useful. Figure

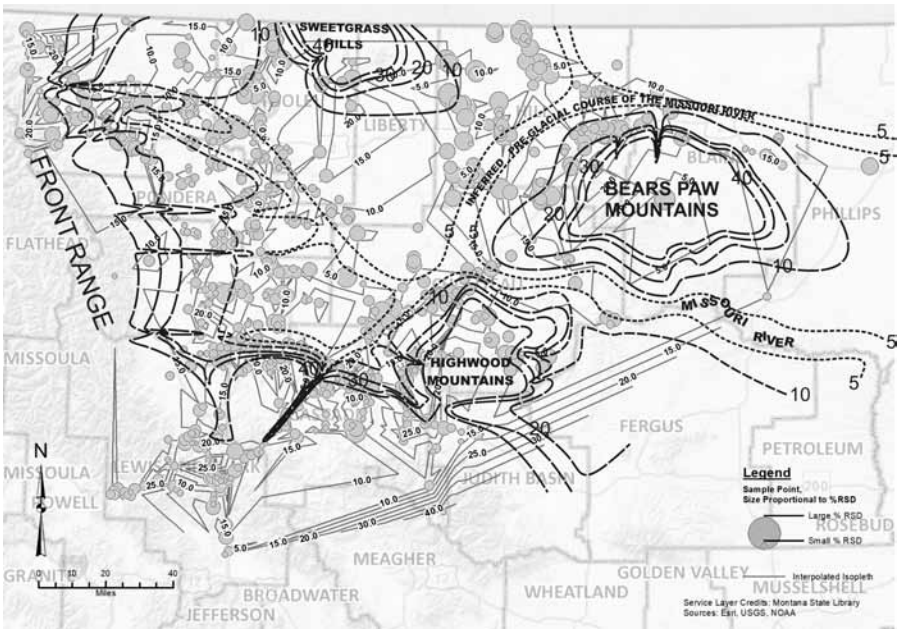

Figure 4 *(right)*. Idealized map showing expected change in particle size based on Sternberg's Law and topography (dashed lines) superimposed on measured D_{95} grain size isopleths (solid lines). Rough correspondence is evident.

7 shows little correspondence, with r^2 an insignificant 0.0022 for a linear fit through the Folk and Ward plot. Figure 8, comparing sorting to skewness, shows a similar lack of correspondence. Large numbers for both negative and positive skewness indicate polygenetic deposits, and similar scattered data have been collected from known polygenetic deposits (Srivastava et al., 2012). Examination of Figure 9 shows the lack of a meaningful trend in these data also, which is not surprising since none was clear in either variable alone. While kurtosis [outlier frequency distribution] increasing eastward (Table II) may be consonant with eastward-flowing currents, it is not conclusive and not well displayed in the data (Figure 10). Higher kurtosis in canyons could result from lag deposits from large floods. While grain size distribution data tend to produce large scatter, the data usually have more discernable trends, even in glacial environments (Mycielska-Dowgiałło and Ludwikowska-Kędzia, 2011). Fining occurs more rapidly during higher discharge (Hoey and Ferguson, 1997). Sorting trends may fail to develop in fluvial transport due to multiple sediment sources, cohesion of fines, and flocculation, among other factors (McLaren, 1981). End member analysis (a type of principal component analysis) can sometimes be used to help distinguish mixed sediments. Sediment input from tributaries can greatly affect observed grain-size relationships downstream (Unde and Dhakal, 2009), make them more bimodal, or even obliterate them when capacity is limited (Rădoane et al., 2008).

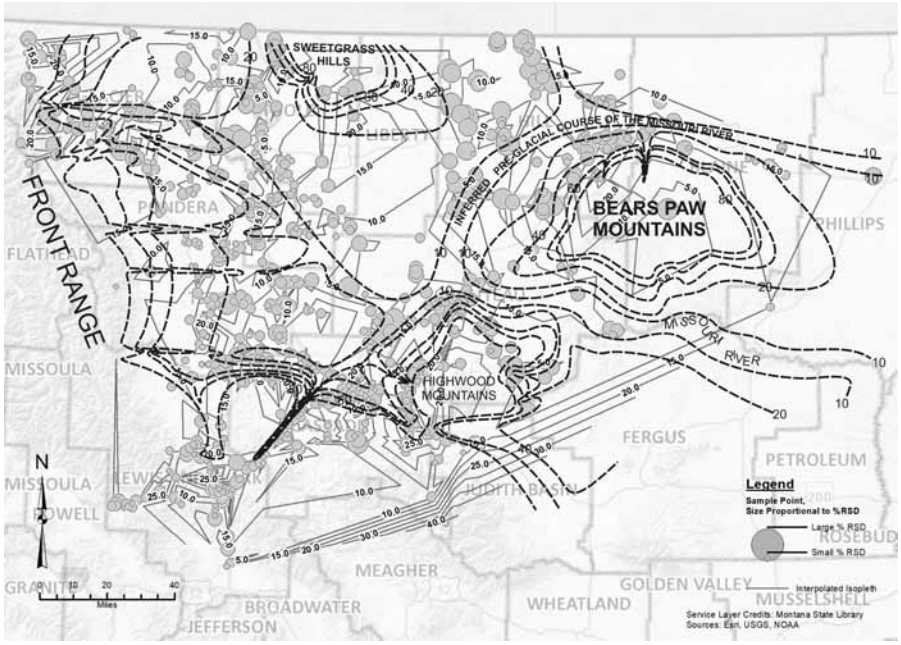

Figure 5. Idealized Sternberg's Law contours (dashed lines) superimposed on measured mean grain size isopleths (solid lines) based on Trask (1932) definition. Correspondence is similar to the D_{95} data.

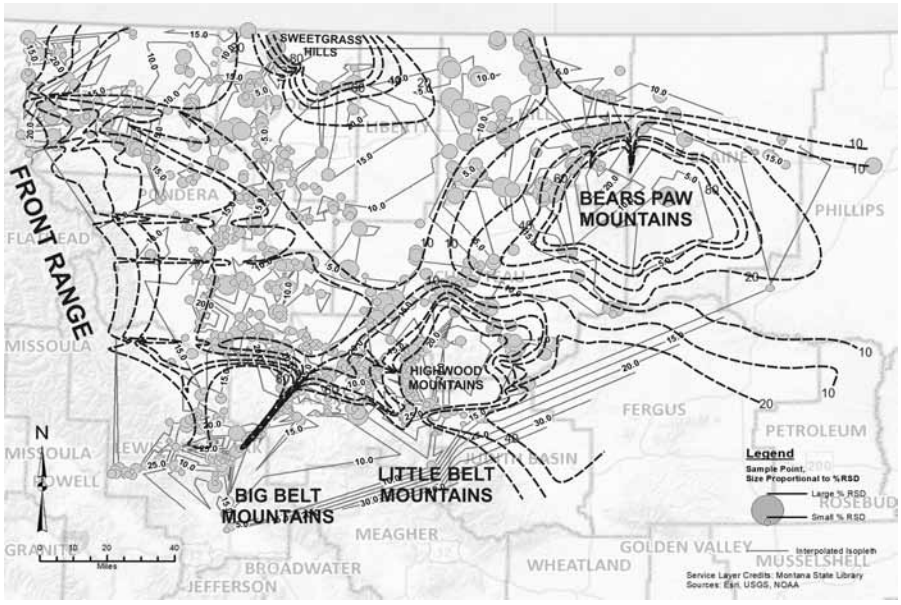

Figure 6. Idealized Sternberg's Law contours (dashed lines) superimposed on measured sorting isopleths (solid lines) based on Folk and Ward (1957) definition. Correspondence is slightly lower than D_{95} or mean.

Sternberg's downstream fining was originally explained by abrasion, but sorting was later found more important *after* an initial abrasive phase (Domokos et al., 2014). Pelletier (1980) documents that anisotropy develops from progradation. A prograding wave of fine sediment moves downstream ahead of coarser sediments, and exchange with sediment in the bed of the stream also takes place (Hoey and Ferguson, 1997). Thus, downstream fining, cross-bedding thickness, unit thickness, silt/clay ratio, clast rounding,

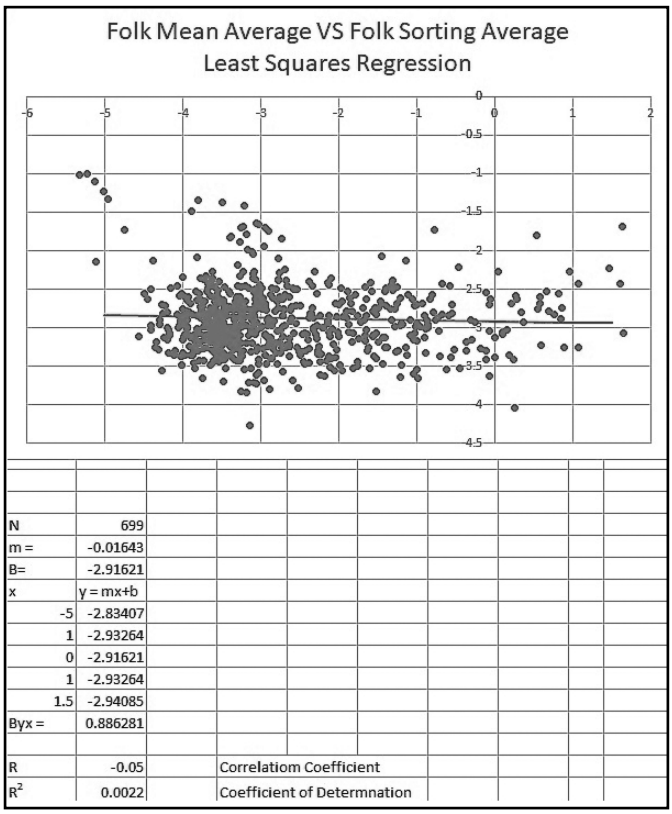

N	699								
m =	-0.01643								
B=	-2.91621								
x	y = mx+b								
-5	-2.83407								
1	-2.93264								
0	-2.91621								
1	-2.93264								
1.5	-2.94085								
Byx =	0.886281								
R	-0.05		Correlatiom Coefficient						
R^2	0.0022		Coefficient of Determnation						

Figure 7. Plot of sorting versus mean grain size per Folk and Ward (1957) with linear regression.

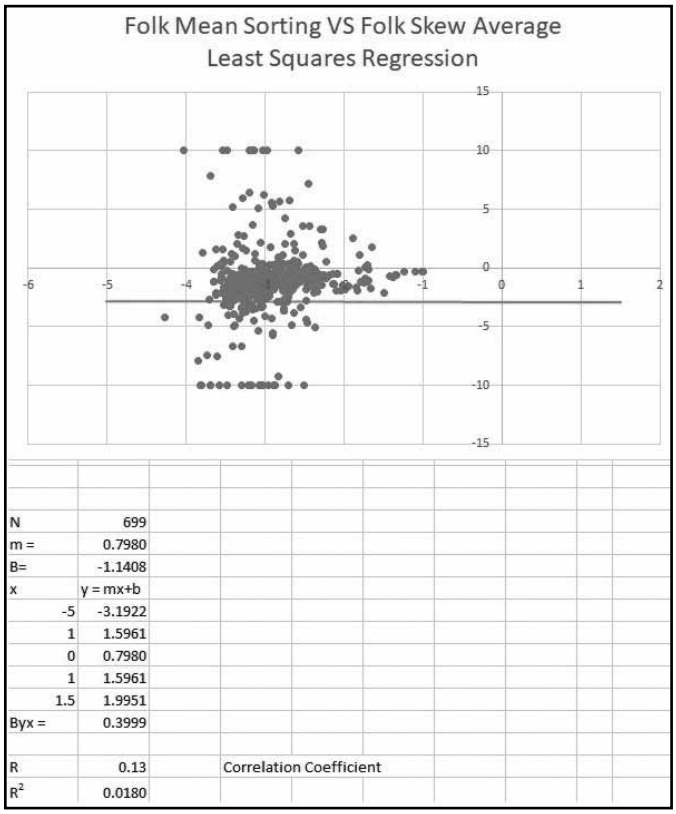

N	699								
m =	0.7980								
B=	-1.1408								
x	y = mx+b								
-5	-3.1922								
1	1.5961								
0	0.7980								
1	1.5961								
1.5	1.9951								
Byx =	0.3999								
R	0.13		Correlation Coefficient						
R^2	0.0180								

Figure 8. Mean versus skewness using Folk and Ward (1957). Linear regression applied.

heavy mineral content, and other vector properties (e.g., foreset dip, asymmetric ripple orientation, festoon bed plunge) reflect anisotropy developed by progradation and described by Sternberg's Law.

Pelletier (1980, p. 46) noted the applicability of Sternberg's Law to a wide variety of observed conditions in Canada:

> Variations in Sternberg's Law can be applied to sediments that were deposited under prograding conditions. Because currents move over beds that are characterized by a topographic gradient, the size decrease in the sediments is exponential in nature over given linear distances of transport (rivers in the Canadian Arctic Archipelago).

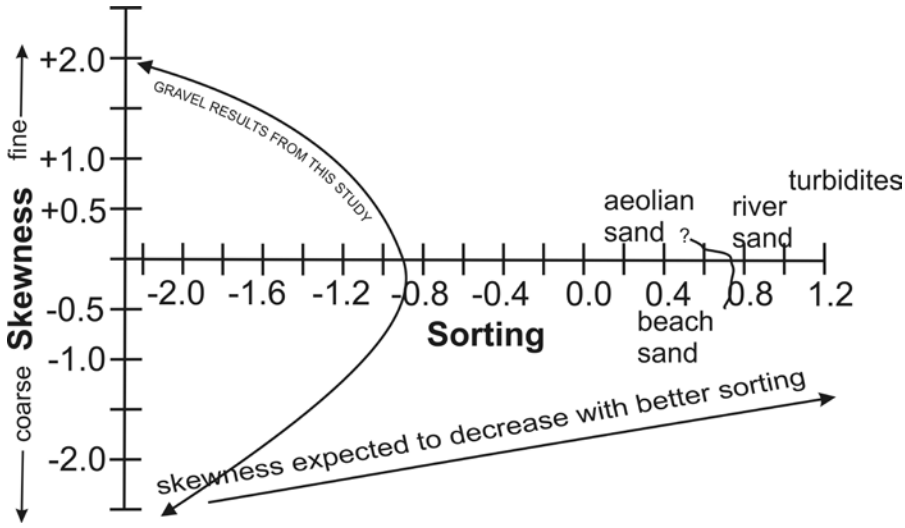

Figure 9. Sorting coefficient versus skewness showing domains of transport processes in sand range and parabola tracing the edge of gravel data from this study (left side of figure). Arrow shows expected decrease in skewness with increase in sorting resulting from action of current during transport.

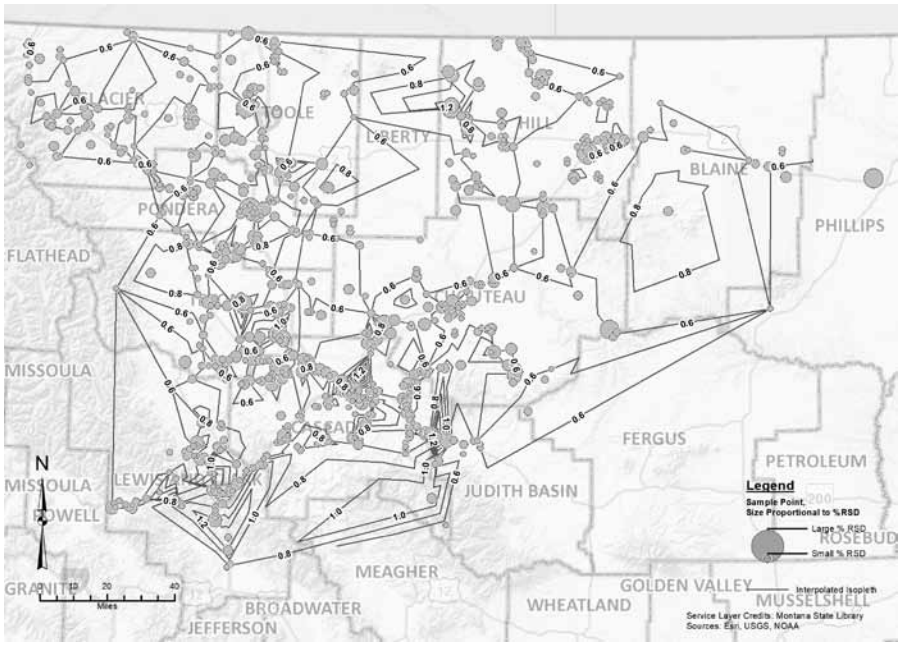

Figure 10. Map showing measured kurtosis per Inman (1952). Per Sternberg's Law, kurtosis should decrease down the stream course. Glacial deposits should have very high values of kurtosis.

Figure 11. Typical surficial gravel deposit on ridge in Chouteau County, Montana, ten miles east of The Knees. This area is mapped as glacial deposits over fine-grained clastic rocks. View east across road cut. (Location indicated on Figure 13.)

In examining this phenomenon in beds of geologic antiquity, it was found that the semi-logarithmic, size-distance curves could be applied to successive units deposited under prograding conditions. This rule, expressed mathematically as $Y=Y_0e^{-ax}$ (see text) was found to be operational over long periods of geologic time. For example, it applied for different parts of the same geological member (lower and upper Grimsby), as well as for two successive members (Grimsby and Thorold of the Silurian of the Niagara Penninsula); it held for a single formation (Toad) as well as for successive formations (Toad, Liard, and Grey Beds of the Triassic of northeastern British Columbia); and it could be demonstrated for successive rock systems (Upper Devonian sandstones, the Mississippian Pocono Formation, and the Pennsylvanian Pottsville Conglomerate in the Central Appalachians).

While many sedimentary features, including vector properties, are related to progradation, simple application of Sternberg's Law and grain-size statistics does not provide unique genetic solutions (Watson et al., 2013). As McLaren asserted (1981, p. 623), "… grain-size analyses of sediments from unknown environments and given no other supporting data will provide too large a range of possibilities to predict the exact environment of deposition."

Diamict

In the author's three decades of drilling in North Central Montana, the diamict (i.e., a poorly-sorted, clay-to-boulder-size-range sediment) identified as till largely consists of high-plasticity lean clay with varying amounts of sand and a slight amount of gravel. While till or glacial drift in many glaciated areas consists primarily of sand and gravel, most of the material in the study area is sandy lean clay or lean clay with sand per ASTM D2487. Gravel is found in discrete bodies, as a small percentage of the total earth material (Figures 11 and 12). It is, however, widely distributed, so the samples included in this

research project effectively cover the area believed to have been glaciated (see Figure 13). However, it is important to note that there is an *inherent bias* in the sampling scheme.

This study specifically focuses on gravels. Virtually all the diamict originating as glacial till that blankets much of Montana is rich in clay. While fluvial or diluvial processes would separate the coarse and fine fractions through sorting, diamict by its nature is unsorted. Could the samples included in this study be skewing the results and indicating a much smaller role for glacial transport than really was the case?

As explained in Part I of this paper (Klevberg, 2024), virtually none of the gravel samples landed in the till envelope on the C-M diagram (Figure 3). This figure is reproduced here as Figure 14 with the addition of 48 till samples (indicated by ▲). Sieve analysis reports for these samples were pulled from geotechnical records available to the author. A few of the samples were from sites apparently impacted by cordilleran rather continental glaciation, and these are indicated by black triangles. Most of these classify as clayey gravel. The rest of the till samples are from the area mapped as impacted by continental glaciation and are marked by gray triangles. These samples generally classify as high-plasticity lean clay with various amounts of sand (typically 20% or less) and minor gravel. While some of the till samples are coarse enough to fall into the size range included in this study (Figure 14), these are few and cordilleran.

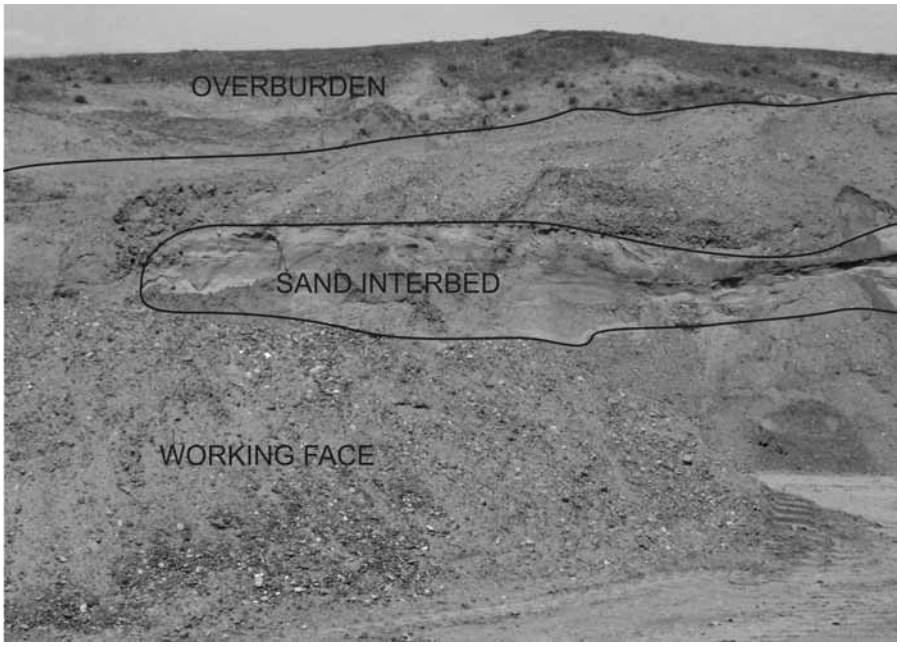

Figure 12. Working face in gravel pit a few miles north of Cartwright, McKenzie County, North Dakota. Cartwright gravel deposits consist almost solely of reworked cypflax (see Figure 13).

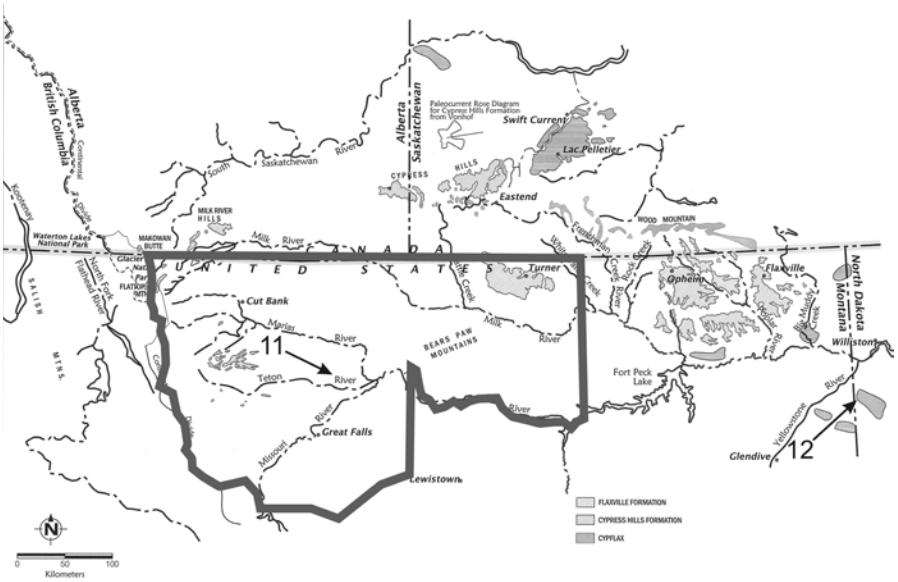

Figure 13. Map showing Cypress Hills Formation and Flaxville Formation deposits on erosional remnants in Montana, Alberta, and Saskatchewan. These appear to grade into each other with equivocal deposits (labelled simply "cypflax"). Rose diagram on figure north of Cypress Hills is based primarily on crossbeds in sand interbeds. Locations of Figures 11 and 12 indicated.

Conclusions

Analysis of the data, seen through Sternberg's Law, does not conclusively point to any of the three genetic hypotheses. Table III provides a detailed summary of Table II, with a scoring system to reduce subjectivity in comparing the three hypotheses. None obtains an overwhelming score. Although the most characteristics favor the diluvial mechanism, its total score is not dramatically greater than the glacial or fluvial hypotheses. While the

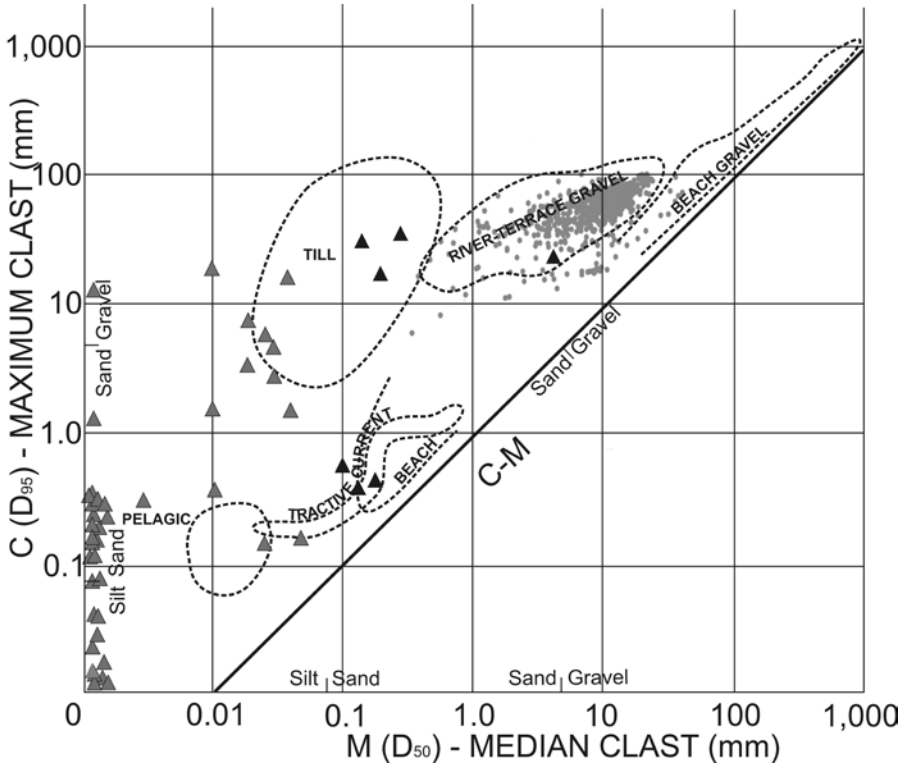

Figure 14. Figure 3 (C-M diagram) with addition of data from till (diamict) from several geotechnical projects. Black triangles are from site mapped as cordilleran glacial deposits. Gray triangles are from sites mapped as continental glacial deposits. Very fine-grained materials have M simply estimated from grain size distribution curves.

scoring is not truly quantitative, the order of the results may be significant. The highest levels (benches) in the study area are the cypflax surface (notably large parts of the Cypress Hills, Boundary Plateau, and equivalent benches in Figure 13), above the level of glaciation and stream incision, and not overprinted by later processes. The lowest areas, river valleys, would tend to show the most complex histories, and fluvial deposition scores nearly as low as glacial deposition in Table III. The study can be summarized as follows:

- While various methods weight different parts of the grain-size distribution, these differences do not explain observed contrasts between predictions and observations (Figure 5).
- Patterns are complex and poorly developed, but not chaotic, indicating more than a glacial origin for the gravels, especially since glaciation is believed absent on the highest benches and in the southeastern study area.
- Incorporation of rock eroded by highly competent currents could mask or supplant the ordinary Sternberg relationships. This would happen during generation of planation surfaces.
- Paleocurrents flowing east-northeast were highly modified by local topography, which includes several mountain ranges.
- Polyfinality is not only possible but likely for many deposits (McLaren, 1981), and grain size analysis does not provide unique solutions to natural history processes.
- Absence of Sternberg patterns does not preclude fluvial deposition, as alluvial deposits do not always exhibit expected trends, especially in gravel-bedded rivers (Mohtar et al., 2017).
- Rating of factors based on the gravel statistics and scatter plots makes the strongest case for the diluvial hypothesis and the weakest for glacial transport. The rating coincides with geography and concurrent multiple processes—from high diluvial plateaus to low river valleys subject to glaciation and fluvial reworking.
- The strong correlation shown on the C-M diagram (Figure 3), with most points plotting in the "river-terrace gravels" sector and a substantial number in the "beach gravels" (i.e., bidirectional transport) sector, supports the fluvial and diluvial hypotheses.
- Gravels in glaciated areas are likely *glaciofluvial*, not strictly glacial, based on the grain size statistics and their presence as isolated bodies within the till plains. Comparison with till samples for which more detailed information was available than the MDT samples indicates only minor effects to the data set would be likely (Figure 14), and these should be limited to the mountain front.

The reader should note that the comparison in Table III is between hypotheses about genetic mechanisms, not models or theories. Various mechanisms can be fit into innumerable models or theories, be they catastrophic or uniformitarian, diluvial or not. However, to be sound, any model or theory must accommodate the mechanisms indicated by field data.

Table III. Conclusions and Process Rankings.

Parameter	Process	Observation	Conclusion	Scoring
Grain size diminution	Fluvial	Fining evident by Front Range but gradual and complex eastward with local reflections of topography	No clear Sternberg's Law relationship	3
	Glacial		Complexity may result from glaciation, topography, or both, but largely fluvial	1
	Diluvial		Results accord with diluvial sheet flow but complicated by subsequent local factors	3
Sorting	Fluvial	Sorting is generally weak with no clear pattern, though possibly weaker along major streams.	No clear Sternberg's Law relationship	1
	Glacial		Accords with glacial model	4
	Diluvial		Accords with diluvial sheet flow but not with waning, channelized flow except locally	2
Skewness	Fluvial	Patterns inconsistent between methods with no strong trend, though more positive than negative	Sternberg relationship not evident from data	2
	Glacial		Accords with glacial model	4
	Diluvial		Weak and probably negative trend would be expected, lack of it is not supportive of diluvial deposition	3
Kurtosis	Fluvial	Consistent pattern between methods, kurtosis slightly higher near mountains and in Missouri canyons	More outliers in higher energy environments accords with Sternberg's Law	4
	Glacial		Glaciation not evident from kurtosis patterns	1
	Diluvial		Gradual decrease in outliers onto Great Plains expected, though pattern is weak	4
Mean versus Sorting	Fluvial	Sorting actually seems to become somewhat less with fining, though poor correlation	Opposite Sternberg's Law relationship unless significant addition of sediment from streams no longer extant	1
	Glacial		Glacial deposits are unsorted, though melting glaciers contribute to fluvial processes	2
	Diluvial		Accords with planation incorporating subjacent, finer materials	3
Sorting versus Skewness	Alluvial	Skewness varies widely in both positive and negative directions, with best fit curve level and showing very poor correlation	Correlation should be evident at least on reach level, possibly masked by data spacing	2
	Glacial		Extreme skewness values may be glacial, but clustering of data does not indicate glacial origin	1
	Diluvial		Accommodated by diluvial sheet flow but not a supporting prediction	3
Sorting versus Kurtosis	Fluvial	Poor correlation, but some indication of more kurtosis (heavy tail) with better sorting—increased sorting = addition of bed material?	Requires more powerful streams than at present	2
	Glacial		Glacial deposits are unsorted, though melting glaciers contribute to fluvial processes	3
	Diluvial		Accords with planation incorporating subjacent, finer materials	3
C-M Diagram	Fluvial	Excellent correlation, most being "river terrace," i.e. unidirectional fluvial transport, some "beach," i.e. bidirectional flow.	Most samples land squarely in this field.	4
	Glacial		Virtually nothing lands in "till" field.	0
	Diluvial		Nearly all samples land in the two fields that could apply.	5
Scoring: 0 = complete lack of correlation or complete incompatibility, 5 = perfect correlation or diagnostic criterion.			Alluvial (fluvial process) =	19
			Glacial (glacial process) =	16
			Diluvial (sheet or current deposition) =	26

Further Research

This study provides less subjective and more independent geologic information that should be combined with traditional field examination of paleocurrent indicators, stratigraphy, and provenance studies (e.g., Edwards and Scafe, 1996; see Klevberg, 2024). The author has already collected a significant amount of lithologic data for surficial gravel deposits in the study area, toward that end.

The correlation between elevation and multiple processes could be tested by combining the present work with a digital elevation model that segregates data by discrete levels known locally as "benches." This could be combined with lithologic data to infer provenance. Field examination of an adequate number of sites could qualitatively confirm conclusions from such studies and further elucidate depositional environments and transport mechanisms.

Additional data entry could "plug" the "Liberty hole" and include the Boundary (Turner) Plateau. These sieve reports are available but were not included for budgetary reasons. Sieve reports from the sites east of the study area would provide a longer baseline for increased accuracy in assessing any west-east trends.

Acknowledgements

This project was truly a team effort. Data collection 25 years ago was performed by Beverly Oard and Krista Koljonen with the cooperation of Montana Department of Transportation personnel. The completion of analysis was made possible by a research grant from the Creation Research Society, and TD&H Engineering provided bare-bones hourly rates. Cindy Wojciechowski went beyond requirements entering data with amazing accuracy. James Hiersche donated hours of his time programming the spreadsheet and processing the data. While my coworkers may not be convinced of my position on Earth history, they gladly contributed to the advancement of science through this project. Michael Oard provided an invaluable review of the first draft of this paper and encouragement and assistance over many years. *Deum laudo* (Proverbs 20:15,17).

Glossary

cordilleran—related to glaciation of the Rocky Mountains spreading eastward onto the plains as opposed to ice moving into the study area from the north or northeast.

diamict—an unstratified, unconsolidated deposit of various particle sizes, typically ranging from clay to boulder sizes.

diluvial—produced by or pertaining to the cataclysm described in Genesis 6–8, the Noahican Deluge, *mabbul*, Genesis Flood.

festoon bedding—a type of sedimentary cross-bedding characterized by ellipsoidal troughs with conformable beds or laminae that make a scoop-like shape.

kurtosis—a statistical term for the deviation of the tails of the population distribution from a normal (Gaussian) distribution.

lean clay—clay with a liquid limit less than 50%.

fat clay—clay with a liquid limit of 50% or more, indicating moisture sensitivity.

planation surface—a type of erosional surface that is relatively flat without regard to the hardness or toughness of the underlying geologic materials.

polyfinality—geologic phenomena that can be generated by two or more unrelated processes.

polygenetic—deposits with evidence of two or more different processes that may have been sequential rather than contemporaneous.

progradation—non-horizontal deposition of sediment that migrates horizontally, such as the sloping depositional surface of a delta front as it advances into a body of water.

skewness—a statistical term for the asymmetry of a population distribution, i.e. the mode and median do not coincide with the mean.

till—diamict formed by glacial transport.

References

Alden, W.C. 1932. Physiography and glacial geology of eastern Montana and adjacent areas. *U.S. Geological Survey Professional Paper 174*. U.S. Government Printing Office, Washington, D.C.

ASTM D2487. Standard practice for classification of soils for engineering purposes (Unified Soil Classification System). ASTM International, West Conschoken, PA.

Buffington, J.M., and D.R. Montgomery. 1999. A procedure for classifying textural facies in gravel-bed rivers. *Water Resources Research* 35(6):1903–1914.

Edwards, W.A.D., and D. Scafe. 1996. Mapping and resource evaluation of the Tertiary and preglacial sand and gravel formations of Alberta. *Alberta Geological Survey Open File Report 1994–06*.

Folk, R.L., and W.C. Ward. 1957. Brazos River bar: A study in the significance of grain size parameters. *Journal of Sedimentary Petrology* 27:3–26.

Hoey, T.B., and R.I. Ferguson. 1997. Controls of strength and rate of downstream fining above a river base level. *Water Resources Research* 33(11):2601–2608.

Inman, D.L. 1952. Measures for describing the size distribution of sediments. *Journal of Sedimentary Research* 22(3):125–145.

Klevberg, P. 2024. Sternberg's Law statistical study of surficial gravels in North-Central Montana—Part I: Methods and findings. *CRSQ* 61(1):58–80.

Klevberg, P., and M.J. Oard. 1998. Paleohydrology of the Cypress Hills Forma-

tion and Flaxville Gravel, *In* Walsh, R.E. (editor). *Proceedings of the Fourth International Conference on Creationism* (technical symposium sessions), pp. 361–378. Creation Science Fellowship, Pittsburgh, PA.

Kondolf, G.M., and M.G. Wolman. 1993. The sizes of salmonid spawning gravels. *Water Resources Research* 29(7):2275–2285.

McLaren, P. 1981. An interpretation of trends in grain size measures. *Journal of Sedimentary Petrology* 51(2):611–624.

Mohtar, W.H.M.W., S.A. Bassa, and M. Porhemmat. 2017. Grain size analysis of surface fluvial sediments in rivers in Kelantan, Malaysia. *Sains Malaysiana* 46(5):685–693.

Mycielska-Dowgiałła, E., and M. Ludwikowska-Kędzia. 2011. Alternative interpretations of grains-size data from Quaternary deposits. *Geologos* 17(4):189–203.

Pelletier, B.R. 1980. A sedimentological continuum occurring through geologic time: A study for students. *Maritime Sediments* 16(1–3):35–48.

Rădoane, M., N. Rădoane, D. Dumitriu, and C. Miclăuş. 2008. Downstream variation in bed sediment size along the East Carpathian Rivers: Evidence of the role of sediment sources. *Earth Surface Processes and Landforms* 33(5):674–694.

Schlee, J. 1973. Atlantic continental shelf and slope of the United States: Sediment texture of the northeastern part. *Geological Survey Professional Paper 529-L*. U.S. Geological Survey, Washington, D.C.

Srivastava, A.K., P.S. Ingle, H.S. Lunge, and N. Khare. 2012. Grain-size characteristics of deposits derived from different glacigenic environments of the Schirmacher Oasis, East Antarctica. *Geologos* 18(4):251–266.

Sternberg, H. 1875. Über Längen- und Querprofil geschiebeführender Flüsse. *Zeitschrift für Bauwesen* 25:483–506.

Trask, P.D. 1932. *Origin and Environment of Source Sediments of Petroleum*. Gulf Publishing Co., Houston, TX.

Unde, M.G., and S. Dhakal. 2009. Sediment characteristics at river confluences: A case study of the Mula-Kas Confluence, Maharashtra, India. *Progress in Physical Geography* 33(2):208–223.

Watson, E.B., G.B. Pasternick, A.B. Gray, M. Gozi, and A.M. Woolfolk. 2013. Particle size characterization of historic sediment deposition from a closed estuarine lagoon, Central California. *Estuarine, Coastal and Shelf Science* 126:23–33.

Notes from the Panorama of Science

Parting the Red Sea: A Compressible Flow Assessment

Abstract

Exodus 14:2 says that God parted the Red Sea with a strong east wind. If God complied with the natural laws, a compressible flow assessment can be applied. A notional scenario using stagnated flow was proposed and the penetration depth into the water column was calculated. Additionally, the temperature of the flow increases dramatically with increasing Mach number. For subsonic flow, the penetration depth is limited to less than 30 feet and the air temperature increase can be over 100°F. Hence, it seems the Red Sea was a *bona fide* miracle, and not merely a miracle of providential timing.

Introduction

Per the Bible, Exodus 14:21: "Moses stretched out his hand over the sea, and the Lord drove the sea back by a strong east wind all night and made the sea dry land, and the waters were divided." There is reference to a strong east wind blowing all night. Was the parting of the Red Sea simply a miracle of providential timing? If so, the miracle might be understandable in terms of compressible fluid flow. Or was parting the Red Sea an outright miracle that is simply beyond our understanding?

Compressible Flow Background

If the parting of the Red Sea was merely a miracle of providential timing, then it might be possible to use the physics of air flow to find the air speed, pressure, and temperature associated with the crossing event. If these values turn out to be tolerable for the fleeing Israelites, then no further miraculous explanation is necessary. On the other hand, if the air speed, temperature, and pressure values derived from the physics of compressible fluid flow are intolerable for humans, or unlikely to occur 'naturally,' this would suggest that the miracle is beyond our current understanding.

The working fluid for parting the sea seems to be air, which is a compressible fluid. Compressible flow is characterized by pressure, temperature, and velocity. The pressure of the flow consists of the static pressure, and a dynamic pressure that is related to the flow energy. For a free steam flow, which is the reference flow, the static pressure is usually the ambient pressure. Ambient pressure varies with altitude. The sum of the static pressure and the dynamic pressure equals the total pressure.

$$P_t = P_{dyn} + P_s \quad (1)$$

Where

P_t = Flow Total Pressure (psia)
P_{dyn} = Flow Dynamic Pressure (psi)
P_s = Flow Static Pressure (psia)

If the flow is brought to rest (stagnates), the dynamic pressure is zero and the measured static pressure would be equal to the total pressure as the dynamic pressure is recovered (converted to static pressure). The total pressure of a flow stream does not change and is the thermodynamic pressure potential of the flow stream. Similarly, there is a total temperature and static temperature. The total temperature is the thermodynamic temperature potential. If the flow is brought to rest (stagnates), the static temperature approximately increases to the total temperature. The velocity of the flow is generally expressed in terms of the Mach number, which is the ratio of the flow velocity divided by the sonic velocity. The following compressible flow equations are fundamental and can be found in any compressible flow textbook, such as Reference 1.

Total Pressure Calculation

Because the air flow is compressible, the stagnation pressure, known as the total pressure (P_t) is

$$P_t = P_s\left(1+\frac{\gamma-1}{2}M^2\right)^{\frac{\gamma}{\gamma-1}} \quad (2)$$

Where

P_t = Flow Total Pressure (psia)
P_s = Flow Static Pressure (psia)
M = Flow Mach Number
γ = property of air (constant at 1.4)

Note that the pressures for compressible flow calculations are absolute pressure (psia), which is pressure relative to a vacuum. Gauge pressure (psig) is the absolute pressure minus the ambient pressure. For example, a tire pressurized to 35 psig at sea level has an absolute pressure of 35 psi + 14.7 psi = 49.7 psia, as the ambient pressure at sea level is 14.7 psia.

For air, equation (2) can be expressed as

$$P_t = P_s\,(1 + 0.2M^2)^{3.5} \quad (3)$$

Mach Number is the ratio of the flow velocity to the sonic velocity

$$M = v/a \quad (4)$$

Where

v = Flow Velocity (ft./s)
a = Speed of Sound (ft./s)

The speed of sound is calculated as

$$a = \sqrt{\gamma R g_c T_s} \quad (5)$$

Where

R = Gas constant for air (53.35 $lb._f$-ft./$lb._m$-R)
g_c = 32.2 $lb._m$-ft./$lb._f$-s^2
T_s = Flow Static Temperature (Rankine, R)

Note that compressible flow calculation temperatures are based on an absolute scale, Rankine (R). The Rankine scale starts at absolute zero, the absolute minimum temperature. The Fahrenheit scale (F.) uses the same increments as the Rankine scale, but is offset by 460 degrees (R = F.+460). In English units, lb_m is pounds mass and lb_f is pounds force.

Sonic velocity (M=1) at sea level is sqrt (1.4 * 53.35 $lb._f$-ft./$lb._m$-R * 32.2 $lb._m$-ft./$lb._f$-s^2 * 519 R) = 1116 ft./s. At sonic conditions (M=1), the pressure ratio (P_t/P_s) from equation (2) is 1.89.

Total Air Temperature

The total temperature of the flow is

$$T_t = T_s\left(1+\frac{\gamma-1}{2}M^2\right) \quad (6)$$

Where

T_t = Flow Total Temperature (R)
T_s = Flow Static Temperature (R)

At sonic conditions (M=1), the temperature ratio (T_t/T_s) is 1.2.

A Proposed Scenario

Aircraft Wing Leading Edge Analogy

Consider an airfoil cutting through the air. Some of the air goes over the wing and the rest travels under the wing. At the leading edge where the flow splits, there is a stagnation region where the flow does not move and the pressure is higher than the ambient pressure having recovered the dynamic portion of the flow as it stagnates as illustrated in Figure 1. This stagnation region runs the entire length of the wing. Theoretically, an ant could walk the entire span of the wing in this stagnation region without being swept off by the flow.

Imagine a vertical sheet of air flow originating at altitude and impinging on a flat surface, like a body of water and splitting, half going right and the other half going left. Where the flow impinges, it will stagnate. There will be a stagnation line similar to that of an airfoil leading edge as shown in Figure 2. This region of higher pressure will displace the water to a depth where the water pressure equals the stagnation pressure. For this flow scenario, the total pressure does not change.

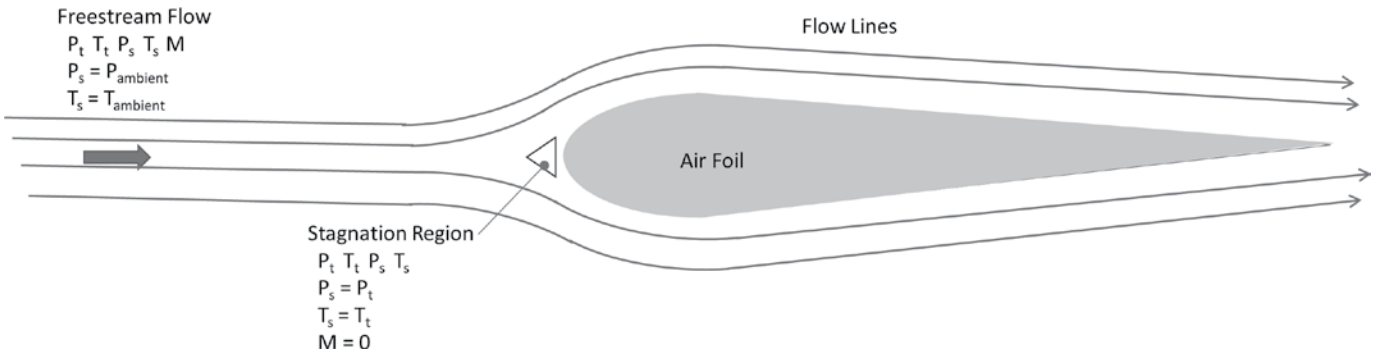

Figure 1. Compressible flow over an airfoil (two-dimensional cut).

The static pressure of the free stream will change with altitude and so will the Mach number. At the stagnation point, the Mach number is zero (since velocity is zero) and the total pressure and static pressure are equal. This is the best possible scenario for maximum penetration depth and ability to transit the channel formed by the parted waters.

Subsonic Conditions at Sea Level

If the flow is assumed to be at the subsonic (M<1.0), the pressure ratio (P_t/P_s) would be less than 1.89 per equation (2). If the altitude was sea level, at the threshold of sonic transition (M = 1) the stagnation pressure would be 1.89 * 14.696 psia = 27.78 psia (13.08 psig). If the flow stream originated at altitude, the flow would be supersonic at altitude as the static pressure (ambient pressure) is less than that at sea level and the total pressure of the flow does not change ($P_t/P_s > 1.89$). So, there would be a transition from supersonic to subsonic at some altitude where the Mach number equals 1.0.

Total Temperature at Altitude

At sonic conditions (M=1), the temperature ratio (T_t/T_s) is 1.2. If the flow is sonic and the ambient temperature (static) is 60°F (520 R), the increase in temperature is 104°F. (1.2 * 520 R = 624 R = 164°F.). 520 R is the ambient temperature for the International Standard Atmosphere (ISA) at sea level (assumed for this example). So, the temperature in the stagnation region would be 164°F. However, if the flow originates at altitude, the static temperature could be much less, but the Mach number would also be higher. So, the total temperature is calculated based on the static temperature at altitude and the flow Mach number. For example, if the flow originated at 10,000 feet, the ambient temperature is 24°F. (484 R) and the ambient pressure is 10.2 psia (ISA conditions at 10,000 feet altitude). Rearranging and solving equation (2) for the Mach number with P_t/P_s = 27.78/10.2 = 2.72 yields M = 1.286. The total temperature can be calculated with equation (6) as 484 R * (1+0.2 * 1.286^2) = 484 * 1.33 = 644 R = 184°F. So, the total temperature is defined at altitude at the origin of the flow based on the Mach number and static (ambient) temperature. The total pressure is defined at sea level as we want sonic conditions (or even better, subsonic conditions) at sea level.

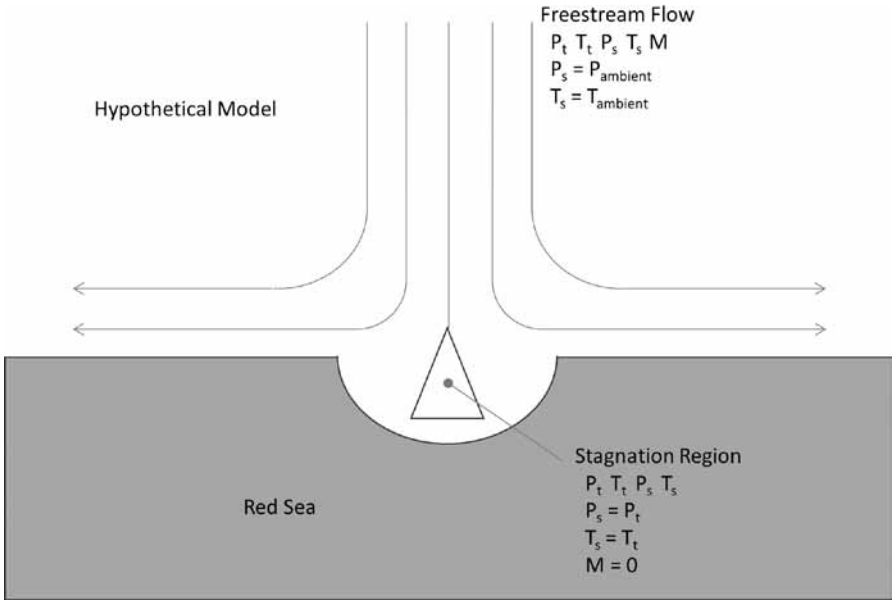

Figure 2. Hypothetical compressible flow impinging on a water surface (two-dimensional cut)

Penetration Depth

Water is an incompressible fluid and the pressure increases linearly by one atmosphere (14.7 psi) every 33 feet. So, the water pressure at depth (P_d) is

$$P_d = P_{surf} + \frac{14.7psi}{33ft} d \qquad (7)$$

Where

P_d = Pressure at depth (psia)
P_{surf} = pressure at the surface (psia = 14.7 psia at sea level)
d = penetration depth (ft)

For example, at a depth of 99 ft., the pressure would be 4 atmospheres or about 58.8 psia. For sonic flow impinging on the water, the total pressure is 1.89 × 14.7 psia = 27.78 psia. Equating this pressure to the pressure at depth, the sonic flow could theoretically penetrate 29 ft. below the surface. That is the maximum depth for a thermodynamic pressure potential (P_t) from sonic flow.

Supersonic Flow

Let's assume that the flow can be supersonic. Figure 3 shows the penetration depth and temperature ratio as a function of Mach number. It can be seen that the penetration depth increases dramatically with increasing Mach number as does the temperature ratio. At a Mach number of 2, the penetration depth is over 200 feet, but the temperature ratio is 1.8 yielding a total temperature of 1.8 * 520 = 936 R

= 476°F. In this case, the ISA ambient temperature at sea level (520 R) was used to calculate the total temperature, but it could be higher depending on the origin of the flow.

Three-Dimensional Effects

The Bible does say that there was a strong east wind. With a component of the flow parallel to the parted waters, the flow is not fully stagnant. The static pressure would be less than the total pressure, so the penetration depth would be less than fully stagnant flow and there would be an associated flow velocity along the parted water channel. Even a relatively low Mach number, like M = 0.1 would yield a flow velocity of over 100 ft./s (68 mph.) and it would be nearly impossible to walk into such a headwind.

Thermodynamic Assessment

The proposed scenario for parting the Red Sea is theoretically possible, but there is no precedent. for a vertical flow impinging on water forming a channel. This scenario, or any other scenario using sonic or subsonic flow, provides an upper bound as all the dynamic pressure is recovered when the flow stagnates. The maximum penetration depth is less than 30 ft. for a stagnated flow with this maximum subsonic condition at sea level and the total temperature of the flow is probably higher than can be tolerated by fleeing Israelites. If supersonic conditions were proposed, the penetration depth would be deeper but the total temperature of the stagnated flow would be intolerable.

Conclusion

If an air flow was used to part the Red Sea and natural laws were in effect, the crossing would probably be confined to shallow parts of the sea. Maybe the east wind was only used to dry the sea floor to keep the Israelites from becoming bogged down in mud. The Bible does state that "the children of Israel went into the midst of the sea upon the dry ground" (Exodus 14:22). The parting of the sea was most likely an outright miracle.

Walter Heim

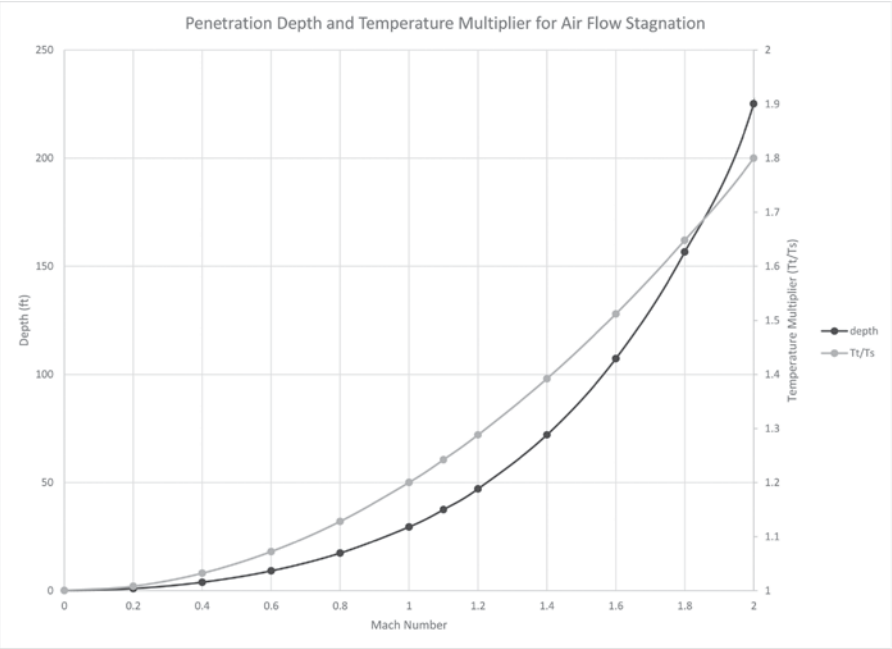

Figure 3. Penetration depth and temperature ratio as a function of flow mach number.

References

Anderson. J. 1982. *Modern Compressible Flow: With Historical Perspective*. McGraw-Hill, New York, NY.

Media Reviews

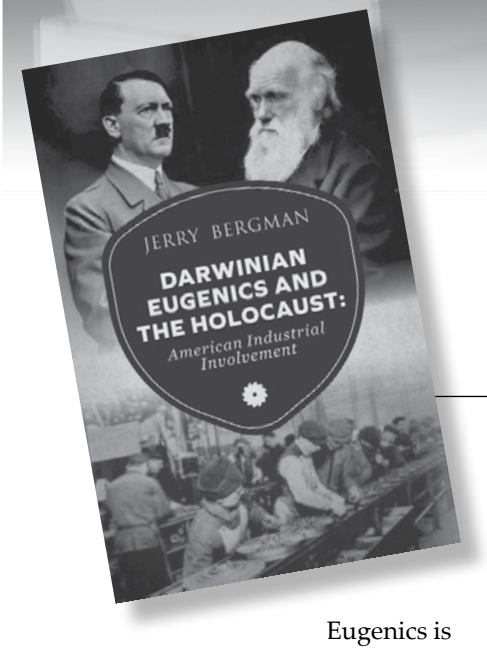

Darwinian Eugenics and the Holocaust: American Industrial Involvement

by Jerry Bergman

Involgo Press, 2020,
199 pages, $22.99

Eugenics is the study of hereditary improvement of the human race by controlled selective breeding. But how do you define what is inferior to what is superior? And how are environmental influences contrasted from hereditary conditions? These are some of the questions posed in Dr. Jerry Bergman's book. He documents in this book in detail the tragic effect of Darwinian eugenics not only in Nazi Germany, but also here in the United States of America.

The first step in establishing Darwinian eugenics is to attack the Creation foundation which begins with the book of Genesis found in the Holy Bible. Darwinian evolution attempts to demonstrate that human beings are not a creation of God, but instead are only animals, just another part of nature as is every other form of life. According to their theology or thinking, human beings may have some unique characteristics, but that we are no more advanced than any other species. This thought process, belief, or idea was critical in the rationale that started the eugenics movement by Charles Darwin's cousin Francis Galton, this premise that eventually led as well to the Holocaust. Again their thinking is that if we are all descendants of the first man and woman, we would all then be created equal as is taught in Genesis. This teaching was against the caveat that some humans are superior to others as would be the case if we came to be by Darwinian evolution.

Bergman demonstrated that Ernst Haeckel's underlying theme through his many books was that the material world is all that exists and that Darwinism explained its existence. The premises of Darwinism was the critical link (i.e. race breeding) that connected the genocide of the Herero people and the Nazi Holocaust to the Rwandan genocide and thus set a separate group up as an enemy, and be able to essentially wipe them out in good conscious.

This book covers in detail a history of how Darwin's *The Origin of Species by Means of Natural Selection or The Preservation of Favored Races in the Struggle for Life* changed America, particularly for the worse, with the introduction of eugenics and how the Carrie Buck Case changed both America and Germany, and how scientists argued for it (eugenics). It covers H.G. Wells endorsement of Darwinism in Europe and the USA through his books, along with his atheistic beliefs and the influence he had on society. Wells, along with many others, openly advocated eugenics. The acceptance of Darwinism led to the rejection of Genesis. Racism has had a long history in America and became much greater after the rise of the acceptance of Darwinism. We learned that the Nazis were inspired by American laws and authors. The central foundation behind WWII, and the Holocaust, was that it is based on the goal of extermination of the inferior races to give the superior Aryan race room to expand, eventually to the entire Earth. Bergman not only demonstrates that eugenics was well established in the American academic community and many universities, but also in industry which included Ford, GM, the Standard Oil Company, Eastman Kodak, the Kellogg Cereal Company, the Andrew Carnegie Institution, the John D. Rockefeller Foundation, the Coca-Cola Company, Aniline Film Corporation, the Harriman Railroad Fortune, IBM, and the Human Betterment Foundation.

Bergman's book ends with a warning that eugenics is alive and well today and for us not to forget the past, so that this does not happen again.

Mark Stewart
stewart1102m@gmail.com

Instructions to Authors

Submission

Electronic submissions of all manuscripts and graphics are preferred and should be sent to the editor of the *Creation Research Society Quarterly* in Word, WordPerfect, or Star-Office/Open Office (see the inside front cover for address). Printed copies also are accepted. If submitting a printed copy, an original plus two copies of each manuscript should be sent to the editor. The manuscript and copies will not be returned to authors unless a stamped, self-addressed envelope accompanies submission. If submitting a manuscript electronically, a printed copy is not necessary unless specifically requested by the *Quarterly* editor. Manuscripts containing more than 35 pages (double-spaced and including references, tables, and figure legends) are discouraged. An author who determines that the topic cannot be adequately covered within this number of pages is encouraged to submit separate papers that can be serialized.

All submitted manuscripts will be reviewed by two or more technical referees. However, each section editor of the *Quarterly* has final authority regarding the acceptance of a manuscript for publication. While some manuscripts may be accepted with little or no modification, typically editors will seek specific revisions of the manuscript before acceptance. Authors will then be asked to submit revisions based upon comments made by the referees. In these instances, authors are encouraged to submit a detailed letter explaining changes made in the revision, and, if necessary, give reasons for not incorporating specific changes suggested by the editor or reviewer. If an author believes the rejection of a manuscript was not justified, an appeal may be made to the *Quarterly* editor (details of appeal process at the Society's web site, www.creationresearch.org).

Authors who are unsure of proper English usage should have their manuscripts checked by someone proficient in the English language. Also, authors should endeavor to make certain the manuscript (particularly the references) conforms to the style and format of the *Quarterly*. Manuscripts may be rejected on the basis of poor English or lack of conformity to the proper format.

The *Quarterly* is a journal of original writings, and only under unusual circumstances will previously published material be reprinted. Questions regarding this should be submitted to the Editor (CRSQeditor@creationresearch.org) prior to submitting any previously published material. In addition, manuscripts submitted to the *Quarterly* should not be concurrently submitted to another journal. Violation of this will result in immediate rejection of the submitted manuscript. Also, if an author uses copyrighted photographs or other material, a release from the copyright holder should be submitted.

Appearance

Manuscripts shall be computer-printed or neatly typed. Lines should be double-spaced, including figure legends, table footnotes, and references. All pages should be sequentially numbered. Upon acceptance of the manuscript for publication, an electronic version is requested (Word, WordPerfect, or Star-Office/Open Office), with the graphics in separate electronic files. However, if submission of an electronic final version is not possible for the author, then a cleanly printed or typed copy is acceptable.

Submitted manuscripts should have the following organizational format:

1. Title page. This page should contain the title of the manuscript, the author's name, and all relevant contact information (including mailing address, telephone number, fax number, and e-mail address). If the manuscript is submitted by multiple authors, one author should serve as the corresponding author, and this should be noted on the title page.

2. Abstract page. This is page 1 of the manuscript, and should contain the article title at the top, followed by the abstract for the article. Abstracts should be between 100 and 250 words in length and present an overview of the material discussed in the article, including all major conclusions. Use of abbreviations and references in the abstract should be avoided. This page should also contain at least five key words appropriate for identifying this article via a computer search.

3. Introduction. The introduction should provide sufficient background information to allow the reader to understand the relevance and significance of the article for creation science.

4. Body of the text. Two types of headings are typically used by the *CRSQ*. A major heading consists of a large font bold print that is centered in column, and is used for each major change of focus or topic. A minor heading consists of a regular font bold print that is flush to the left margin, and is used following a major heading and helps to organize points within each major topic. Do not split words with hyphens, or use all capital letters for any words. Also, do not use bold type, except for headings (italics can be occasionally used to draw distinction to specific words). Italics should not be used for foreign words in common usage, e.g., "et al.", "ibid.", "ca." and "ad infinitum." Previously published literature should be cited using the author's last name(s) and the year of publication (ex. Smith, 2003; Smith and Jones, 2003). If the citation has more than two authors, only the first author's name should appear (ex. Smith et al., 2003). Contributing authors should examine this issue of the *CRSQ* or consult the Society's web site for specific examples as well as a more detailed explanation of manuscript preparation.

Frequently-used terms can be abbreviated by placing abbreviations in parentheses following the first usage of the term in the text, for example, polyacrylamide gel electrophoresis (PAGE) or catastrophic plate tectonics (CPT). Only the abbreviation need be used afterward. If numerous abbreviations are used, authors should consider providing a list of abbreviations. Also, because of the variable usage of the terms "microevolution" and "macroevolution," authors should clearly define how they are specifically using these terms. Use of the term "creationism" should be avoided. All figures and tables should be cited in the body of the text, and be numbered in the sequential order that they appear in the text (figures and tables are numbered separately with Arabic and Roman numerals, respectively).

5. Summary. A summary paragraph(s) is often useful for readers. The summary should provide the reader an overview of the material just presented, and often helps the reader to summarize the salient points and conclusions the author has made throughout the text.

6. References. Authors should take extra measures to be certain that all references cited within the text are documented in the reference section. These references should be formatted in the current *CRSQ* style. (When the *Quarterly* appears in the references multiple times, then an abbreviation to *CRSQ* is acceptable.) The examples below cover the most common types of references:

Robinson, D.A., and D.P. Cavanaugh. 1998. A quantitative approach to baraminology with examples from the catarrhine primates. *CRSQ* 34:196–208.

Lipman, E.A., B. Schuler, O. Bakajin, and W.A. Eaton. 2003. Single-molecule measurement of protein folding kinetics. *Science* 301:1233–1235.

Margulis, L. 1971a. The origin of plant and animal cells. *American Scientific* 59:230–235.

Margulis, L. 1971b. *Origin of Eukaryotic Cells*. Yale University Press, New Haven, CT.

Hitchcock, A.S. 1971. *Manual of Grasses of the United States*. Dover Publications, New York, NY.

Walker, T.B. 1994. A biblical geologic model. In Walsh, R.E. (editor), *Proceedings of the Third International Conference on Creationism* (technical symposium sessions), pp. 581–592. Creation Science Fellowship, Pittsburgh, PA.

7. Tables. All tables cited in the text should be individually placed in numerical order following the reference section, and not embedded in the text. Each table should have a header statement that serves as a title for that table (see a current issue of the *Quarterly* for specific examples). Use tabs, rather than multiple spaces, in aligning columns within a table. Tables should be composed with *14-point type* to insure proper appearance in the columns of the *CRSQ*.

8. Figures. All figures cited in the text should be individually placed in numerical order, and placed after the tables. Do not embed figures in the text. Each figure should contain a legend that provides sufficient description to enable the reader to understand the basic concepts of the figure without needing to refer to the text. Legends should be on a separate page from the figure. All figures and drawings should be of high quality (hand-drawn illustrations and lettering should be professionally done). Images are to be a minimum resolution of 300 dpi at 100% size. Patterns, not shading, should be used to distinguish areas within graphs or other figures. Unacceptable illustrations will result in rejection of the manuscript. Authors are also strongly encouraged to submit an electronic version (.cdr, .cpt, .gif, .jpg, and .tif formats) of all figures in individual files that are separate from the electronic file containing the text and tables.

Special Sections

Letters to the Editor:

Submission of letters regarding topics relevant to the Society or creation science is encouraged. Submission of letters commenting upon articles published in the *Quarterly* will be published two issues after the article's original publication date. Authors will be given an opportunity for a concurrent response. No further letters referring to a specific *Quarterly* article will be published.

Editor's Forum:

Occasionally, the editor will invite individuals to submit differing opinions on specific topics relevant to the *Quarterly*. Each author will have opportunity to present a position paper (2000 words), and one response (1000 words) to the differing position paper. In all matters, the editor will have final and complete editorial control. Topics for these forums will be solely at the editor's discretion, but suggestions of topics are welcome.

Book Reviews:

All book reviews should be submitted to the book review editor, who will determine the acceptability of each submitted review. Book reviews should be limited to 1000 words. Following the style of reviews printed in this issue, all book reviews should contain the following information: book title, author, publisher, publication date, number of pages, and retail cost. Reviews should endeavor to present the salient points of the book that are relevant to the issues of creation/evolution. Typically, such points are accompanied by the reviewer's analysis of the book's content, clarity, and relevance to the creation issue.

Author Copies:

CRSQ policy is that authors get 10 free copies of the issue containing their article, regardless of the number of co-authors. These free copies must be pre-ordered before the issue goes to press.

Creation Research Society Membership/Subscription Application and Renewal Form

The membership/subscription categories are defined below:

1. **Voting Member** ....Those having at least an earned master's degree in a recognized area of science.
2. **Sustaining Member** ....Those without an advanced degree in science, but who are interested in and support the work of the Society.
3. **Student Member** ....Those who are enrolled full time in high schools, undergraduate colleges, or postgraduate science programs (e.g., MS, PhD, MD, and DVM). Those holding post-doctoral positions are not eligible. A graduate student with a MS degree may request voting member status while enrolled as a student member.
4. **Senior Member** ....Voting or sustaining members who are age 65 or older.
5. **Life Member** ....A special category for voting and sustaining members, entitling them to a lifetime membership in the Society.
6. **Subscriber** ....Libraries, churches, schools, etc., and individuals who do not subscribe to the Statement of Belief.

All members (categories 1–5 above) must subscribe to the Statement of Belief as defined on the next page.

Please complete the lower portion of this form and mail it with payment to CRS Membership Secretary, 1 W. Firestorm Way #145, Glendale, AZ 85306, or fax for credit card payment to (928) 636-1153. Applications may also be completed online at creationresearch.org.

✂ -

This is a ❑ new ❑ renewal application for the subscription year beginning Summer 20____. *(Please type or print legibly.)*

Name ______________________ Address ______________________

City ______________________ State ________ Postal/Zip code ________ Country ______________

Phone (optional) ______________________ Email ______________________

Degree ______________________ Field ______________________

Year granted ______________ Institution ______________________

Presently associated with ______________________

I have read and subscribe to the CRS Statement of Belief. Signature ______________________

For foreign orders, including Canadian, payment must be made in U.S. dollars by a check drawn on a U.S. bank, international money order, or credit card. *Please do not send cash.*

Indicate applicable category ➊	*Indicate payment* ➊			
	Paper**			**Paper-less‡**
❑ Voting ❑ Sustaining	USA	Canada Mexico	Other countries	
❑ Regular [per year]	❑ $53	❑ $73	❑ $93	❑ $35
❑ Senior [per year]	❑ $48	❑ $68	❑ $85	❑ $30
❑ Life member	❑ $600	❑ $600	❑ $600	❑ $600
❑ Student* [per year]	❑ $48	❑ $68	❑ $85	❑ $30
❑ Subscriber [per year]	❑ $56	❑ $76	❑ $96	❑ $38

* Student members are required to complete the bottom portion of this form.
NOTE: Student members may qualify for the *Future Leaders Sponsorship* program.
See the CRS website at www.creationresearch.org for details.
** Rates for the paper option include postage for First Class Mail International

‡ **PAPERLESS option:** You may opt out of receiving paper copies of the CRS periodicals (*CRS Quarterly* and *Creation Matters*). By choosing this option you may register for access to the Premium Area of the website, where you may view or download electronic (PDF) versions of these publications. Of course, regular members and subscribers may also have access to the Premium Area. Only members, however, will have access to the Members Exclusive Area of the website.

Member/Subscriber $_____ per year
x ______ years

SUBTOTAL $__________

Optional contribution + $__________

Life membership + $__________

TOTAL $__________

❑ Visa ❑ MasterCard ❑ Discover
❑ American Express ❑ Check/money order

Card number ______________________

Expiration date (mo/yr) ______________________

Phone number (______) ______________________

Signature ______________________

Student Members **are required to complete the following:**

School or institution now attending ______________________

____

Your current student status: ❑ high school; ❑ undergraduate;
graduate program ❑ MS ❑ PhD; ❑ other ______________

Year you expect to graduate or complete your degree ____________

Major, if college or graduate student ______________________

Signature ______________________

Order Blank for Past Issues

Cost of complete volumes (per volume): ..... members (all categories) – $18.00 + S/H
nonmembers and subscribers (libraries, schools, churches, etc.) – $25.00 + S/H

Cost of single issues (per issue): ..... members (all categories) – $5.00 + S/H
nonmembers and subscribers (libraries, schools, churches, etc.) – $7.00 + S/H

	Number					Number					Number			
Volume	1	2	3	4	Volume	1	2	3	4	Volume	1	2	3	4
23	☐	☐	☐	☐	36	☐	☐	☐	☐	49	☐	☐	☐	☐
24	☐	☐	☐	☐	37	☐	☐	☐	☐	50	☐	☐	☐	☐
25	☐	☐	☐	☐	38	☐	☐	☐	☐	51	☐	☐	☐	☐
26	☐	☐	☐	☐	39	☐	☐	☐	☐	52	☐	☐	☐	☐
27	☐	☐	☐	☐	40	☐	☐	☐	☐	53	☐	☐	☐	☐
28	☐	☐	☐	☐	41	☐	☐	☐	☐	54	☐	☐	☐	☐
29	☐	☐	☐	☐	42	☐	☐	☐	☐	55	☐	☐	☐	☐
30	☐	☐	☐	☐	43	☐	☐	☐	☐	56	☐	☐	☐	☐
31	☐	☐	☐	☐	44	☐	☐	☐	☐	57	☐	☐	☐	☐
32	☐	☐	☐	☐	45	☐	☐	☐	☐	58	☐	☐	☐	☐
33	☐	☐	☐	☐	46	☐	☐	☐	☐	59	☐	☐	☐	☐
34	☐	☐	☐	☐	47	☐	☐	☐	☐	60	☐	☐	☐	☐
35	☐	☐	☐	☐	48	☐	☐	☐	☐	61	☐	☐		

Add 20% for postage (**for U.S. orders:** min. $6, max. $18; **for Canadian orders:** min. $10, no max.; **for other foreign orders:** min. $15, no max.) **Total enclosed: $**_____

Make check or money order payable to Creation Research Society. Please do not send cash. For foreign orders, including Canadian, please use a check in U.S. funds drawn on a U.S. bank, an international money order, or a credit card.

(Please type or print legibly)

Name _____ Address _____

City _____ State _____ Zip _____ Country _____

❑ Visa ❑ MasterCard ❑ Discover ❑ American Express Card number _____

Expiration date (mo/yr) _____ Signature _____

Mail to: Creation Research Society, 1 W. Firestorm Way #145, Glendale, AZ 85306, USA

Creation Research Society

History—The Creation Research Society was organized in 1963, with Dr. Walter E. Lammerts as first president and editor of a quarterly publication. Initially started as an informal committee of 10 scientists, it has grown rapidly, evidently filling a need for an association devoted to research and publication in the field of scientific creation, with a current membership of over 600 voting members (graduate degrees in science) and about 1000 non-voting members. The *Creation Research Society Quarterly* is a peer-reviewed technical journal. It has been gradually enlarged and modified, and is currently recognized as one of the outstanding publications in the field. In 1996 the *CRSQ* was joined by the newsletter *Creation Matters* as a source of information of interest to creationists.

Activities—The Society is a research and publication society, and also engages in various meetings and promotional activities. There is no affiliation with any other scientific or religious organizations. Its members conduct research on problems related to its purposes, and a research fund and research center are maintained to assist in such projects. Contributions to the research fund for these purposes are tax deductible. As part of its vigorous research and field study programs, the Society operates the Van Andel Creation Research Center in Glendale, Arizona.

Membership—Voting membership is limited to scientists who have at least an earned graduate degree in a natural or applied science and subscribe to the Statement of Belief. Sustaining membership is available for those who do not meet the academic criterion for voting membership, but do subscribe to the Statement of Belief.

Statement of Belief—Members of the Creation Research Society, which include research scientists representing various fields of scientific inquiry, are committed to full belief in the biblical record of creation and early history, and thus to a concept of dynamic special creation (as opposed to evolution) both of the universe and the earth with its complexity of living forms. We propose to re-evaluate science from this viewpoint, and since 1964 have published a quarterly of research articles in this field. *All members of the Society subscribe to the following statement of belief:*

1. The Bible is the written Word of God, and because it is inspired throughout, all its assertions are historically and scientifically true in all the original autographs. To the student of nature this means that the account of origins in Genesis is a factual presentation of simple historical truths.
2. All basic types of living things, including humans, were made by direct creative acts of God during the Creation Week described in Genesis. Whatever biological changes have occurred since Creation Week have accomplished only changes within the original created kinds.
3. The Great Flood described in Genesis, commonly referred to as the Noachian Flood, was a historical event worldwide in its extent and effect.
4. We are an organization of Christian men and women of science who accept Jesus Christ as our Lord and Savior. The act of the special creation of Adam and Eve as one man and woman and their subsequent fall into sin is the basis for our belief in the necessity of a Savior for all people. Therefore, salvation can come only through accepting Jesus Christ as our Savior.

iDINO II

Investigation of Dinosaur Intact Natural Osteo-tissue

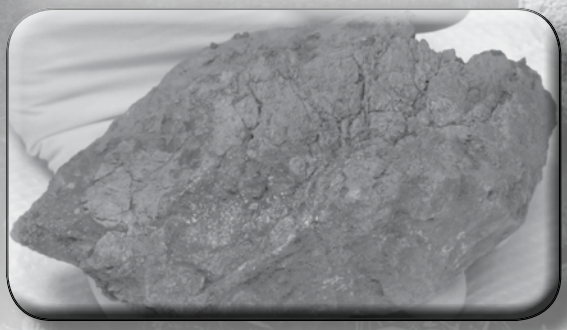

A fragment of the *Triceratops* brow horn. Fragments, such as this one, still contain tissue and cells.

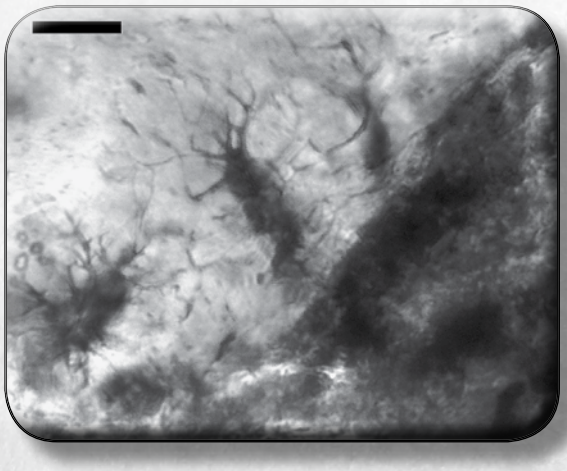

Microscopic examination of tissue extracted from a *Triceratops* horn reveals bone cells still present.

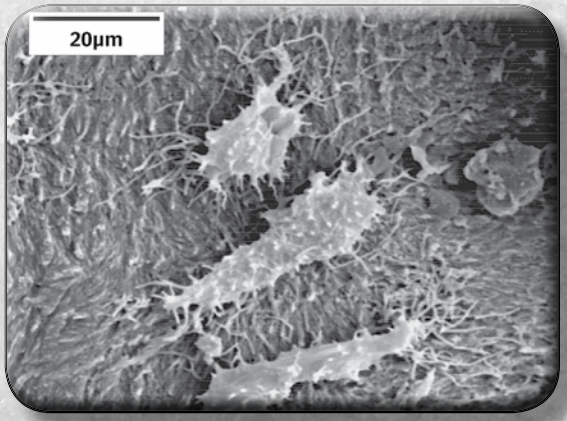

Electron microscope picture of intact bone cells still in tissue extracted from a *Triceratops* horn.

How can pliable, stretchable tissue survive inside dinosaur fossils for over 65 million years?

How can this tissue still contain intact cells and even dinosaur proteins?

How can this fragile biological material survive for so long?

The answer to these questions directly challenges the current, evolutionary-biased, geologic timescale.

The Creation Research Society began its iDINO research initiative for the purpose of studying soft tissue in dinosaur fossils. The first phase of the project detected pliable, unfossilized tissue in a brow horn of a *Triceratops*. Within this tissue were intact osteocytes (bone cells). Some results from the iDINO project have been published in a technical microscopy journal and presented at an international microscopy conference. The Spring 2015 issue of the *Creation Research Society Quarterly* also features a special report of the iDINO project. Plus, to further spread the important information about soft tissue, the Society is developing a video (Echoes of the Jurassic).

The **second phase** of the project (iDINO II) will look more extensively at the process of tissue preservation. Evolutionists have offered various theories of how this tissue could survive for millions of years. iDINO II will methodically investigate these preservation claims, assessing their plausibility.

The iDINO results have already provided a strong challenge to the evolutionary worldview. More extensive and detailed examination may provide even stronger evidence that the age of dinosaur fossils is far less than 65 million years. To this end, the Society continues to seek those willing to fund this project with either one-time gifts or monthly donations.

For more information contact us at (928) 636-1153 or crsvarc@crsvarc.com.

Also visit http://tinyurl.com/nphm2c4 for project updates and details.

V61N2